DISSERTATIONES
NEUROSCIENTIAE
UNIVERSITATIS
TARTUENSIS
39

MARIA KAARE

The involvement of NEGR1 and LSAMP in the psychiatric disorders are mediated through monoaminergic neurotransmission and changes in the systemic metabolism

DISSERTATIONES NEUROSCIENTIAE UNIVERSITATIS TARTUENSIS
39

DISSERTATIONES NEUROSCIENTIAE UNIVERSITATIS TARTUENSIS
39

MARIA KAARE

The involvement of NEGR1 and LSAMP in the psychiatric disorders are mediated through monoaminergic neurotransmission and changes in the systemic metabolism

UNIVERSITY OF TARTU
Press
1632

Institute of Biomedicine and Translational Medicine, University of Tartu, Tartu, Estonia.

The dissertation was accepted for the commencement of the degree of Doctor of Philosophy in Neurosciences on 06.01.2023 to 11.01.2023 by the council for the Curriculum of Neurosciences.

Supervisors: Mari-Anne Philips, PhD, Associate Professor,
Department of Physiology, Institute of Biomedicine and Translational Medicine, University of Tartu, Estonia

Eero Vasar, MD, PhD, Professor,
Department of Physiology, Institute of Biomedicine and Translational Medicine, University of Tartu, Estonia

Este Leidmaa, PhD, Research Fellow,
Department of Physiology, Institute of Biomedicine and Translational Medicine, University of Tartu, Estonia

Reviewers: Aet O´Leary, PhD, Associate Professor,
University Hospital Frankfurt, Germany

Külli Jaako, PhD, Associate Professor,
Department of Pharmacology, Institute of Biomedicine and Translational Medicine, University of Tartu, Estonia

Opponent: Tomi Rantamäki, PhD, Professor,
Faculty of Pharmacy, University of Helsinki

Commencement: 21.02.2023

This study was supported by research grants IUT20-41 and PRG685 from the Estonian Research Council. This research was also supported by the European Union through the European Regional Development Fund (Project No. 2014-2020.4.01.15-0012).

ISSN 1736-2792 (print)
ISBN 978-9916-27-133-9 (print)
ISSN 2806-2418 (pdf)
ISBN 978-9916-27-134-6 (pdf)

University of Tartu Press
www.tyk.ee

CONTENTS

LIST OF ORIGINAL PUBLICATIONS 8

ABBREVIATIONS 9

1. INTRODUCTION 11

2. REVIEW OF LITERATURE 13
   - 2.1. IgLON Family 13
   - 2.2. General characterization of NEGR1 and LSAMP 13
   - 2.3. Psychiatric disorders 14
   - 2.4. NEGR1 in psychiatric disorders 15
   - 2.5. LSAMP in psychiatric disorders 17
   - 2.6. IgLONs and monoamines 17
   - 2.7. NEGR1 and body weight phenotype 19
   - 2.8. Concluding remarks 20

3. AIMS OF THE STUDY 21

4. MATERIALS AND METHODS 22
   - 4.1. Animals (Paper I, II and III) 22
   - 4.2. *Lsamp* isoform-specific stainings in brain slices (Paper I) 23
   - 4.3. qRT-PCR analysis in mouse brain areas (Papers I, II) 23
     - 4.3.1. qRT-PCR analysis by using Taqman assays (Paper I) 23
     - 4.3.2. qRT-PCR analysis by using Sybr green assay (Paper II) 24
   - 4.4. Escitalopram treatment (Papers I, II) 24
   - 4.5. Dose-response and chronic amphetamine treatment (Paper II) 25
   - 4.6. Behavioral testing 26
     - 4.6.1. Elevated plus maze (Paper I, II) 26
     - 4.6.2. Open field test (Paper I, II) 27
     - 4.6.3. Tail Suspension Test (Paper I, II) 27
   - 4.7. Measurement of monoamines (Paper I, II) 27
   - 4.8. Immunohistochemistry (Paper II) 28
   - 4.9. Diet composition (Paper III) 29
   - 4.10. HF diet (Paper III) 29
   - 4.11. Food preference test (cohort IX) (Paper III) 30
   - 4.12. Measurement of metabolites (Paper III) 30
   - 4.13. GTT, cohort VIII (Paper III) 31
   - 4.14. Sample collection (Paper I, II, III) 31
   - 4.15. Western blot 31
   - 4.16. Statistical Analysis (Paper I, II, III) 32

5. RESULTS 33
5.1. Expression and impact of LSAMP neural adhesion molecule in the serotonergic neurotransmission system (Paper I)..... 33
5.1.1. *Lsamp* transcripts are expressed in the dorsal, median, and caudal raphe nuclei..... 33
5.2. Chronic administration of escitalopram has impact to the behavior *of Lsamp*$^{-/-}$ mice and *Lsamp*$^{-/-}$ mice has lower baseline bodyweight..... 34
5.2.1. Chronic administration of escitalopram alters the level of monoamine in several brain areas..... 37
5.2.2. The baseline 5-HT system related gene expression in *Lsamp*-deficient mice..... 38
5.3. *Negr1* gene-deficiency induces alterations in the monoaminergic neurotransmission enhancing time-dependent sensitization to amphetamine in mice (Paper II)..... 39
5.3.1. The impact of chronic administration of escitalopram to the body weight and behavior of *Negr1*$^{-/-}$ and WT mice..... 39
5.3.2. Chronic administration of escitalopram alters the level of monoamines and their metabolites in raphe 40
5.3.3. *Negr1*$^{-/-}$ mice display higher sensitivity to amphetamine compared to WT mice..... 42
5.3.4. Chronic administration of amphetamine increases the level of tyrosine hydroxylase (*Th*) in VTA..... 46
5.3.5. Amphetamine increases the level of dopamine in DSTR 47
5.3.6. Chronic amphetamine administration alters the level of monoamines in Hip and chronic escitalopram treatment causes weight difference of the Hip 49
5.4. High-fat diet induces pre-diabetes and distinct sex-specific metabolic alterations in *Negr1*-deficient mice (Paper IV) 51
5.4.1. *Negr1* deficiency induces lower intake of HF food but higher body weight gain in male mice 51
5.4.2. HF diet leads to higher levels of blood glucose in *Negr1*$^{-/-}$ mice, whereas phenotype difference in glucose tolerance test was apparent only in males..... 53
5.4.3. HF diet induces an altered profile of circulating lipids sex-specifically *in Negr1*$^{-/-}$ mice..... 54
5.4.4. HF diet induced an increase in circulating amino acids in *Negr1*$^{-/-}$ mice, more prominently in males..... 55
5.4.5. Altered profile of circulating organic acids in *Negr1*$^{-/-}$ mice..... 57
5.5. *Negr1*$^{-/-}$ mice have increased levels of oxidative stress related proteins in Hip (Cohort X) (unpublished)..... 58

6. DISCUSSION 59
6.1. Expression of *Lsamp* and *Negr1* in the monoaminergic nuclei and pathways 59
6.2. Effects of escitalopram on the *Lsamp*- and *Negr1*- deficient mice . 61
6.3. Effects of amphetamine in the *Negr1*-deficient mice 65
6.3.1. Increased behavioral sensitization to amphetamine and upregulation of *Dat* transcript in *Negr1*$^{-/-}$ mice 65
6.3.2. Altered molecular reactivity to the amphetamine in the brains of *Negr1*$^{-/-}$ mice 66
6.3.3. *Negr1*$^{-/-}$ mice display reduced sensitivity to stress and show less activity during chronic injections/testing 68
6.4. *Negr1* deficiency-induced alterations in the monoaminergic neurotransmission could explain links of *NEGR1* with both depression and obesity phenotypes 68
6.5. Body weight and metabolic profile of *Negr1*-deficient mice on HF diet 69
6.5.1. Effects of HF diet on the body weight and food consumption of *Negr1*-deficient mice 69
6.5.2. HF diet alters the glucose tolerance of male *Negr1*-deficient mice 70
6.5.3. Gender-specific changes in the metabolism of lipids of *Negr1*-deficient mice caused by HF diet 71
6.5.4. Gender-specific changes in the metabolism of amino acids of *Negr1*-deficient mice caused by HF diet 71
6.5.5. Gender-specific changes in the metabolism of citric of *Negr1*-deficient mice caused by HF diet 73
6.6. Concluding remarks and future prospects 75
CONCLUSIONS 76
REFERENCES 79
SUMMARY IN ESTONIAN 90
ACKNOWLEDGEMENT 92
ORIGINAL PUBLICATIONS 93
CURRICULUM VITAE 158
ELULOOKIRJELDUS 160

LIST OF ORIGINAL PUBLICATIONS

I. Bregin, A.*, **Kaare, M**.*, Jagomäe, T., Karis, K., Singh, K., Laugus, K., Innos, J., Leidmaa, E., Heinla, I., Visnapuu, Oja, E.-M., Kõiv, K., Lilleväli, K., Harro, J., Philips, M.-A., Vasar, E. (2020). Expression and impact of Lsamp neural adhesion molecule in the serotonergic neurotransmission system. Pharmacol. Biochem. Behav. 198, 173017. https:/doi.org/10.1016/j.pbb.2020.173017.

II. **Kaare, M**., Jayaram, M., Jagomäe, T., Singh, K., Kilk, K., Leevik, M., Varul, J., Leidmaa, E., Visnapuu, T., Nõmm, H., Rähn, K., Plaas, M., Lilleväli, K., Schäfer, M. K.E., Philips, M.-A., Vasar, E. (2022). Depression-associated *Negr1* gene-deficiency induce alterations in the monoaminergic neurotransmission enhancing time-dependent sensitization to amphetamine in male mice. Brain Sciences.

III. **Kaare, M**., Mikheim, K., Lilleväli, K., Kilk, K., Jagomäe, T., Leidmaa, E., Piirsalu, M., Porosk, R., Singh, K., Reimets, R., Taalberg, E., Schäfer M. K. E., Plaas, M., Vasar, E., Philips, M.-A. (2021). High-Fat Diet Induces Pre-Diabetes and Distinct Sex-Specific Metabolic Alterations in Negr1-Deficient Mice. Biomedicine 9(9), 1148. https:/doi.org/10.3390/biomedicines9091148.

Contribution of the author:

I. * – Shared first authorship. The author participated in the behavioral experiments. Prepared cDNAs and performed qPCR analyzes, performed in situ hybridization stainings. Participated in data interpretation, writing and revision of the paper.

II. The author participated in designing the study and was responsible for formation of study groups. Author performed behavioral and pharmacological experiments, HPLC analysis of the ventral and dorsal striatum, performed and supervised qPCR analysis, carried out all statistical analysis, participated in the data interpretation and writing of the manuscript.

III. The author participated in designing the study and was responsible for the formation of the study groups. Author performed the body weight and food intake measurements and behavioral experiments, carried out statistical analysis, participated in the data interpretation and writing of the manuscript and handled correspondence.

ABBREVIATIONS

ADHD	–	attention deficit hyperactivity disorder
ASD	–	autism spectrum disorder
AUC	–	area under curve
BCAA	–	branched-chain amino acids
BMI	–	body-mass index
BST	–	bed nucleus of the striata terminalis
cDNA	–	complementary deoxyribonucleic acid
CHOL	–	cholesterol
Comt	–	catechol-O-methyltransferase
CT	–	cycle threshold
DA	–	dopamine
Dat	–	dopamine transporter
DG	–	dentate gyrus
DLPFC	–	dorsolateral prefrontal cortex
DOPAC	–	3,4-dihydroxyphenylacetic acid
DR	–	dorsal raphe
Drd1	–	dopamine receptor 1
Drd2	–	dopamine receptor 2
*Dr*d5	–	dopamine receptor 5
DSM-4	–	Diagnostic and Statistical Manual of Mental Disorders IV
DSTR	–	dorsal striatum
GABA	–	gamma-aminobutyric acid
$GABA_A$	–	gamma-aminobutyric acid-A (receptor)
GSH	–	glutathione
GTT	–	glucose tolerance test
GWAS	–	genome wide association studies
HF	–	high-fat
Hip	–	hippocampus
HPLC	–	high performance liquid chromatography
HVA	–	homovanillic acid
ICD-10	–	International Statistical Classification of Diseases and Related Health Problems 10^{th} version
IgLON	–	name of a protein family
i.p	–	intraperitoneal
LD	–	lipid droplets
LDL	–	low density lipoprotein
LSAMP	–	limbic system associated membrane protein in general
LSAMP	–	limbic system associated membrane protein human gene
Lsamp	–	limbic system associated membrane protein mice gene
$Lsamp^{-/-}$	–	homozygous mutants lacking both functional alleles of *Lsamp* gene
LSD	–	lysergic acid diethylamide

MaoA – monoamine oxidase A
MaoB – monoamine oxidase B
MDD – major depressive disorder
MnR – median raphe
NA – noradrenaline
NEGR1 – neuronal growth regulator 1 protein in general
NEGR1 – neuronal growth regulator 1 human gene
Negr1 – neuronal growth regulator 1 mice gene
Negr1$^{-/-}$ – homozygous mutants lacking both functional alleles of the *Negr1* gene
NMN – normetanephrine
NOX1 – NADPH oxidase 1
NOX2 – NADPH oxidase 2
NPC2 – NPC intracellular cholesterol transporter 2
NTM – neurotrimin protein
NTM – neurotrimin human gene
Ntm – neurotrimin mice protein
Ntm – neurotrimin mice gene
OPCML – opioid-binding protein/cell adhesion molecule like human gene
Opcml – opioid-binding protein/cell adhesion molecule like mice protein
PC – phosphatidylcholines
RMg – raphe magnus
RNA – ribonucleic acid
RT-qPCR – quantitative reverse transcription polymerase chain
SAT – subcutaneous adipose tissue
SERT – serotonin transporter
SFA – saturated fatty acids
Slc6a4 – serotonin transporter gene
SM – sphingomyelin
SOD1 – superoxide dismutase 1
SSD – schizophrenia spectrum disorders
TAAR1 – trace amine associated receptor 1
Temp – temporal lobe
Th – tyrosine hydroxylase
VSTR – ventral striatum
VTA – ventral tegmental area
WT – wild-type
3-MT – 3-methoxytyramine
5-HT – serotonin
5-HIAA – 5-hydroxyindoleacetic acid

1. INTRODUCTION

Obesity, metabolic syndrome, and diabetes are major global health problems. One in every 8 people (970 million) in the world live with mental disorders, with anxiety and depressive disorder being the most common. Mental disorders involve significant disturbances in cognitive processes, emotional regulation, or behavior. According to the World Health Organization (WHO), 1.9 billion adults and over 340 million children and adolescents aged 5–19 were overweight in 2016. Several studies have shown that mental disorders and obesity may have the same etiology.

Cell adhesion molecules are important proteins that mediate either intercellular contacts or contacts between cells and the extracellular matrix. Neural adhesion molecules are important in creating connections between neurons in the development of the nervous system, as well as in the adult brain. Neural cell adhesion molecules, such as IgLON proteins, are also very important for the correct formation of neuronal circuits and for keeping the integrity of those circuits. Therefore, changes in the expression or function of adhesion molecules can lead to changes in adaptive behavior and lead to psychopathological conditions. Neuronal growth regulator 1 (NEGR1) and limbic system associated membrane protein (LSAMP) are the members of IgLON gene family. IgLONs play an important role in cell-to-cell adhesion and have been shown to promote growth cone migration, axon target guidance, synapse formation, and dendritic tree formation throughout development and adulthood (Hashimoto et al., 2009; Pischedda et al., 2014; Singh et al., 2018). Polymorphisms in the human IgLON genes have been linked with a variety of psychiatric conditions. In genome wide association studies (GWAS), the neural adhesion molecule encoding NEGR1 gene has been linked with a wide spectrum of psychiatric conditions (Cross-Disorder Group, 2019). Nevertheless, the genome-wide studies link NEGR1 most strongly with depression (Hyde et al., 2016). In addition to psychiatric disorders, NEGR1 is a candidate gene regulating human obesity. In GWAS studies, *NEGR1* gene locus has been repeatedly shown to have strong associations with human body-mass index (BMI) indicating a role in body weight regulation and obesity (the GIANT Consortium, 2009; Thorleifsson et al., 2009; Speliotes et al., 2010; Locke et al., 2015; Winkler et al., 2016; Schlauch et al., 2020). Altered expression of LSAMP protein has been also linked with psychopathology. Accumulating evidence suggests that increased levels of the LSAMP transcript in mice are associated with lower activity, higher levels of anxiety or acute fear reaction, and that the genetic deletion of the *Lsamp* gene in mice results in increased activity in novel environments and reduced anxiety-like behavior (Catania et al., 2008; Innos et al., 2011; Innos et al., 2012).

The aim of this study was to assess the effects of *Lsamp*- and *Negr1*-deficiency on the monoaminergic circuitry as adhesion molecules regulate neurite outgrowth, play a vital role in the formation of correct neuronal pathways and connections, and disruption of these processes can also alter the monoaminergic

pathways and proper functioning of monoaminergic systems. In addition, adhesion molecules are important in the formation of synapses and maintaining the integrity of synapses. Consequently, changes in the function of adhesion molecules can lead to changes in the location of monoamine transporters and receptors at synapses, as well as changes in receptor density. Amphetamine and escitalopram were used as pharmacological agents to challenge monoaminergic neurotransmission in *Negr1*-deficient mice and escitalopram was used to study monoaminergic neurotransmission in *Lsamp*-deficient mice. Another aim of the current study was to explore the effect of *Negr1* deficiency on food intake, systemic metabolism, and oxidative stress levels in the brain. Shared genetic risk factors between depression and obesity have been reported, which could be mediated through shared etiological pathways, such as dysfunction of the hypothalamic–pituitary axis. Although IgLONs are neural adhesion molecules that are primarily expressed in the brain, several studies have shown that they may play a role in several non-neural organs. For example, IgLONs have been shown to act as tumor suppressors in a variety of organs, such as the ovaries, lungs, bones, and stomach (Sellar et al., 2003; Ntougkos et al., 2005; Wang et al., 2006; Tsou et al., 2007; Barøy et al., 2014). Furthermore, recent data from depression patients suggest that the functional impact of NEGR1 might involve systemic regulation. A significant upregulation of NEGR1 has been shown in the cerebrospinal fluid (Maccarrone et al., 2013) and peripheral blood of depression patients (Dall'Aglio et al. 2021; Deng et al., 2022). Considering the recent data, the current study aimed to add evidence that would enable us to determine whether the impact of NEGR1 is established mainly through its function as a cell adhesion molecule in the brain or whether this protein also has a distinct role in the systemic metabolism, which could, in turn, contribute to the etiology of psychiatric disorders.

2. REVIEW OF LITERATURE

2.1. IgLON Family

IgLON gene family consists of five members: Neuronal growth regulator 1 (*Negr1*), limbic system associated membrane protein (*Lsamp*), neurotrimin (*Ntm*), opioid-binding protein/cell adhesion molecule like (Opcml) and IgLON-5 (Vanaveski et al., 2017). All these molecules are highly glycosylated membrane proteins, characterized by three immunoglobulin domains and glycosylphosphatidylinositol-anchor. IgLONs plays an important role in cell to cell adhesion and neurite outgrowth and synaptogenesis (Hashimoto et al., 2008; Pischedda et al., 2014; Singh et al., 2019). The expression of IgLON family members is the strongest during embryonal state of development, it starts to fade a little after birth being more faintly expressed during adulthood. Three of the IgLON family members *Lsamp, Ntm* and *Opcml* have two alternative isoforms 1a and 1b. Those isoforms are differentially expressed during development, indicating the regulation of alternative promoter usage. Expression of IgLONs has been shown as early as E10.5, the earliest expression is detected from *Negr1, Lsamp 1a, Ntm 1a* and *Opcml 1b* (Jagomäe et al., 2021). This timing correlates with the neurogenic and expansion phase of brain development. IgLONs are known to form dimers through homophilic and heterophilic interactions and through this control neuronal growth and synaptogenesis. IgLONs function predominantly as subunits of heterodimeric proteins (Diglons) (Reed et al., 2004). Thus, the four IgLONs can form six Diglons (LSAMP-OPCML, LSAMP-NTM, NTM-OPCML, NEGR1-OPCML, NEGR1-NTM and NEGR1-LSAMP) (Reed et al., 2004). Ntm mediates bifunctional effects on neurite outgrowth through attractive and repulsive mechanisms, which are cell type specific. IgLONs act synergistically, each forming the context for the work of the other in the regulation of neural circuit formation which manifests both at the level of neuronal morphology and behavior (Singh et al., 2018a, Vanaveski et al., 2017). Polymorphisms in the human IgLON genes have been linked with a variety of psychiatric conditions.

2.2. General characterization of NEGR1 and LSAMP

In mice, NEGR1 is highly expressed in the temporal lobe (Temp), cerebellum, cerebral cortex, and forebrain. Lower NEGR1 expression has been detected in the brainstem and eyes. In addition to the nervous system, NEGR1 is expressed in a number of organs and tissues (e.g., skeletal muscle, adrenal gland, heart, lung, liver, kidney, ovary, testis) (Vanaveski et al., 2017).

Experiments with cell cultures have shown that NEGR1 plays an important role in regulating the neurite outgrowth, branching and number of synapses. Pischedda et al. showed that suppression of NEGR1 expression in cell cultures *in vitro* produces neurons with fewer neurites than controls and the resulting neurites are shorter and less branched than in a normal cell. A similar result was

shown in *in vivo* experiments in mice with reduced numbers of neurites and their outgrowths and reduced length of neurites (Pischedda et al., 2014).

In addition to other IgLON family members NEGR1 also interacts with several other molecules, through these interactions NEGR1 may have an important role in neuronal development. For example, it has been shown that NEGR1 connects ADAM10 and FGFR2 in a pathway that regulates neurite outgrowth in a ERK1/2 dependent manner. NEGR1 acts as a novel ADAM10 substrate involved in neuronal morphogenesis. Soluble NEGR1 stimulates an intracellular signaling cascade, NEGR1 triggers ERK1/2 phosphorylation and modulates neurite outgrowth via activation of FGRF2 (Pischedda et al., 2015). It has been shown that NEGR1 may have the ability to influence neuronal signaling during neuronal development acting both as a membrane bound protein as well as a soluble factor.

LSAMP is expressed in bodies and dendrites of neurons located in the cortical and subcortical regions of the limbic system (Levitt, 1984). Functional studies have shown that LSAMP can promote or inhibit neurite outgrowth and synapse formation, depending on interactions with other members of the IgLON family (Mann et al., 1998; Gil et al., 2002; Hashimoto et al., 2009). Additionally, LSAMP has been identified as a negative regulator of myelination (Sharma et al., 2015).

Lsamp has two alternative promoters 1a and 1b, those two alternative promoters have heterogeneous anatomical distribution in the developing and adult brain. The isoform expression patterns are important for normal brain development. In mice *Lsamp* 1a is expressed in hippocampus (Hip), Temp, amygdala, ventral striatum (VSTR) and in the cingulate and insular cortex. *Lsamp* 1b is expressed in sensory pathways extending from the brainstem and the sensory nuclei of the thalamus to the primary sensory areas of the cerebral cortex. In addition, *Lsamp* 1b is also expressed in regions that form the limbic system and are involved in the regulation of stress and arousal (Philips et al., 2015). In addition to the nervous system, low expression of *Lsamp* 1a and 1b is also present in the urogenital system, and *Lsamp* 1b is also expressed in the heart, skeletal muscle, and small intestine. *Lsamp* expression is also detectable in the liver (Vanaveski et al., 2017).

2.3. Psychiatric disorders

Psychiatric disorders are generally characterized by a combination of abnormal thoughts, perception, emotions, behavior, and relationship with others. Mental disorders include major depressive disorder, bipolar disorder, schizophrenia and other psychoses, dementia, and developmental disorders including autism.

Major depressive disorder (MDD) is a common mental disorder and one of the main causes of disability worldwide. According to the WHO, an estimated 280 million people are affected by depression globally. More women are affected than men. International Statistical Classification of Diseases and Related Health Problems 10th version (ICD-10) defines three typical depressive symptoms (depressed mood, anhedonia, and reduced energy), two of which should be present to

determine the depressive disorder diagnosis. The symptoms of MDD are associated with structural and neurochemical deficits in the corticolimbic brain regions. Presently, MDD is considered a multifactorial disease with various causes and triggers such as genetic susceptibility, stress, and other pathological processes such as inflammation. For example, in some cases, genetic factors can promote or even trigger the occurrence of depression. Some mutations and polymorphisms can affect the response of receptors to neurotransmitters or biologically active substances, which, in turn, could affect the resistance of the brain chemical balance to the stressor (Filatova et al., 2021). It is estimated that only 60–70% of depressed patients are responsive to currently available antidepressant treatments. Around 40% of patients with depression do not adequately respond to antidepressant medication and one-third patients do have remission of their depressive symptoms (Fox et al. 2019). Of those who do not respond, 10–30% exhibit treatment-resistant symptoms. Since a large proportion of patients with depression do not respond to available drugs, it would be necessary to develop new possible drugs for the treatment of depression.

Schizophrenia is a severe neuropsychiatric disorder with complex etiology that affects approximately 1% of the world's population (21 million people out of 7.9 billion) (WHO; Costain et al., 2012). Schizophrenia is more common in men (12 million) than women (9 million) (WHO). Family studies have shown that schizophrenia has high inheritability (80%) (Mäki et al., 2005), and cross-genomic association studies have identified a number of chromosomal loci that may be associated with schizophrenia (Stefansson et al., 2009; Prucell et al., 2009; Yue et al., 2017). Evidence from GWAS studies and protein expression studies, that have shown changes in protein expression in patients with schizophrenia, indicate that most of the pathophysiological processes seen in patients with schizophrenia are associated with neural transmission, synaptic maturation and plasticity, neurite outgrowth and neurogenesis (Hosak et al., 2012; Nascimento et al., 2015; Singh et al., 2018). The symptoms of schizophrenia are usually divided into three categories. Positive symptoms include behavioral signs that occur in patients with schizophrenia but not healthy people. Positive symptoms include hallucinations (most commonly auditory hallucinations), paranoia, and delusions (These et al., 2009). Negative symptoms are behavioral deficits that are not characteristic for healthy individuals. Negative symptoms include loss of interest and joy (apathy, anhedonia) and social withdrawal (Sarkar et al., 2015). The third category is cognitive symptoms. Cognitive symptoms include attention problems, memory problems, difficulty solving problems and processing information, and difficulty making decisions (Need et al., 2009).

2.4. NEGR1 in psychiatric disorders

Several GWAS studies have shown a link between the *NEGR1* gene and depression. Accumulating data from GWAS studies indicate that genomic area in chromosome 1p31.1 around the start ATG of *NEGR1* gene, is one of the most

significant risk loci for MDD (Wray et al. 2018, Hyde et al., 2016). Transcriptome and protein analysis suggest increased expression of NEGR1 in depression patients; an increased level of *NEGR1* has been reported in the brain areas, namely in the dorsolateral prefrontal cortex (DLPFC) (Chang et al., 2014) and in the hypothalamic area (Levey et al., 2021) of patients with MDD in comparison with healthy controls. Additional data from depression patients suggest that the functional impact of NEGR1 might involve systemic regulation as significant upregulation of NEGR1 has been shown in the cerebrospinal fluid (Maccarrone et al., 2013) and peripheral blood of depression patients (Dall'Aglio et al., 2021).

Although the linkage between NEGR1 and depression is strongest, evidence suggests involvement of NEGR1 in a wide spectrum of psychiatric conditions (Cross-Disorder Group, 2019). The levels of NEGR1 protein and transcripts are elevated in the post-mortem prefrontal cortex (PFC) (Cox et al., 2016) and DLPFC (Karis et al., 2018) of schizophrenic patients. NEGR1 has also been shown to be associated with intelligence (Sniekers et al., 2017), dyslexia (Veerappa et al., 2013) and autism spectrum disorders (ASD) (Marshall et al., 2008; Michaelson et al., 2012). A microdeletion in the *NEGR1* gene was described in two siblings that presented cognitive disabilities, attention deficit hyperactivity disorder (ADHD), speech problems and features of ASD in one of them (Genovese et al., 2015).

Homozygous deletion of *Negr1* gene in mice (*Negr1*$^{-/-}$) has been shown to induce no detectable changes in sensory and motor development but is causing impaired social behavior and reversal learning deficits compared to wild-type (WT) littermates (Singh et al., 2018b; Singh et al., 2019). *Negr1*$^{-/-}$ mice displayed also neuroanatomical alterations, such as enlargement of ventricles and decrease in the volume of whole brain, including corpus callosum, Hip, globus-pallidus whereas decreased number of parvalbumin-positive inhibitory interneurons was evident in *Negr1*$^{-/-}$hippocampi (Singh et al., 2019). In alternatively created *Negr1*$^{-/-}$ mice, it has been shown that *Negr1* deficiency results in alterations in adult neurogenesis and hippocampal dentate gyrus (DG) synaptic transmission and leads to anxiety- and depression-like behaviors (Noh et al., 2019). Szczurkowska et al. (2018) showed that downregulation of *Negr1* in mice causes ASD-related developmental and behavioral abnormalities in the brain. They showed that these mice have defective neuronal migration and morphological maturation in the somatosensory cortex which are associated with deficits in core behaviors related to ASD in mice (Szczurkowska et al., 2018). In conclusion accumulating evidence show that *NEGR1* is associated with several psychiatric disorders and that in mice *Negr1* has important role in neuronal development.

2.5. LSAMP in psychiatric disorders

Altered expression of LSAMP protein has been linked with psychopathology; the level of the LSAMP protein is increased in the postmortem DLPFC both in patients with depression and schizophrenia (Behan et al., 2009) and in the synaptosome fraction of the orbitofrontal cortex (Velásquez et al., 2017) in patients with schizophrenia. Furthermore, the level of LSAMP protein is significantly upregulated in the post-mortem anterior PFC of patients with schizophrenia compared to healthy controls (Cox et al., 2016), whereas lower expression of LSAMP transcripts has been shown to be related with concurrent depressive endophenotype in schizophrenic patients (Karis et al., 2018). Polymorphisms in the human *LSAMP* gene in the chromosomal locus 3q13.31 have been shown to be associated with the risk of schizophrenia and MDD both in the European (Koido et al., 2012; Koido et al., 2014) and Chinese populations (Chen et al., 2017). Furthermore, *LSAMP* gene has been associated with suicide susceptibility (Must et al., 2008; Sokolowski et al., 2016).

Homozygous deletion of the *Lsamp* gene in mice (*Lsamp*$^{-/-}$) induced no detectable changes in sensory and motor development but caused increased activity in novel environments and reduced anxiety like behavior in two independently created knockout models (Catania et al., 2008; Innos et al., 2011). Increased anxiety in rats has been shown to be related with increased levels of the *Lsamp* transcripts in the periaqueductal gray (Nelovkov et al., 2003), amygdaloid area (Philips et al., 2015), raphe nuclei, Hip, and frontal cortex (Alttoa et al., 2010). Elevated levels of the *Lsamp* transcript in the amygdaloid area of rats have been associated with increased acute fear reaction (Kõks et al., 2004) and impairments in fear conditioning (Lamprecht et al., 2009). In conclusion, accumulating evidence suggests that increased levels of the *Lsamp* transcript are associated with lower activity, higher levels of anxiety or acute fear reaction, and that the genetic deletion of the *Lsamp* gene in mice results in increased activity in novel environments and reduced anxiety-like behavior (Catania et al., 2008; Innos et al., 2011; Innos et al., 2012).

2.6. IgLONs and monoamines

The monoamine hypothesis of depression states that monoamine neurotransmitter system dysfunction is the cause of the symptoms. Although accumulating evidence also suggests involvement of other pathways, monoamines still play a crucial role in the mood disorders and are the main targets of antidepressant drugs that are currently available (Belujon & Grace, 2017). The expression of NEGR1 has been shown in both dopaminergic and serotonergic nuclei and pathways. NEGR1 is expressed in the whole fasciculus retroflexus, which serves as a molecular scaffold for dopaminergic axons that grow from the midbrain toward the habenula. High *Negr1* expression is also detected in the islands of Calleja which modulate dopamine signaling between the frontal cortex and the Temp, in the

ventral striatopallidal system. These nuclei play a significant role in maintaining normal connectivity of the brain and their alterations are related to the pathophysiology of psychiatric disorders (Singh et al., 2019). The modest signal of NEGR1 and LSAMP was detected in the dorsal raphe serotonergic neurons of macaques (Bethea & Reddy, 2012). In another study, NEGR1 was identified as differentially expressed gene across molecularly defined 5HT neuron subtypes, the expression of NEGR1 was highest in the medial raphe, especially ventral areas of medial raphe (clusters R2 and R3) and less than average in the dorsal raphe (Okaty et al., 2015).

The expression of NEGR1 has been shown to be altered after administration of several antidepressants that target monoaminergic neurotransmission. Chronic treatment with one of the widely used antidepressants, venlafaxine, has been shown to increase *Negr1* expression in the cerebral cortex in rats (Tamási et al., 2014). Carboni et al. 2020, however showed a decrease of *Negr1* transcript in rodent models after administration of two other common antidepressants; after escitalopram in the hypothalamus and fluoxetine in the Hip. Additionally, nortriptyline downregulated *Negr1* in the hippocampal primary neurons. Another study showed increased NEGR1 levels in human cell lines which were treated with clozapine which binds both dopaminergic and serotonergic receptors, suggesting that NEGR1 is a target of antipsychotic drugs as well (Mustard et al., 2021).

Lsamp is involved in the proper establishment of specific neural pathways, such as thalamic, septo- and intrahippocampal circuits (Keller et al., 1989; Pimenta et al., 1995; Mann et al., 1998). These circuits can be paths for specific neurotransmission, for example, Schmidt et al. (2014) showed that *Lsamp* is critical in the fasciculation of dopaminergic afferents from the midbrain to lateral habenula.

Further evidence that *Lsamp* has an impact on specific neurotransmission systems comes from pharmacological studies with *Lsamp*-deficient mice. *Lsamp*-deficient mice displayed increased sensitivity to the sedative effect of benzodiazepines, possibly due to alterations in the balance of the gamma-aminobutyric acid-A ($GABA_A$) receptor subtypes in the brain, and lower sensitivity to the locomotor activating effect of amphetamine. Likewise, in the place preference test, the rewarding effect of amphetamine was absent in $Lsamp^{-/-}$ mice (Innos et al., 2013a). In the same study, the elevated serotonin (5-HT) turnover rate in several brain areas of the *Lsamp*-deficient mice and changes in the baseline levels of 5-HT were detected (Innos et al., 2013a). The cell bodies of serotonergic neurons are located mainly in the raphe nuclei in the brainstem and the axons of these neurons innervate virtually the entire central nervous system, especially parts of the limbic areas. Dorsal and median raphe nuclei are responsible for the projections to and receive innervation from the PFC, amygdala, Hip, and dorsal and VSTR (Dorocic et al., 2014). Modest signal of LSAMP (along with NEGR1) has been detected in laser captured 5-HT neuron preparations from the dorsal raphe nucleus of rhesus monkeys (Bethea and Reddy, 2012). A recent study has identified LSAMP and another IgLON gene Ntm among the genes that are differentially expressed between serotonergic neuron subtypes in the dorsal raphe

(Huang et al., 2019). In addition to monoamine pathways IgLONs can also be associated to other pathways involved in the development of depression. Noh et al. showed that the expression of lipocalin-2 (Lcn 2) was decreased in the Hip of *Negr1*-deficient mice. They also showed that NEGR1 interacts with leukemia inhibitory factor receptor (LIFR) and modulates LIF-induced Lcn2 expression. Lcn2 was originally identified in the secretory granules of neutrophils and can also be induced by other immune cells upon infection or tissue injury. In the brain, Lcn2 expression can be induced in hippocampal neurons, microglia, and astrocytes by various inflammatory stimuli, and thereby it regulates neuroinflammation (Noh et al., 2019).

There are several pathways which may be associated with the development of depression. In this study we focused on the monoamine hypothesis of depression, although, most likely several pathways act together and contribute to the development of depression.

2.7. NEGR1 and body weight phenotype

In addition to psychiatric disorders, NEGR1 is a candidate gene regulating human obesity. In GWAS studies, *NEGR1* gene locus has been repeatedly shown to have strong associations with human BMI indicating a role in body weight regulation and obesity (the GIANT Consortium, 2009; Thorleifsson et al., 2009; Speliotes et al., 2010; Locke et al., 2015; Winkler et al., 2016; Schlauch et al., 2020). Besides SNP markers, it has been found that two deletions (43 kb and 8 kb) upstream of *NEGR1* are strongly associated with early onset of extreme obesity (Wheeler et al., 2013).

Higher levels of NEGR1 in hypothalamic nuclei were linked with lower food intake; administration of NEGR1 ectodomains into the paraventricular nucleus of the hypothalamus induced ~ 20% decrease of food intake in rats (Venkannagari et al., 2020). Kim et al. (2017) have demonstrated that NEGR1 interacts with cholesterol (CHOL) transporter 2 (NPC2), a key player in intracellular CHOL trafficking and increases the stability of NPC2 in the late endosomes. Furthermore, Sandholt et al. (2011) have shown that NEGR1 tag SNP (rs2568958) has significant associations with low density lipoprotein (LDL) cholesterol levels. Bernhard et al. (2012) detected lower *NEGR1* expression in the subcutaneous adipose tissue (SAT) compared with visceral adipose tissue, whereas *NEGR1* expression was lower in the SAT of obese humans compared to lean subjects. Walley et al. (2012) demonstrated that in the human SAT, *NEGR1* appears to be central to the set of functionally related genes most differentially expressed between lean and obese subjects. An et al. (2020) have shown that the level of lipid droplets (LD) was reduced in NEGR1-overexpressing cells whereas the intracellular LD level was higher in primary adipocytes obtained from *Negr1*$^{-/-}$ mice than those from WT mice (An et al., 2020). In addition, the expression level of LD-associated protein perilipin-2/ADRP increased in white adipose tissue of *Negr1*-deficient mice. Evidence from Bernhard et al. (2012) suggests that

NEGR1, which is upregulated during adipogenesis, is important in the adipocytes from early development. They also found that knockdown of NEGR1 significantly inhibited adipocyte maturation.

Data from mouse models with non-functional *Negr1* gene have revealed somewhat conflicting findings. In the study of Lee et al. (2012) both *Negr1*-deficiency and loss-of-function mutation of *Negr1* resulted in a slight but steady decrease in body mass whereas by Joo et al. (2019) found no change in body weight in *Negr1*$^{-/-}$ mice. However, these works agree that lacking or non-functional NEGR1 protein causes alterations in the body composition. Joo et al. (2019) showed a significant increase in fat mass with hypertrophic adipose cells containing enlarged cytosolic lipid droplets in *Negr1*$^{-/-}$ mice compared with the WT mice. Moreover, these mice showed significant hepatic lipid accumulation, decrease in muscle mass and -capacity (Joo et al., 2019).

2.8. Concluding remarks

Several studies have linked IgLON family members *Lsamp* and *Negr1* with various psychiatric disorders. And it has been shown that both genes have associations with monoaminergic systems. The expression of *Negr1* has been shown in both dopaminergic and serotonergic nuclei and pathways and pharmacological studies have shown that *Lsamp* has an impact on specific monoaminergic systems. Despite the high linkage between *Negr1* and depression, the serotonergic and dopaminergic neurotransmission has not been studied until now in *Negr1*-deficient mice. Although relationships between *Lsamp* and monoaminergic systems have been studied in mice before, they need to be further characterized. Prior evidence about *Lsamp* expression in the raphe area comes from gene chip expression data in Wistar rats (Alttoa et al., 2010). First aim of the study was to describe the isoform-specific expression of *Lsamp* transcript in the mid- and hindbrain of the mice with the focus on the raphe nuclei. The second aim of the current study is to explore the brain monoaminergic system in a mouse model deficient in either *Negr1* or *Lsamp* gene/protein for better understanding whether these neural circuits could be responsible for the links between *Negr1* and *Lsamp* polymorphisms and phenotypes of depression. Thirdly, we challenged the monoaminergic neurotransmission of mice lacking *Negr1* or *Lsamp* and their WT littermates with chronic injection of escitalopram. Chronic injections were chosen because in humans the effect of escitalopram appears around two weeks after starting to take the medication. As forth, amphetamine was used to challenge monoaminergic neurotransmission in *Negr1*-deficient mice.

In addition to psychiatric disorders, NEGR1 is a candidate gene regulating human obesity. Shared genetic risk factors between depression and obesity have been reported, which could be mediated through shared etiological pathways. Therefore, the fifth aim of the current study is to clarify the role of NEGR1 in the maintenance of systemic metabolism, including glucose homeostasis, by using both male and female *Negr1*-deficient mice receiving a standard or high-fat diet.

3. AIMS OF THE STUDY

The general aim of the current study was to explore the function on the IgLON nCAMs NEGR1 and LSAMP by using gene deficient mouse models.
More specific aims were following:

1. To describe the isoform-specific expression of *Lsamp* transcripts in the mid- and hindbrain of mice with the focus on the raphe nuclei. (Paper I)
2. To explore the effect of chronic administration of selective 5-HT reuptake inhibitor (SSRI) escitalopram on the behavior and monoamine metabolism of both *Lsamp*- and *Negr1*-deficient mice compared to their WT littermates. (Paper I and II)
3. To assess the effects of *Negr1*-deficiency on the monoaminergic circuitry using chronic (10-days) amphetamine, indirect dopamine agonist. (Paper II)
4. To study the effect of *Negr1* deficiency on the food intake, systemic metabolism, and oxidative stress levels in the brain. (Paper III)

4. MATERIALS AND METHODS

4.1. Animals (Paper I, II and III)

In this study several cohorts of mice were used (Table 1). Male and female WT mice and their homozygous *Negr1*-deficient littermates (*Negr1*$^{-/-}$) used in the study are described previously (Singh et al., 2019). Generation of the mouse line with *Lsamp* deletion has been described previously (Innos et al., 2011), male WT mice and their homozygous *Lsamp*-deficient (*Lsamp*$^{-/-}$) littermates mice were used. For isoform-specific stainings *Lsamp*$^{+/-}$ mice were used. All mice had the genetic background of 129S6/ SvEvTac × C57BL/6 and were F2 hybrids derived from heterozygous F1 intercrosses. Mice were group-housed in standard laboratory cages measuring 42.5 (L) × 26.6 (W) × 15.5 (H) cm, 10 animals per cage in the animal colony at 22 ± 1 °C, under a 12:12 h light/dark cycle (lights off at 19:00 h). A 2 cm layer of aspen bedding (Tapvei, Estonia) and 0.5 l of aspen nesting material (Tapvei, Estonia) were used in each cage and changed every week. Water and food pellets (R70, Lactamin AB, Sweden) were available *ad libitum*. Breeding and the maintenance of the mice were performed at the animal facility of the Institute of Biomedicine and Translational Medicine, University of Tartu, Estonia. The use of mice was conducted in accordance with the regulations and guidelines approved by the Laboratory Animal Center at the Institute of Biomedicine and Translational Medicine, University of Tartu, Estonia. All animal procedures were conducted in accordance with the European Communities Directive (2010/63/EU) with permit No 150 (September 27, 2019; experiments with *Negr1*$^{-/-}$ mice) and permit No. 29 (April 28, 2014; experiments with *Lsamp*$^{-/-}$ mice) from the Estonian National Board of Animal Experiments.

Table 1. Cohorts of the mice used in the experiments.

Cohort I	*Lsamp* $^{+/+}$ and $^{-/-}$	Male	n = 6–14	3 months old in the end of experiment, chronic escitalopram experiment
Cohort II	*Negr1* $^{+/+}$ and $^{-/-}$	Male	n = 13–15	3 months old in the end of experiment, chronic escitalopram experiment
Cohort III	*Negr1* $^{+/+}$ and $^{-/-}$	Male	n = 10	5 months old in the end of experiment, amphetamine dose response curve experiment
Cohort IV	*Negr1* $^{+/+}$ and $^{-/-}$	Male	n = 10	5 months old in the end of experiment, chronic amphetamine experiment
Cohort V	*Lsamp* $^{+/+}$ and $^{-/-}$	Male	n = 8 (qPCR) n = 3 (*in situ*)	4 months old, group housed in home cages, qPCR and *in situ* stainings

Cohort VI	*Negr1* $^{+/+}$ and $^{-/-}$	Male	n = 10–11 (qPCR) n = 5 (immuno-histochemistry)	4 months old, group housed in home cages, qPCR and immunohistochemical stainings
Cohort VII	*Negr1* $^{+/+}$ and $^{-/-}$	Male and female	n = 12	5 months old, metabolomics experiment
Cohort VIII	*Negr1* $^{+/+}$ and $^{-/-}$	Male and female	n = 10	4 months old, glucose tolerance test (GTT)
Cohort IX	*Negr1* $^{+/+}$ and $^{-/-}$	Male and female	n = 10	3 months old, food preference test
Cohort X	*Negr1* $^{+/+}$ and $^{-/-}$	Male	n = 10	3 months old, western blot analysis to assess oxidative stress

4.2. *Lsamp* isoform-specific stainings in brain slices (Paper I)

Non-radioactive in situ RNA hybridization analysis with digoxigenin-UTP and X-Gal staining for detecting the distribution of *Lsamp* 1b promoter activity was performed as described earlier (Philips et al., 2015). Briefly, cDNA fragments specific for 1a promoter (400 bp) consisted of 1a-specific 5′UTR, exon 1a and exon 1a′. Universal *Lsamp* probe (567 bp) contained cDNA fragments consisting of *Lsamp* exons 2–6. For X-Gal staining, the brains of the mice with *Lsamp*$^{-/+}$ genotype were used with heterozygous in-frame NLSLacZNeo cassette resulting in insertion of gene encoding beta-galactosidase immediately after *Lsamp* 1b promoter.

4.3. qRT-PCR analysis in mouse brain areas (Papers I, II)

Gene expression was determined by two-step RT-qPCR (qPCR). Total RNA was extracted from each tissue sample by using Trizol reagent (Invitrogen) according to the manufacturer's protocol.

4.3.1. qRT-PCR analysis by using Taqman assays (Paper I)

First strand cDNA was synthesized by using Random Hexamer (Applied Biosystems) and SuperScript^{TM} IV Reverse Transcriptase (Invitrogen) according to the manufacturer's protocol. Predesigned Taqman Gene Expression Assays (Applied Biosystems) were used for the measurement of the expression of monoamine

oxidase A (*MaoA*; assay number: Mm00558004_m1), monoamine oxidase B (*MaoB*, Mm00555412_m1) and 5-HT transporter (*Slc6a4*, Mm00439391_m1). The same assays have been previously used also by Hansson et al. (2014). TaqMan Universal PCR Master Mix was used according to the manufacturer's protocol as a reaction buffer. Two micrograms of RNA were used in a 20µl end-reaction for cDNA synthesis from brain tissues. Each reaction mix was divided into 10µl quadruplicates.

ABI Prism 7900HT Sequence Detection System with ABI Prism 7900 SDS 2.4.2 software (Applied Biosystems) was used for qPCR detection. qPCR data has been presented on linear scale, in form of $2^{-\Delta\Delta CT}$ (Livak and Schmittgen, 2001) where ΔCT is the difference in cycle threshold (CT) between the gene of interest (FAM) and the housekeeper gene (VIC).

4.3.2. qRT-PCR analysis by using Sybr green assay (Paper II)

First strand cDNA was synthesized by using FIREScript RT cDNA Synthesis MIX with Oligo (dT) and Random primers (Solis BioDyne, Tartu, Estonia) according to the manufacturer's protocol. In qPCR 8 dopamine related genes were studied, tyrosine hydroxylase (*Th*), dopamine receptor 1 (*Drd1*), dopamine receptor 2 (*Drd2*), dopamine receptor 5 (*Drd5*), dopamine transporter (*Dat*), catechol-O-methyltransferase (*Comt*), monoamine oxidase A (*MaoA*) and monoamine oxidase B (*MaoB*). Dopamine system-related primers used in the experiment have been previously described in Varul et al. 2021. As a housekeeper gene beta-actin (ActB_mm_F ACCATGTACCCAGGCATTGC, ActB_mm_R AGC CACCGATCCACACAGAG) was used. Every reaction was made in four parallel samples to minimize possible errors. All reactions were performed in a final volume of 10 µL, using 5 ng of cDNA. Real-time qPCR was performed using 5× HOT FIREPol® EvaGreen® qPCR Supermix (Solis BioDyne, Tartu, Estonia).

4.4. Escitalopram treatment (Papers I, II)

All mice were age-matched with littermates and were tested at 3–4 months of age. *Lsamp*$^{-/-}$ (cohort I), *Negr1*$^{-/-}$ (cohort II) (Figure 1) and WT mice were randomly divided into groups that received an intraperitoneal (i.p.) injection of either saline or 10 mg/kg of escitalopram at a volume of 10 ml/kg. In the experiment with *Lsamp*$^{-/-}$ mice escitalopram was administered for 18 consecutive days and in the experiment with *Negr1*$^{-/-}$ mice for 23 consecutive days. The number of mice per group in the *Lsamp*$^{-/-}$ experiment was: 10 mice in the *Lsamp*$^{-/-}$ escitalopram group and 10 mice in WT escitalopram group. There were fourteen animals in the WT-saline group altogether but only 10 mice of these were tested in all experiments, an exception was the open field test in which all 14 mice were included. *Lsamp*$^{-/-}$ saline group consisted of 10 animals but only 9 mice of these were tested in all experiments, an exception was the open field test, where all 10 mice were included. The number of mice per group was: 13 mice in *Negr1*$^{-/-}$

escitalopram group and 15 mice in WT escitalopram group, in saline groups there were 13 mice in both WT and *Negr1*$^{-/-}$ groups. Escitalopram (Sigma-Aldrich, USA) was freshly prepared in a sterile pyrogen free 0.9% solution of sodium chloride. Body weight of *Negr1*$^{-/-}$ was measured weekly for 8 weeks before administration of escitalopram and on days 1, 3, 5, 7, 9, 11, 13, 15, 17, 19 and 21 during the period of injections.

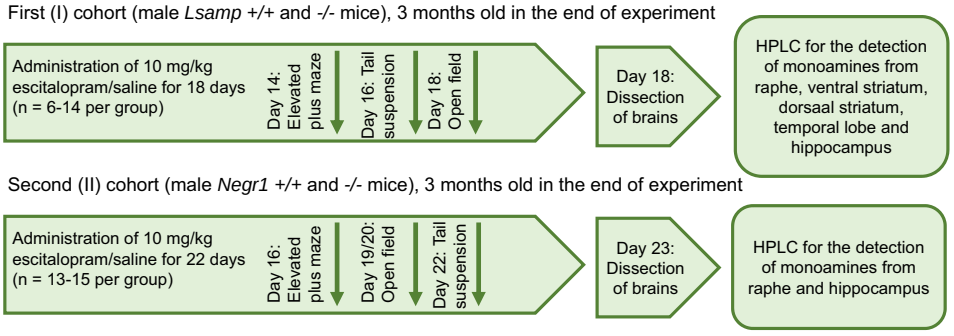

Figure 1. Schematic overview of the cohorts of escitalopram treatment mice and tests/measurements performed in the current study. Cohort I and II was used for the estimation of the treatment of chronic escitalopram.

4.5. Dose-response and chronic amphetamine treatment (Paper II)

For the estimation of acute and chronic effects of amphetamine two subgroups of 5 months old mice were used: cohort III for the estimation of dose curve and cohort IV for the chronic amphetamine administration (Figure 2). All *Negr1*-deficient mice and their age-matched WT littermates were randomly assigned to groups (n = 10 per group). We used the D-isomer of amphetamine (d-amphetamine) because L-amphetamine is a weaker agonist of the dopamine system (Taylor et al., 1970). In the acute administration group (III), mice received a single injection of d-amphetamine in two different dosages: 3 mg/kg and 6 mg/kg, or saline. In the chronic amphetamine experiment (cohort IV), all mice were tested in the open field test (I testing) two weeks prior to the amphetamine injections in order to detect their baseline motor/exploratory activity. Thereafter, they received an i.p. injection of saline or 3 mg/kg amphetamine for 10 days followed by a daily open field test 30 min after injection. D-amphetamine (Sigma-Aldrich, St. Louis, MO, USA) was freshly prepared in a sterile pyrogen free 0.9% solution of sodium chloride (B. Braun Melsungen AG, Germany). Amphetamine was injected intraperitoneally at a volume of 10 ml/kg 30 min before testing. The results of the chronic amphetamine experiment were analyzed daily as we considered raising the dosage of amphetamine, if necessary, but 3mg/kg ended up having a sufficient effect.

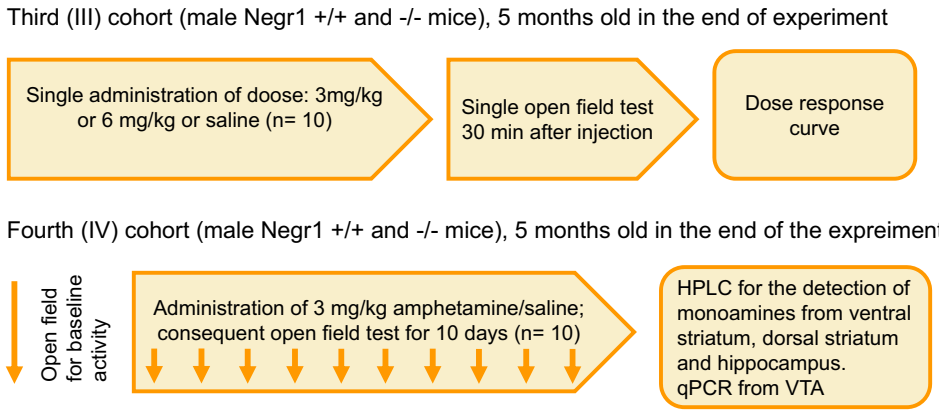

Figure 2. Schematic overview of the cohorts of amphetamine experiment mice and tests/measurements performed in the current study. Small arrows indicate the timing of behavioral tests in the schematic timeline. Cohort III mice were used for the estimation of dose response curve and cohort IV for the chronic amphetamine administration. Open field test for baseline activity of cohort IV mice was performed 7 days before administration of amphetamine.

4.6. Behavioral testing

In the experiment with *Lsamp*$^{-/-}$ mice, behavioral tests were performed on day 14 (elevated plus maze), day 16 (tail suspension test) and day 18 (open field test). In the experiment with *Negr1*$^{-/-}$ mice, behavioral changes were evaluated in the elevated plus maze (day 16), open field test (half of the mice on day 19 and other half of the mice on day 20), and tail suspension (day 22) tests.

4.6.1. Elevated plus maze (Paper I, II)

The elevated plus maze apparatus consisted of two opposite open (17.5 × 5 cm) arms without sidewalls and two enclosed arms of the same size with 14 cm high sidewalls and an end wall. The apparatus was elevated to a height of 30 cm and placed in a room with the light intensity of 100 lx in open arms. Testing began by placing the animal on the central platform of the maze facing an open arm. After each mouse the floor of the testing apparatus was cleaned with 70% ethanol and dried thoroughly. Standard 5 min test duration was employed, and all the sessions were video recorded. An arm entry was counted only when all four limbs were within a given arm.

4.6.2. Open field test (Paper I, II)

Locomotor activity of individual mice was measured with the illumination level of 450 lx for 30 min in soundproof photoelectric motility boxes (44.8 × 44.8 × 45 cm) connected to a computer (TSE, Technical & Scientific Equipment GmbH, Germany). The floor of the testing apparatus was cleaned with 70% ethanol and dried thoroughly after each mouse. The system automatically registered the movement of the animal.

4.6.3. Tail Suspension Test (Paper I, II)

Mice were suspended for 6 min from the edge of a shelf 60 cm above a tabletop by adhesive tape, placed approximately 1 cm from the tip of the tail. The duration of immobility, the number of immobility episodes (an episode defined as hanging passively and being motionless for at least 3 s), and the number of short immobility episodes lasting 1–2 s were scored during the last 4 min from the recorded videos by an observer blind to the genotype.

4.7. Measurement of monoamines (Paper I, II)

Monoamines – serotonin (5-HT), noradrenaline (NA) and dopamine (DA) – and their metabolites – normetanephrine (NMN), 3,4-dihydroxyphenylacetic acid (DOPAC), homovanillic acid (HVA), 5-hydroxyindoleacetic acid (5-HIAA), and 3-methoxytyramine (3-MT) – were assayed by high performance liquid chromatography (HPLC) with electrochemical detection. Monoamine and their metabolites were measured from VSTR and dorsal striatum (DSTR) tissues of *Negr1*$^{-/-}$ chronic amphetamine experiment mice and from VSTR, DSTR, raphe, Temp, and Hip of *Lsamp*$^{-/-}$ escitalopram experiment mice.

Monoamine quantification in raphe nuclei and Hip were done by liquid chromatography mass spectrometry. Briefly, the samples were weighed and transferred into 50 µl PBS. Fifty µl internal standard [$^{2}H_3$]leucine, [$^{13}C_6$]tyrosine, [$^{2}H_5$]phenylalanine (Cambridge Isotope Laboratories, Tewksbury, MA, USA) and 0.9–2.0 mm stainless steel beads (Next Advance, Troy, NY, USA) were added. Homogenization was achieved within 2 min in bullet blender (Next Advance). Thereafter 400 µl ice-cold methanol (resulting the final concentration of 80% methanol) was added and the samples were let stand at –20 °C for 20 min. After centrifugation 10 min at 21,000 ×g two 200 µl aliquots were taken from supernatant and dried under a stream of nitrogen. First aliquot was treated with 50 µl phenylisothiocyanate in water and pyridine (v/v/v 50/320/635) for 40 min at 40 °C. The second aliquot was treated with 100 µl 200 mM 2-nitrophenylhydrazine and 20 µl 120 mM 1(3-dimethylaminopropyl)-N-ethylcarbodiimide for 1 h at room temperature. After subsequent drying under nitrogen the samples were resolved in 100 µl 5 mM ammonium acetate in methanol. Ten µl was injected into Acquity Premier 1.7 µm CSH Phenyl-Hexyl 2.1 × 100 mm column

in Waters Acquity UPLC H-class – Xevo TQ-XS mass spectrometer (Waters, Milford MA, USA). Gradient was composed of solvent A: H_2O with 0.2% formic acid and solvent B: acetonitrile with 0.2% formic acid. Starting from 85% solvent A for 0.5 min the gradient rose to 50% B in 1 min and to 90% B in next 0.5 min. Total run time was 4.5 min with flow rate 0.5 ml/min. The phenylisothiocyanate derivatives were analyzed in positive ionization multiple reaction monitoring mode with the following quantification ion pairs: 5-HT 312/160, NA 287/135, DA 289/137, NMN 301/166, 5-HIAA 192/146 and 3-MT 303/94. Nitrophenyl-hydrazine derivatives were quantified in negative ionization mode with the following ion pair signals: DOPAC 302/137, HVA 316/146.

4.8. Immunohistochemistry (Paper II)

Fluorescent immunohistochemistry was performed on floating 30 µm thick coronal sections collected after every 300 µm into phosphate buffered saline (PBS). Incubations were performed with gentle rocking and at room temperature unless mentioned otherwise. After washing with PBS for 10 min, sections were permeabilized with 0.25% Triton X-100 (Naxo, Tartu, Estonia)/PBS solution for 45 min. Sections were subsequently blocked in solution containing 0.3M glycine/5% donkey serum//1% bovine serum albumin (BSA, Sigma-Aldrich)/PBS for 2 h at room temperature and incubated with rat anti-dopamine transporter/DAT (1:100) (sc-32258, Santa Cruz Biotechnology) dilutions in 0.1% Tween-20/1% BSA/PBS 72 hours at 4 °C. Subsequently sections were then washed with 5 times 0.1% Tween-20//PBS for 10 min and incubated with the appropriate secondary antibody donkey anti-rat antibody (1:1000) (712-607-003, Jackson ImmunoResearch Labs) at room temperature for 2 h. After subsequent washes with PBS 3 times 10 min nuclei were stained with 5 µg/ml Bisbenzimide H 33258 (Hoechst 33258, Sigma Aldrich) in PBS for 2 min. Subsequently sections were rinsed with PBS for 5 min, mounted in Fluoromount mounting medium (Sigma Aldrich), and covered with a 0.17-mm coverslip (Deltalab). Specificity of the immunohistochemistry was determined by incubations without the primary antibodies. Fluorescent images were obtained with the Olympus FV1200MPE (Olympus, Hamburg, Germany) laser scanning confocal microscope and Leica Aperio VERSA Brightfield, Fluorescence & FISH Digital Scanner using 10x air objective.

Fluorescent intensity of DAT immunostaining in the striatum was quantified using the Positive pixel count 2004-08-11 algorithm of Aperio Image Scope [v12.4.3.5008]. The image of striatal surface was divided into DSTR containing caudate-putamen and VSTR consisting of nucleus accumbens and olfactory tubercle, according to the Scalable Brain Atlas (Bakker et al. 2015). Isosurface was created separately from both the parts of the striatum and was used to make quantitative measurements on area and surface fluorescent intensity.

4.9. Diet composition (Paper III)

High fat (HF) chow [DIO-45 kJ% fat (lard)] (Ssniff Spezialiäten GmbH) corresponds to the D12451 diet from Research Diets from and its physiological energetic value was 4.615 kcal/kg. It contained 45 kJ% fat, 20 kJ% proteins and 35 kJ% carbohydrates. This diet is characterized by high fat content (lard) and high sucrose levels. It is used to induce obesity and metabolic syndrome/diabetes in rats and mice.

The caloric value of regular chow (V1534-000 Rat/mice universal maintenance diet, autoclavable (10mm) from Ssniff Spezialiäten GmbH) was 3.225 kcal/kg. It contains 9 kJ% fat, 24 kJ% proteins and 67 kJ% carbohydrates. This diet is suitable for long term experiments.

4.10. HF diet (Paper III)

Chronic HF diet experiment was performed with two different cohorts of mice (Figure 3). For the cohort VII of mice 19 (± 1) weeks old WT and *Negr1*$^{-/-}$ male and female mice were divided into two groups, one group received regular food and another group received HF diet (12 male and 12 female WT mice + 12 male and 12 females *Negr1*$^{-/-}$ mice). Mice in the cohort VII received the HF diet for 7 weeks. All the mice were weighed weekly, starting from 10 weeks before the beginning of the HF diet (at the age of 10± 1 weeks), altogether the body weight dynamics of the mice was tracked for 16 weeks. In the cohort VIII of mice 15 (± 1) weeks old WT and *Negr1*$^{-/-}$ male and female mice were divided into two groups, one group received regular food and another group the HF diet (10 male and 10 female WT mice + 10 male and 10 females *Negr1*$^{-/-}$ mice). In the cohort VIII, all mice received the HF diet for 6 weeks. As female mice showed no genotype effect in the glucose tolerance test, females received the HF diet for another 7 weeks (total 13 weeks for females). In the cohort IX of mice, the food consumed was also weighed to evaluate their food consumption. At the end of both experimental periods, brain tissue, liver, and plasma were collected from all mice.

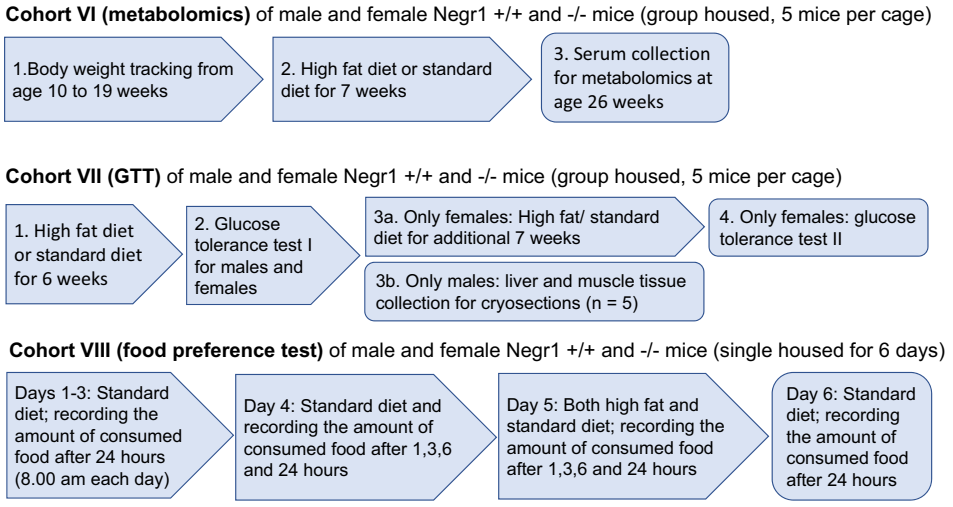

Figure 3. **Schematic overview of the cohorts of mice and tests conducted in the high-fat diet study.** Cohort VII mice were used for metabolomic analyses of high-fat diet and standard diet mice. Cohort VIII mice were used for GTT. Cohort IX mice were used for a food preference test.

4.11. Food preference test (cohort IX) (Paper III)

The food preference was performed with minor modifications as described earlier in Leidmaa et al. All the mice were housed in single cages and on days 1–3, mice received regular food. Both food and mice were weighed every morning at the same time (8.00 am). In the morning of the 4th day, the mice and food were weighed, and the food was further weighed at specific timepoints (1h, 3h, 6h and 24 h) throughout the day. On the 24h time-point the next morning (5th day) mice were weighed, and the HF food was added for the food preference experiment. Both regular food and HF food were weighed at the same time points (1h, 3h, 6h and 24h) as the previous day. On the 24 h weighing (6th day) mice were weighed again, and HF food was removed, only regular food was retained. On the 7th day, the food was weighed for the last time to see if *Negr1*$^{-/-}$ mice showed any withdrawal effects.

4.12. Measurement of metabolites (Paper III)

AbsoluteIDQ™ p180 kit (BIOCRATES Life Sciences AG, Innsbruck, Austria) was used to determine plasma levels of metabolites according to the manufacturer's protocol. Amino acids and biogenic amines in the samples were measured using the liquid chromatography – mass spectrometry techniques. Acylcarnitines (Cx:y), hexoses, sphingolipids [SMx:y or SM (OH)x:y], glycerophospholipids [lysophosphatidylcholines (lysoPCx:y), and phosphatidylcholines (PCaa x:y and PC ae x:y)] were measured using flow injection mass spectrometry.

For both modes of analyzing, multiple reaction monitoring was used. Concentrations of the metabolites were calculated automatically by the MetIDQ™-software (BIOCRATES Life Sciences AG) in µM. The analytical system was QTRAP 4500 (Sciex, Framingham, MA, USA) in combination with Agilent 1260 series HPLC (Agilent Technologies, Waldbronn, Germany).

Citric acid cycle intermediates were analyzed on the same instrument with an in-house protocol. Fifty µl serum was treated with 20 µl 100 µM [2H4] succinate (internal standard) and 750 µl ice-cold methanol for 10 min for protein precipitation. After centrifugation 10 min at 21 000 × g the supernatant was dried under a stream of nitrogen and dissolved in 100 µl of methanol with 0.2% formic acid. The multiple reaction monitoring transitions in negative ionization mode were as follows: malate 133/115, succinate 117/73, citrate 191/87, pyruvate 87/43, alpha-ketoglutarate 145/101, lactate 89/43, oxaloacetate 131/87, beta-hydroxybutyrate 103/59 and the internal standard 121/77.

4.13. GTT, cohort VIII (Paper III)

Animals were deprived of food for 3 h before and during the experiment; water was available throughout the experiment. After measuring the basal glucose levels, the mice were intraperitoneally administered a glucose (Sigma-Aldrich) solution in 0.9% saline (20% w/vol) at a dose of 2 g/kg of body weight. Blood glucose values were subsequently measured after 30, 60, 90, 120 and 180 min from the tail vein using a hand-held glucometer (Accu-Check Go, Roche, Mannheim, Germany). The bioavailability of glucose was estimated by calculating the under the curve area (AUC) of plasma concentration at measured time points. For males, GTT was performed on the 6th week and for females on 6th and on the 13th week of a HF diet.

4.14. Sample collection (Paper I, II, III)

All mice tissues used in this dissertation were collected in the same manner. Mice were euthanized by decapitation, and trunk blood was collected into EDTA-coated microcentrifuge tubes and stored on 4 °C. All the tubes were centrifuged at 2,000 g for 15 min at 4 °C. Plasma supernatant was separated and stored at −80 °C until further analysis. Different brain regions were dissected from the brain and frozen in liquid nitrogen, brain tissues were stored at –80 °C.

4.15. Western blot

Western blot analyses were performed according to general protocol of western blotting (Bio-Rad). Primary antibodies used: rabbit anti-NOX2/gp91phox antibody (1µg/ml) (ab 80508, Abcam), rabbit anti-NOX1 antibody (0.1 µg/ml) (ab131088, Abcam), mouse anti-Glutathione antibody (1:1,000) (ab19534,

Abcam), rabbit anti-Superoxide Dismutase 1 antibody (ab51254, Abcam). Secondary antibodies used: goat anti-rabbit antibody (1:40,000) (35569, Jackson ImmunoResearch) and goat anti-mouse antibody (1:5,000) (A21057, Invitrogen), goat anti-rabbit HRP antibody (1:3,000) (ab205718, Abcam). The values were then normalized to control protein. Optical densities of the bands were measured using ImageJ software and normalized with β-actin.

4.16. Statistical Analysis (Paper I, II, III)

All results are expressed as mean values ± SEM, all differences were considered statistically significant at $p < 0.05$. For analyzing gene expression data, non-parametric tests were applied, because not all of the gene expression data sets were normally distributed according to the Shapiro Wilk's normality test. Statistical analyses for metabolomic data, body weight, GTT and food preference test were performed using GraphPad Prism 6 software. Normal distribution of data was evaluated by the Shapiro-Wilk test. Comparison of metabolomic data between groups was performed using two-way ANOVA (diet × genotype) followed by a Bonferroni *post hoc* test. Comparison of GTT data between groups was performed using two-way ANOVA followed by a Tukey *post hoc* test. Statistical analysis of the food preference test and cross-sectional area of muscle fibers was performed by using Mann-Whitney U test.

Statistica 13 software was used for statistical analysis of experiments with *Lsamp*$^{-/-}$ mice. Shapiro-Wilks test was used to test for normal distribution of the data. For the behavioral experiments, two-way ANOVA for independent groups was used (genotype × treatment). Repeated measures ANOVA was used to analyze body weight changes. Comparisons between individual groups were performed by means of Tukey HSD post hoc test. p-Value below 0.05 was considered significant. Wilcoxon-Mann-Whitney test was used for comparisons of gene expression levels between *Lsamp*-deficient mice and WT littermates.

In the chronic amphetamine experiment normal distribution of data was evaluated with the Shapiro-Wilk test. Results from qPCR and other data comparing two groups were assessed using Student's t-test or Mann–Whitney test for nonparametric data. Comparison of RT-qPCR data from chronic amphetamine experiment in the ventral tegmental area (VTA), of the behavioral results from the escitalopram experiment, levels of monoamines and their metabolites, and body weight differences was performed using two-way ANOVA followed by a Bonferroni *post hoc* test. The body weight dynamics from day –10 to day –3 were analyzed using repeated measures two-way ANOVA (time × genotype) followed by Bonferroni *post hoc* test. Behavioral data from the chronic amphetamine experiment was analyzed by repeated measures three-way ANOVA followed by a Tukey's *post hoc* test. All differences were considered statistically significant at $p < 0.05$. Statistical analysis was performed using GraphPad Prism 8 software.

5. RESULTS

5.1. Expression and impact of LSAMP neural adhesion molecule in the serotonergic neurotransmission system (Paper I)

5.1.1. *Lsamp* transcripts are expressed in the dorsal, median, and caudal raphe nuclei

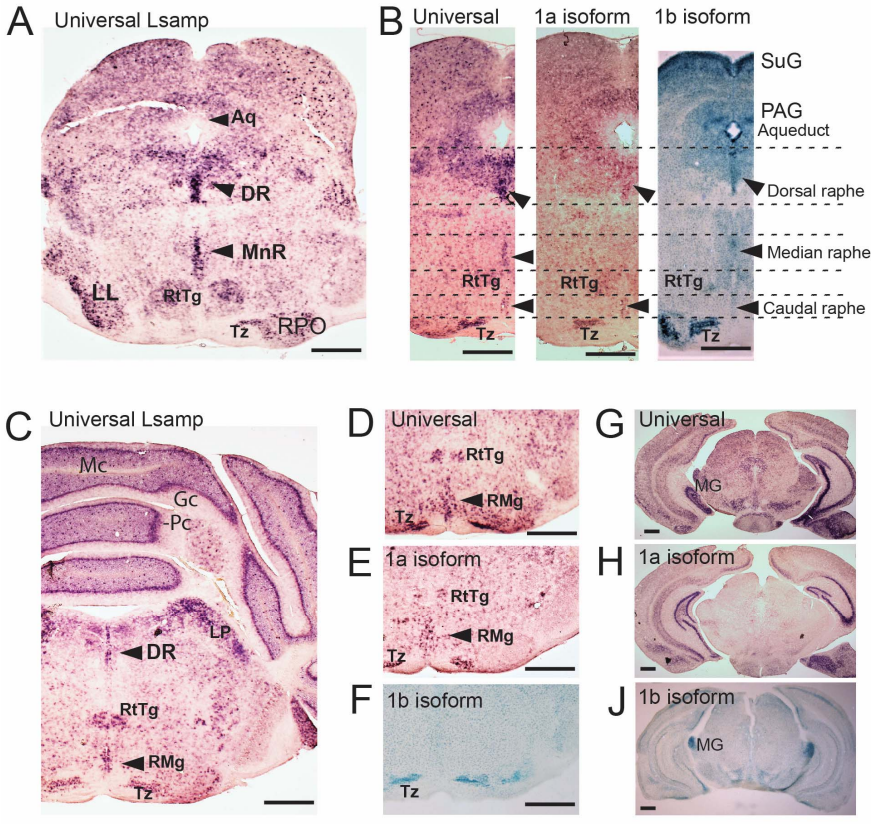

Figure 4. Isoform-specific stainings of *Lsamp* transcripts in the mid- and hindbrain of mice. In situ staining with a probe specific for the universal *Lsamp* transcript (A, B in the left, C, D, G). In situ staining with a *Lsamp*1a-specific probe (B in the middle, E, H). *Lsamp* 1b-specific X-gal staining (B in the right, F, J). Stainings from more rostral sections validating the specificity of the stainings (G, H, J). Abbreviations according to the atlas of Franklin and Paxinos (1997): Aq (aqueduct), DR (dorsal raphe nuclei) Gc/Mc/Pc (granule/molecular/Purkinje cell layer of the cerebellum), LL (nuclei of lateral lemniscus), LP (lateral posterior thalamic nucleus), MG (medial geniculate nucleus), MnR (median raphe nuclei), PAG (periaqueductal gray), RPO (rostral periolivary region), RtTg (reticular tegmental nucleus of the pons), SuG (superficial gray layer of the superior colliculus), Tz (trapezoid body). Scale bars: 500 μm.

Lsamp transcripts are expressed in both the dorsal raphe (DR) and median raphe (MnR) nuclei, whereas the signal is slightly more intensive in the dorsal raphe (Figure 4A). From the isoform specific stainings we could conclude that both *Lsamp* 1a and 1b promoters are active in the DR (Figure 4B); most of the expression in MnR comes from 1b promoter, whereas most of the *Lsamp* expression in the caudal subgroup of raphe, such as raphe magnus (RMg) derives from 1a promoter (Figure 4B, C, D, E). Universal and isoform-specific stainings from more rostral sections validate the specificity of the stainings (Figure 4G, H, J).

5.2. Chronic administration of escitalopram has impact to the behavior *of Lsamp*$^{-/-}$ mice and *Lsamp*$^{-/-}$ mice has lower baseline bodyweight

The body weight of saline-injected *Lsamp*$^{-/-}$ mice was significantly reduced compared to their wild-type littermates (main genotype effect $F = 7.675$; $p = 0.013$; Figure 5, left). There was also a significant time effect (main time effect $F = 18.095$, $p < 0.0001$), but no interaction (time × genotype $F = 1.166$; $p = 0.216$). Under escitalopram treatment, no significant differences could be observed between the body weights of Lsamp$^{-/-}$ and Lsamp$^{+/+}$ mice (main genotype effect $F = 0.109$; $p = 0.745$; Figure 5, right). There was a significant time effect (main time effect $F = 330.157$, $p < 0.0001$), but no interaction (time × genotype $F = 1.765$; $p = 0.185$).

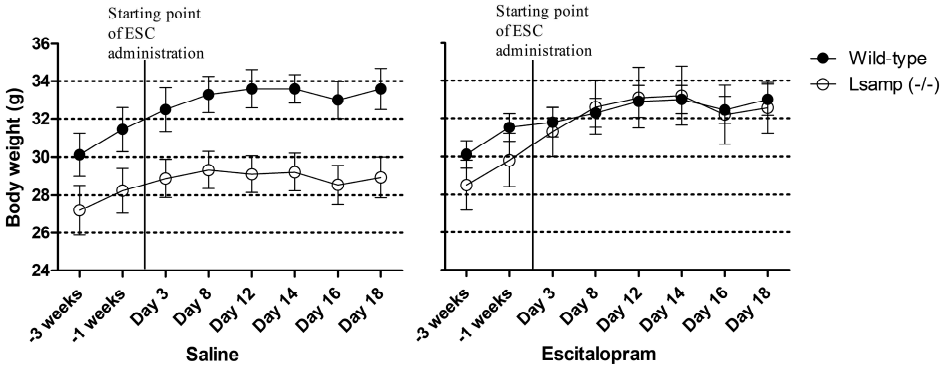

Figure 5. Body weight changes. The body weight was initially measured three weeks before the first administration of escitalopram, the behavioral tests were performed on Day 14 (elevated plus maze), Day 16 (tail suspension test) and Day 18 (open field test). After the last test, the mice were immediately decapitated, and the brains dissected for the measurement of monoamines and their metabolites. The number of mice was nine in the *Lsamp*$^{-/-}$ saline group, n = 10 in all other groups. Error bars represent ± SEM; ESC – escitalopram, g – gram, SEM – standard error of the mean.

To study the effects of chronic escitalopram treatment on anxiety like behaviors, we tested mice in the elevated plus maze. The number of closed arm entries, reflecting locomotor activity, was heavily dependent on genotype ($F_{1,35} = 49.8$; $p < 0.00001$), treatment ($F_{1,35} = 17.5$; $p < 0.001$) and genotype × treatment interaction ($F_{1,35} = 14.6$; $p < 0.001$). Post hoc comparison with Tukey HSD test revealed that in *Lsamp*$^{-/-}$ mice, escitalopram administration significantly increased the number of closed arm entries ($p < 0.001$) both compared to *Lsamp*$^{-/-}$ mice receiving saline and to *Lsamp*$^{+/+}$ mice receiving escitalopram (Figure 6A). Open arm entries, which reflect a low level of anxiety, were dependent on genotype ($F_{1,35} = 7.5$; $p = 0.01$) (Figure 6B). For protected head dips, a significant genotype main effect ($F_{1,35} = 5.7$; $p = 0.023$) was established (Figure 6C). Unprotected head dips were dependent on genotype ($F_{1,35} = 6.1$; $p = 0.018$) (Figure 6D). The latency to enter an open arm was also dependent on genotype ($F_{1,35} = 10.1$; $p = 0.003$). Similarly, time spent on open arms depended on genotype ($F_{1,35} = 4.5$; $p = 0.040$). The percentage of time that mice spent on the open arms was tendentially higher in *Lsamp*$^{-/-}$ mice ($F_{1,34} = 3.9983$; $p = 0.053$).

To assess the locomotor activity and anxiety-like phenotype of the mice, we conducted the open field test. Distance travelled during the 30 min of testing, reflecting locomotor activity, was not dependent on genotype ($F_{1,40} = 0.59$; $p = 0.450$), treatment ($F_{1,40} = 1.19$; $p = 0.280$) or their interaction ($F_{1,40} = 0.08$; $p = 0.780$) (Figure 6E). Time spent in the central square, reflecting anxiety levels, was also not dependent on genotype ($F_{1,40} = 0.037$; $p = 0.850$), treatment ($F_{1,40} = 0.78$; $p = 0.380$) or their interaction ($F_{1,40} = 1.68$; $p = 0.200$). Similarly, for distance travelled in the central square, no significant main effects of genotype ($F_{1,40} = 0.024$; $p = 0.880$), treatment ($F_{1,40} = 1.68$; $p = 0.200$) or their interaction ($F_{1,40} = 0.057$; $p = 0.810$) were established. For distance covered in corners, which is another parameter of locomotor activity, a statistically significant genotype effect ($F_{1,40} = 5.24$; $p = 0.028$) was evident, caused mainly by higher ambulation in the corners in the *Lsamp*$^{-/-}$ group receiving saline; however, distance in the corners was not dependent on treatment ($F_{1,40} = 0.78$; $p = 0.38$) or genotype × treatment interaction ($F_{1,40} = 1.29$; $p = 0.260$). As differences in anxiety-like behavior are often most pronounced early in novel environment, we separately analyzed the first 5 min of the open field behavior. The distance travelled during the first 5 min of testing was affected by treatment as escitalopram-treated mice covered longer distances ($F_{1,40} = 11.1968$; $p = 0.001$) (Figure 6F). This difference was caused by WT mice (post hoc $p = 0.001$). The distance travelled during the first 5 min was not dependent on genotype ($F_{1,40} = 0.6563$; $p = 0.420$) or genotype × treatment interaction ($F_{1,40} = 2.559$; $p = 0.120$). Time spent in the central square during the first 5 min was not dependent on genotype ($F_{1,40} = 2.383$; $p = 0.130$), treatment ($F_{1,40} = 0.664$; $p = 0.420$) or their interaction ($F_{1,40} = 0.390$; $p = 0.540$). However, distance travelled in the central square during the first 5 min was affected by treatment as escitalopram treated mice covered longer distances ($F_{1,40} = 8.387$; $p = 0.006$) (Figure 6G); post hoc comparison did not indicate significant differences in *Lsamp*$^{-/-}$ or WT mice separately. There was no main effect of genotype ($F_{1,40} = 2.1657$; $p = 0.15$) nor genotype × treatment interaction

($F_{1,40} = 0.1281$; $p = 0.720$) in distance travelled in the central square during the first 5 min. Corner visits during the first 5 min were affected by genotype, as *Lsamp*$^{-/-}$ mice showed higher number of visits; the difference originated from saline-treated mice (post hoc $p = 0.047$) (Figure 6H). There was no main effect of treatment on corner visits during the first 5 min ($F_{1,40} = 0.7472$; $p = 0.390$) nor genotype × treatment interaction ($F_{1,40} = 1.8577$; $p = 0.180$).

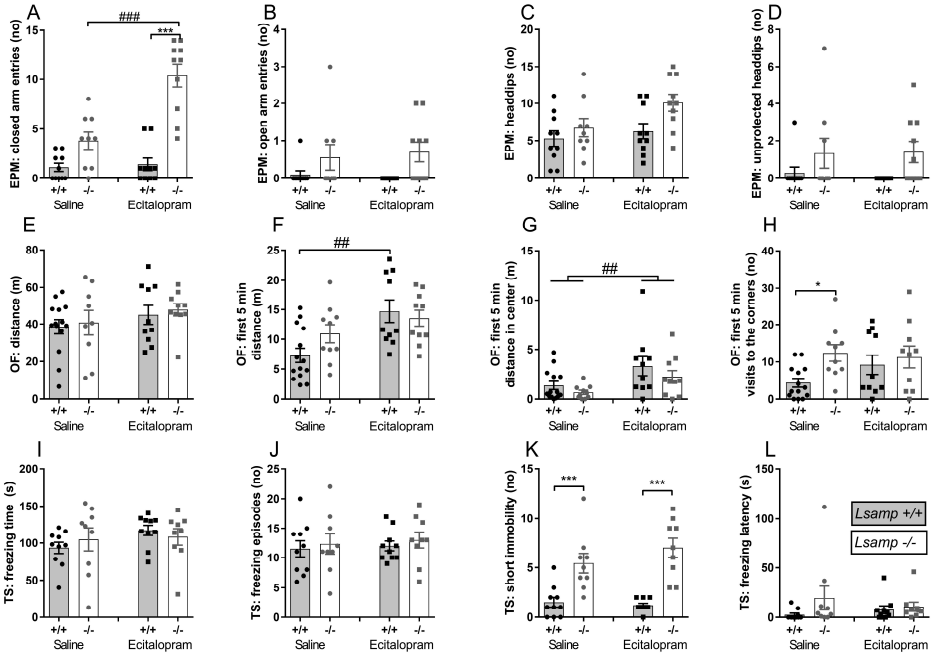

Figure 6. Chronic escitalopram had a significant impact on the behavior in the elevated plus maze, but not in the open field and tail suspension tests. Behavior of *Lsamp*$^{-/-}$ and WT mice in the elevated plus maze, EPM (A–D), open field, OF (E–H) and tail suspension, TS (I–L) tests. In the elevated plus maze, escitalopram significantly increased general motor activity reflected by an increased number of closed arm entries (A) by *Lsamp*$^{-/-}$ mice; this effect was not present in their wildtype littermates. Only genotype effect was present in the open arm entries (B), protected head dips (C) and unprotected head dips (D). In the open field test no statistical differences were found in the general distance during 30 min testing (E), the distance travelled during the first 5 min was significantly increased after administration of escitalopram only in WT mice (F); escitalopram had significant treatment effect to the distance travelled in the center (G); *Lsamp*$^{-/-}$ mice in the saline group made more corner visits during the first 5 min of the open field test compared with their WT littermates (H). No significant effects were found in the tail suspension test related to freezing time (I), number of freezing episodes (J) and latency to freeze (L). *Lsamp*$^{-/-}$ mice displayed a specific behavioral pattern in the tail suspension test that was not dependent on the injected substance: a significantly higher number of short (1–2 s) episodes of immobility compared with their WT littermates (K). *$p < 0.05$, ***$p < 0.001$ – genotype effects; ##$p < 0.01$, ###$p < 0.001$ – treatment effects.

To assess depressive-like phenotype, we conducted the tail suspension test. Freezing time, reflecting behavioral despair, was not dependent on the genotype ($F_{1,35} = 0.023$; $p = 0.880$), escitalopram treatment ($F_{1,35} = 0.999$; $p = 0.324$) or their interaction ($F_{1,35} = 1.461$; $p = 0.235$) (Figure 6I). The number of freezing episodes was also not dependent on genotype ($F_{1,35} = 0.033$; $p = 0.860$), escitalopram treatment ($F_{1,35} = 0.002$; $p = 0.960$) or genotype × treatment interaction ($F_{1,35} = 0.148$; $p = 0.700$) (Figure 6J). Remarkably, *Lsamp*-deficient mice showed an increased number of short immobility episodes compared to the WT controls ($F_{1,35} = 33.4$; $p < 0.00001$). The number of short freezing episodes was neither affected by escitalopram treatment ($F_{1,35} = 0.126$; $p = 0.720$) nor genotype × treatment interaction ($F_{1,35} = 0.545$; $p = 0.470$) (Figure 6K). The freezing latency was neither affected by genotype ($F_{1,35} = 2.41$; $p = 0.130$), escitalopram treatment ($F_{1,35} = 0.559$; $p = 0.460$) nor genotype × treatment interaction ($F_{1,35} = 0.17$; $p = 0.680$) (Figure 6L).

According to these results, *Lsamp*-deficient mice showed signs of reduced anxiety, increased exploratory activity and behavioral disinhibition, entering more frequently to both open and closed arms, as well as making more head dips, both protected and unprotected. The chronic administration of escitalopram amplified this effect even more.

5.2.1. Chronic administration of escitalopram alters the level of monoamine in several brain areas

5-HT and its metabolite 5-HIAA were measured in five brain regions. 5-HT turnover was calculated as the 5-HIAA/5-HT ratio. Remarkably, differences between the *Lsamp*$^{-/-}$ and control mice, most often in 5-HT turnover levels, were observable in all the five brain regions studied. In the raphe nuclei, 5-HT turnover was significantly higher in *Lsamp*-deficient mice receiving saline ($p = 0.034$) compared to the WT mice receiving saline. Escitalopram treatment reduced 5-HT turnover significantly ($p = 0.011$) only in *Lsamp*$^{-/-}$ mice (Figure 7C, in raphe, but also other nuclei). Chronic escitalopram reduced the level of 5-HT significantly ($p = 0.032$) only in *Lsamp*$^{-/-}$ mice (Figure 7A, in raphe). In *Lsamp*$^{-/-}$ mice receiving saline, 5-HIAA level was significantly ($p < 0.001$) higher than in the corresponding WT group. Escitalopram reduced the level of 5-HIAA significantly ($p < 0.001$) only in *Lsamp*$^{-/-}$ mice (Figure 7B, in raphe). In the VSTR, 5-HT turnover was significantly higher in *Lsamp*$^{-/-}$ mice receiving saline, than in the corresponding WT group ($p = 0.028$). Escitalopram administration reduced 5-HT turnover significantly ($p = 0.002$) only in *Lsamp*$^{-/-}$ mice (Figure 7C, V Str). In the DSTR, escitalopram decreased 5-HT turnover significantly ($p < 0.001$) in *Lsamp*$^{-/-}$ mice, but in WT mice the turnover was not significantly different ($p = 0.090$) (Figure 7C, D Str). Also, the level of 5-HIAA was significantly higher in *Lsamp*$^{-/-}$ mice receiving saline ($p = 0.042$) than in WT mice receiving saline. Escitalopram administration reduced the level of 5-HIAA statistically significantly ($p < 0.001$) only in *Lsamp*$^{-/-}$ mice (Figure 7B, D Str). In the Temp, there were no significant differences, however, the 5-HIAA level in *Lsamp*$^{-/-}$ mice receiving saline tended ($p = 0.074$) to be higher than in similarly treated WT mice

(Figure 7B, Temp). In the Hip, the 5-HT turnover in *Lsamp*$^{-/-}$ mice receiving saline tended ($p = 0.066$) to be higher than in WT littermates treated similarly. Escitalopram administration reduced 5-HT turnover significantly ($p < 0.001$) only in *Lsamp*$^{-/-}$ mice (Figure 7C, Hip). There was no difference between the 5-HIAA baseline levels, however, escitalopram reduced 5-HIAA levels in both groups and, notably, in *Lsamp*$^{-/-}$ mice to a greater extent ($p < 0.001$) than in WT animals ($p = 0.01$) (Figure 7B, Hip).

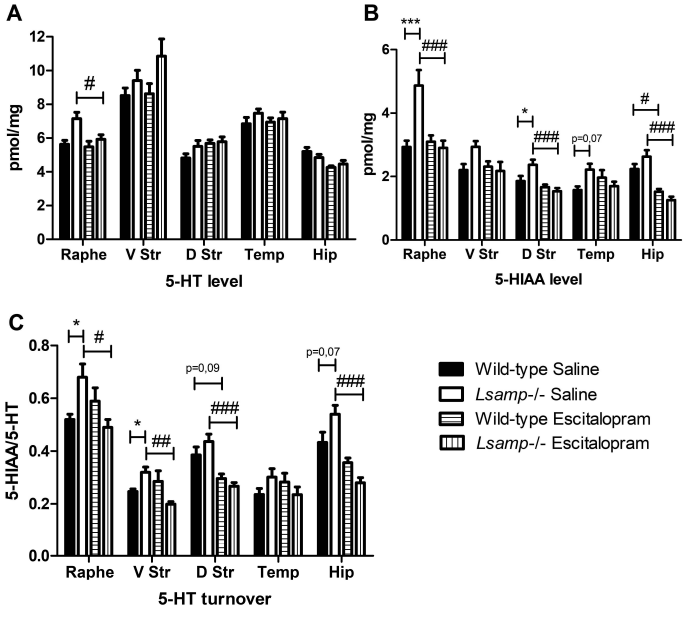

Figure 7. Effects of escitalopram on 5-HT and its metabolism in the five brain regions of *Lsamp*$^{-/-}$ mice (n = 8) and their wildtype littermates (n = 8). 5-HT (A), 5-HIAA (B) and 5-HT turnover (5-HIAA/5-HT) (C) levels in the raphe, ventral striatum (V Str), dorsal striatum (D Str), temporal lobe including amygdala (Temp), and hippocampus (Hip). #$p < 0.05$; ##$p < 0.01$; ###$p < 0.001$ – treatment effects; *$p < 0.05$; ***$p < 0.001$ – genotype effects.

5.2.2. The baseline 5-HT system related gene expression in *Lsamp*-deficient mice

Mann-Whitney U test revealed statistically significant differences between *Lsamp*$^{-/-}$ (n = 8) and control *Lsamp*$^{+/+}$ (n = 8) mice for *MaoA* in the raphe area and *MaoB* in the Temp. *MaoA* was significantly increased in *Lsamp*$^{-/-}$ mice (m = 0.79) compared to controls (m = 0.60) ($p < 0.01$) (Figure 8B), and *MaoB* was significantly decreased in the Temp of *Lsamp*$^{-/-}$ mice (m = 0.66) compared to *Lsamp*$^{+/+}$ mice (m = 0.80) ($p < 0.05$) (Figure 8C).

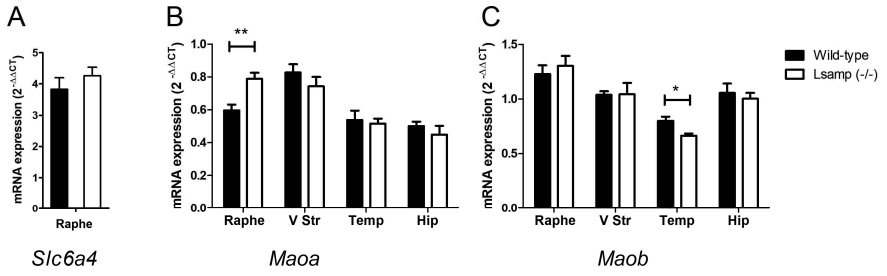

Figure 8. Baseline expression levels of the genes involved in 5-HT turnover. Relative mRNA expression levels of (A) serotonin transporter (*Slc6a4*), (B) monoamine oxidase A (*MaoA*) and (C) monoamine oxidase B (*MaoB*) in *Lsamp*-deficient mice and their WT littermates. *p < 0.05; **p < 0.01.

5.3. *Negr1* gene-deficiency induces alterations in the monoaminergic neurotransmission enhancing time-dependent sensitization to amphetamine in mice (Paper II)

5.3.1. The impact of chronic administration of escitalopram to the body weight and behavior of *Negr1*$^{-/-}$ and WT mice

There were no significant body weight changes in *Negr1*$^{-/-}$ mice caused by chronic administration of escitalopram (Figure 9). *Negr1*$^{-/-}$ and WT received 23 days of escitalopram and the behavior of the mice was assessed in the elevated plus maze (day 16), open field test (days 19 and 20), and tail suspension test (day 22). The test results showed that in the tail suspension test latency to freeze was affected by the treatment ($F_{1,50} = 4.189$; $p = 0.046$). In the elevated plus maze test frequency to enter closed arms was affected by the genotype ($F_{1,50} = 4.713$; $p = 0.035$). In the open field test corner visits made within first 5 minutes of the experiment was affected by the genotype ($F_{1,50} = 4.356$; $p = 0.042$). There were no other significant behavioral changes in the chronic escitalopram treatment experiment (Figure 10).

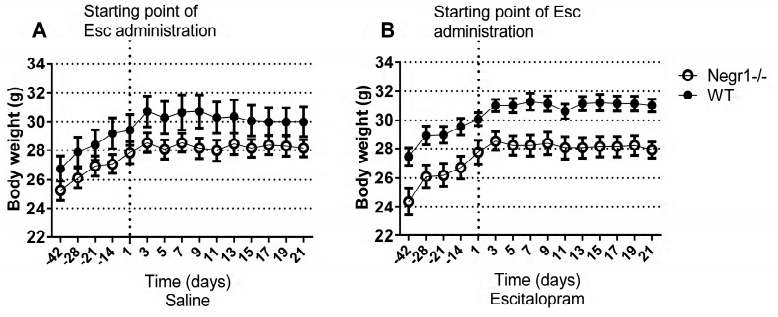

Figure 9. Effects of chronic administration of escitalopram (10 mg/kg) on the body weight of mice. (A) Body weight dynamics of the saline groups and (B) body weight dynamics of escitalopram groups. Data represents mean ± SEM.

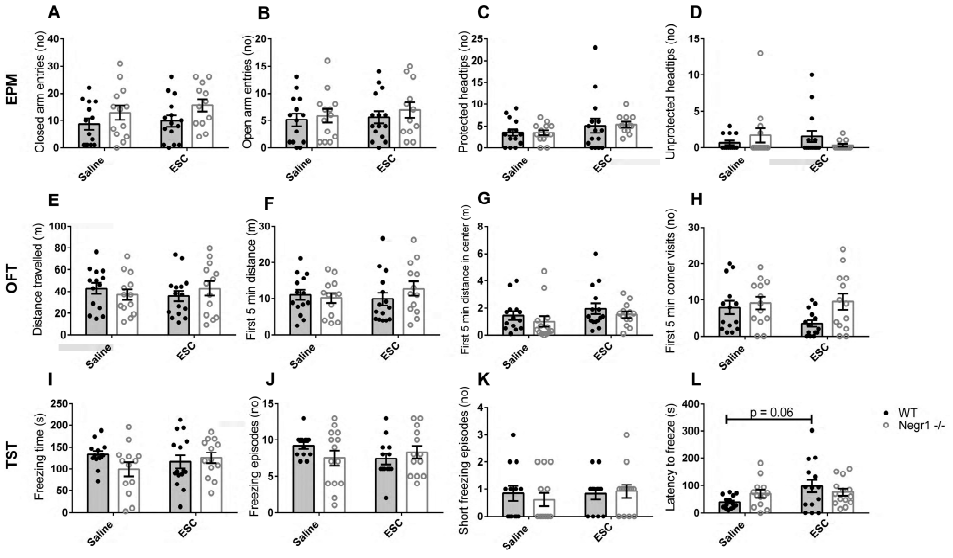

Figure 10. Escitalopram had no effect on the behavior of the mice. Mice received i.p. injection of either saline or 10 mg/kg of escitalopram at a volume of 10 ml/kg for 23 consecutive days. Behavioral changes were evaluated in the (A–D) elevated plus maze (day 16), (E–H) open field test (half of the mice on day 19 and other half of the mice on day 20) and (I–L) tail suspension (day 22) tests. Data represents mean ± SEM.

5.3.2. Chronic administration of escitalopram alters the level of monoamines and their metabolites in raphe

Levels of different monoamines and their metabolites were measured in the raphe nuclei (Figure 11A–J). In the raphe, the levels of 5-HT ($F_{1,48} = 6.36$; $p = 0.015$) (Figure 11B) and its metabolite 5-HIAA ($F_{1,47} = 6.23$; $p = 0.016$) (Figure 11C) were dependent on treatment, but Bonferroni's *post hoc* test did not show any significant changes. In the raphe, escitalopram significantly decreased the 5-HT turnover (5-HIAA/5-HT) in the *Negr1*$^{-/-}$ group ($p = 0.002$) (Figure 11D), 5-HT turnover was dependent on treatment ($F_{1,46} = 19.11$; $p < 0.0001$). The level of tyrosine showed no statistically significant differences between the groups (Figure 11E).

The level of DA was dependent on treatment × genotype interaction ($F_{1,47} = 4.11$; $p = 0.048$). Escitalopram significantly increased the level of DA in the WT group ($p = 0.048$) but not in *Negr1*$^{-/-}$ mice (Figure 11F). The level of DA metabolite DOPAC was also affected by the treatment × genotype interaction ($F_{1,51} = 5.80$; $p = 0.020$), the level of DOPAC was statistically significantly higher in the *Negr1*$^{-/-}$ group receiving saline compared to the *Negr1*$^{-/-}$ escitalopram group ($p = 0.025$) (Figure 11G). DA turnover (DOPAC/DA) was dependent on treatment ($F_{1,49} = 17.53$; $p < 0.001$) and on treatment × genotype interaction ($F_{1,49} = 6.03$; $p = 0.018$). DA turnover was significantly higher in the *Negr1*$^{-/-}$ saline group compared to the WT saline group ($p = 0.035$) and escitalopram significantly decreased the DA turnover in the *Negr1*$^{-/-}$ group ($p < 0.0001$) (Figure 11H).

There was a genotype effect on the level of tyramine ($F_{1,49}$ = 5.38; p = 0.025). The level of tyramine was statistically significantly higher in the *Negr1*$^{-/-}$ saline group compared to the WT saline group (p < 0.05) (Figure 11I). There were no significant changes in the level of 3MeOTyramine (Figure 11J).

The serotonin system-related genes were measured in the raphe using qPCR (Figure 11K-N). In the raphe, the level of *Slc6a4* was significantly higher in *Negr1*$^{-/-}$ mice (p = 0.007) (Figure 11K). There were no significant differences between *Negr1*$^{-/-}$ and WT mice in the level of *Tph2* (Figure 19L), *MaoA* (Figure 11 M) and *MaoB* (Figure 11N).

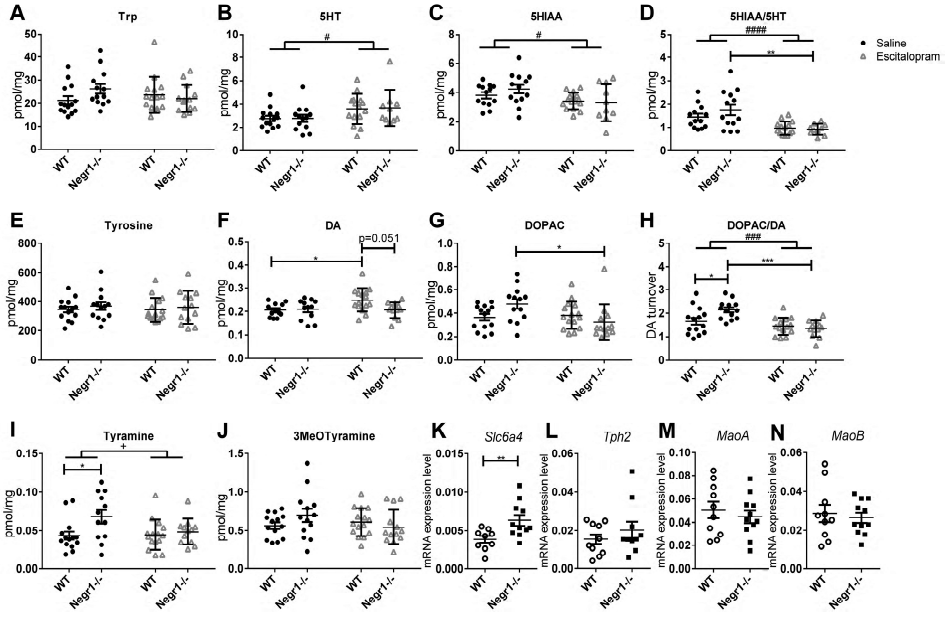

Figure 11. Effect of chronic escitalopram on the level of monoamines and their metabolites in the raphe nuclei. Levels of (A) tryptophan (Trp) (B) serotonin (5-HT), (C) 5-Hydroxyindoleacetic acid (5-HIAA), (D) serotonin turnover (5-HIAA/5-HT), (E) tyrosine, (F) dopamine (DA), (G) 3,4-Dihydroxyphenylacetic acid (DOPAC), (H) dopamine turnover (DOPAC/DA), (I) tyramine and (J) 3MeOTyramine in raphe. The mRNA expression level of (K) serotonin transporter (*Slc6a4*), (L) tryptophan hydroxylase 2 (*Tph2*), (M) monoamine oxidase A (*MaoA*) and (N) monoamine oxidase B (*MaoB*). Monoamines and their metabolites shown as pmol/mg. Data represents mean ± SEM, #p < 0.05, ###p < 0.001, ####p < 0.0001 – treatment effect, +p < 0.05 – genotype effect, *p < 0.05, **p < 0.01, ***p < 0.001 – *post hoc* test, two-way ANOVA (Bonferroni *post hoc* test) (monoamines and their metabolites), Mann-Whitney U test (*Slc6a*4 and *Tph2*).

5.3.3. *Negr1*$^{-/-}$ mice display higher sensitivity to amphetamine compared to WT mice

In the dose-response curve experiment, 6 mg/kg amphetamine induced highly increased motor activity in both genotypes and therefore the 6 mg/kg dose was considered to be too high for chronic experiment, as the behavioral sensitization effect of amphetamine is well known (Scholl et al. 2009). Therefore, chronic amphetamine experiment was performed by using 3mg/kg dose, which, if first time injected, induced only tendency towards increased activity in dose-response curve experiment (Figure 12 A–C). In the dose-response experiment, the distance travelled was affected by the genotype ($F_{2,53}$ = 65.31; $p < 0.0001$), while not affected by the treatment ($F_{1,53}$ = 2.881; $p = 0.095$) and genotype × treatment interaction ($F_{2,53}$ = 2.004; $p = 0.144$) (Figure 12A). Other behavioral parameters, such as distance in center and number of rearings were not significantly affected neither by the genotype, treatment or genotype × treatment interaction (Figure 12B–C)

The 1st day of chronic amphetamine/saline injection was analyzed to see the acute effect of 3 mg/kg amphetamine on mice. The distance travelled (m), was affected by the treatment ($F_{1,36}$ = 13.94; $p < 0.001$, Figure 12D), number of corner visits, was affected by the treatment ($F_{1,34}$ = 13.08; $p = 0.001$, Figure 12E) and number of rotations, was affected by the treatment ($F_{1,36}$ = 12.47; $p = 0.001$, Figure 12F).

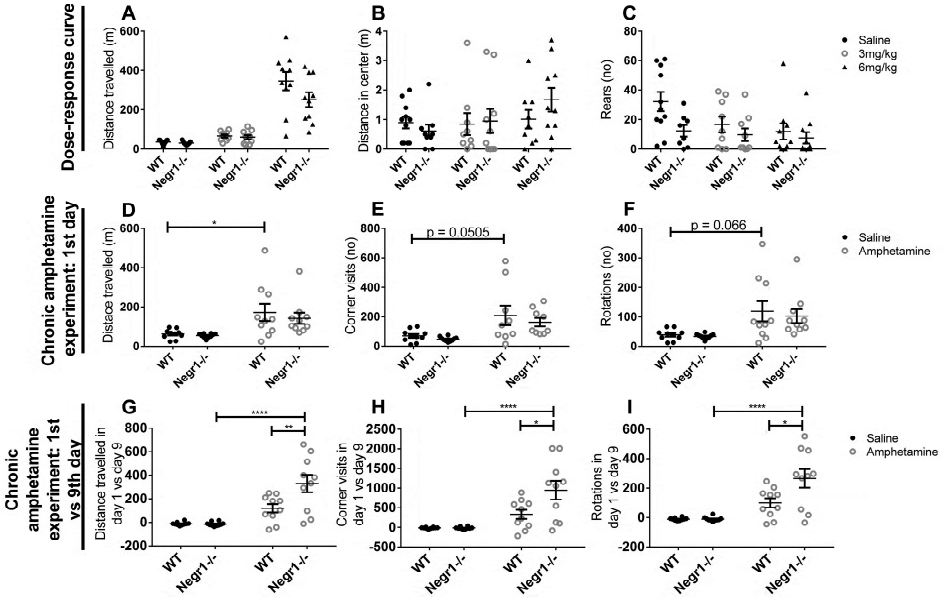

Figure 12. Amphetamine dose curve (A–C) and chronic amphetamine experiment (D–I). All dosage curve mice (cohort III) received a single injection of saline or amphetamine on a dosage either 3mg/kg or 6mg/kg. Figures D–I represent chronic amphetamine experiment mice (cohort IV). Data represents mean ± SEM, *$p < 0.05$, **$p < 0.01$, ****$p < 0.0001$, two-way ANOVA (Bonferroni *post hoc* test).

In order to assess the impact of amphetamine on behavior, *Negr1*$^{-/-}$ and WT mice received 10 days of amphetamine in the dose of 3 mg/kg. The administration of amphetamine for 10 days induced significantly higher motor activity in *Negr1*$^{-/-}$ mice compared to WT mice.

Days 1 and 9 were compared to see the difference of amphetamine effect between those two days (Figure 12 G–I). Distance travelled in day 1 vs day 9, was affected by the genotype ($F_{1,36}$ = 6.32; p = 0.001), treatment $F_{1,36}$ = 33.29; p < 0.0001) and genotype × treatment interaction ($F_{1,36}$ = 6.69; p < 0.05) (Figure 9G), The number of corner visits in day 1 vs day 9 was affected by the genotype ($F_{1,36}$ = 5.31; p = 0.027), treatment ($F_{1,36}$ = 24.1; p < 0.0001) and genotype × treatment interaction ($F_{1,36}$ = 5.31; p < 0.05) (Figure 12H) and number of rotations in day 1 vs day 9 was affected by the genotype ($F_{1,36}$ = 5.52; p < 0.05), treatment ($F_{1,36}$ = 29.90; p < 0.0001) and genotype × treatment interaction ($F_{1,36}$ = 5.53; p = 0.024) (Figure 12I).

Next our analysis included all 10 timepoints of the behavioral recordings: amphetamine-treated *Negr1*$^{-/-}$ mice had travelled, visited corners, and rotated more compared to WT mice, whereas the control (saline) groups for both genotypes did not show any differences in these activities (Figure 13A–F). Clockwise and anticlockwise rotations were summed up in these experiments as there was no difference in the direction of rotation. Three-Way Repeated-Measures ANOVA showed that distance travelled was affected by the time ($F_{3.4,62.6}$ = 5.65; p = 0.001), treatment ($F_{1,18}$ = 67.24; p< 0.0001) and genotype × treatment interaction ($F_{1,18}$ = 22.84; p < 0.001) (Figure 13A). The number of corner visits showed significant time ($F_{3.2,57.9}$ = 5.06; p = 0.002), treatment ($F_{1,18}$ = 63.32; p< 0.0001) and genotype × treatment effects ($F_{1,18}$ = 17.36; p < 0.001) (Figure 13B). Rotations were also affected by the time ($F_{3.6,64.8}$ = 5.48; p = 0.001), treatment ($F_{1,18}$ = 43.95; p < 0.0001) and genotype × treatment interaction ($F_{1,18}$ = 21.03; p < 0.001) (Figure 13C).

Analyzing the AUC showed that amphetamine increased the travelled distance for both WT and *Negr1*$^{-/-}$ mice (p < 0.0001; Figure 13D). Nevertheless, the travelled distance was longer in *Negr1*$^{-/-}$ mice that received amphetamine compared to their WT littermates (p = 0.016; Figure 13D). A similar situation was also seen in case of corner visits (Figure 13B, E) and rotations (Figure 13C, F): while both genotypes visited more corners as well as made more rotations (p < 0.001 for WTs and p < 0.0001 for *Negr1*$^{-/-}$ mice), (Figure 13E) upon chronic amphetamine administration. Besides that, in summary, the amphetamine induced more corner visits (p = 0.012) and rotations (p= 0.032) in *Negr1*$^{-/-}$ mice compared to their WT littermates.

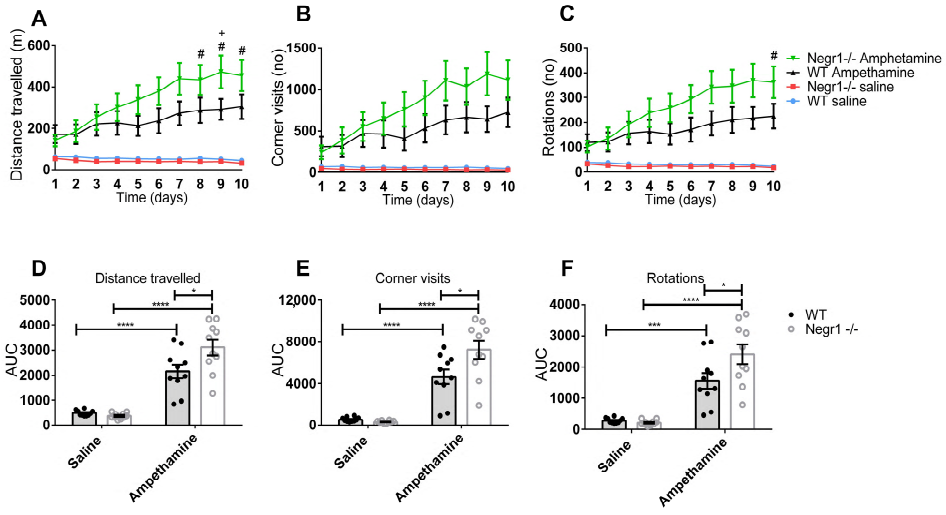

Figure 13. *Negr1*$^{-/-}$ mice are more sensitive to chronic amphetamine administration. Effect of chronic amphetamine on (A, D) distance travelled, (B, E) corner visits and (C, F) rotations in open field test. Data represents mean ± SEM, + – p< 0.01 – difference in treatment in WT mice, # – p< 0.05 – difference in treatment in *Negr1*$^{-/-}$ mice (Tukey post hoc test, A–C); *p < 0.05, ***p < 0.001, ****p < 0.0001 (Mann-Whitney, D–F). AUC, area under curve.

The body weight of the mice was measured 10 days before amphetamine or saline injections (marked as day –10). Body weight dynamics prior to the amphetamine injection (day –10 until –3) showed significant genotype ($F_{1,38} = 9.17$; $p = 0.004$) and genotype × time interaction effects ($F_{2,76} = 5.97$; $p = 0.004$). WT mice showed slight decrease in body weight, whereas *Negr1*$^{-/-}$mice gained weight during the first week of measurements (Figure 14C), at the time when handling due to daily weighing was the only interfering activity. According to Bonferroni's *post hoc* test on day –10 the difference between the body weight of the WT mice and *Negr1*$^{-/-}$ mice was statistically significant ($p = 0.001$). On day –7, the baseline open field test was performed and on day –6 all the mice were single housed. The difference in body weight was still statistically significant on day –6 ($p = 0.018$) but was not anymore seen on day –3. The change of body weight during the first week (days –10 vs day –3) was also calculated (Figure 14D). The average weight loss for WT mice was 0.27 g and the average weight gain of *Negr1*$^{-/-}$ mice was 0.69 g. Mann-Whitney test showed that weight change differences between WT and *Negr1*$^{-/-}$ mice were statistically significant ($p = 0.008$). The weight from the beginning of the experiment to the end of the experiment (day –10 vs day 10) was also calculated (Figure 14E), but there were no statistically significant changes in the body weight change caused by amphetamine. There was, however, a significant genotype effect ($F_{1,36} = 11.62$; $p = 0.002$) showing that *Negr1*$^{-/-}$ mice lost less body weight than WT both upon saline and amphetamine injections.

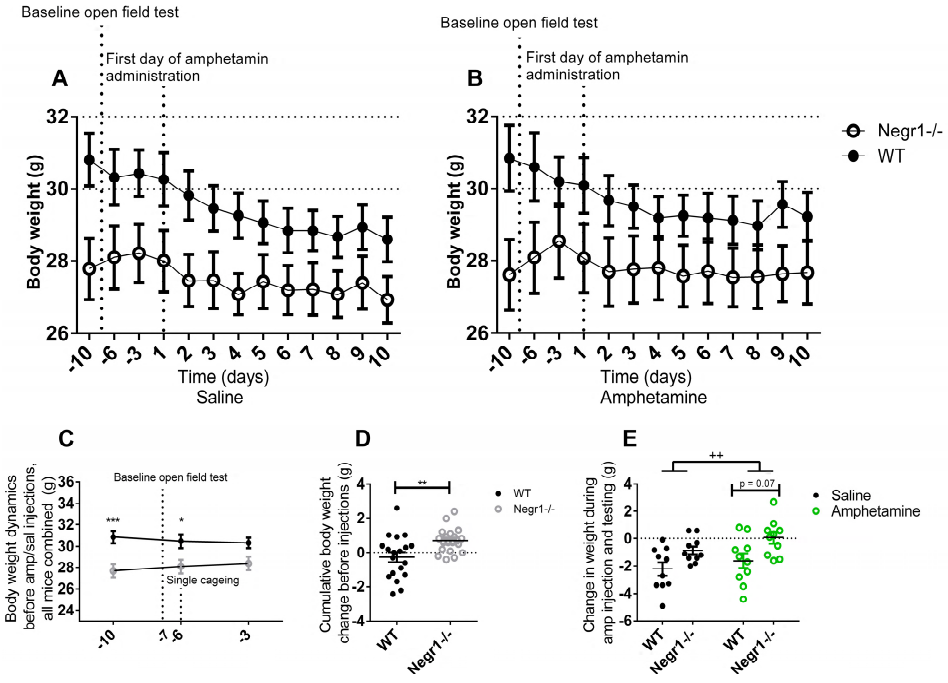

Figure 14. Effects of chronic administration of amphetamine (3 mg/kg) on the body weight of mice. (A) Body weight changes of the saline groups and (B) body weight changes of amphetamine groups. In C and D saline/amphetamine groups have not been separated yet, the body weight change is a reaction for non-pharmacological environmental manipulations. (C) Body weight dynamics measured during 1 week of period before amphetamine injection (from day –10 until day –3) (D) Cumulative body weight change before saline/amphetamine injections (from day –10 until day –3). (E) Body weight change caused by chronic saline or amphetamine injections and behavioral testing (from day 1 until day 10). Data represents mean ± SEM. *p < 0.05, **p < 0.01, ***p < 0.001 (Bonferroni *post hoc* test, C–E), ++p < 0.01 – genotype effect.

If the data from saline groups was analyzed separately. Open field tests showed genotype effects in the distance travelled in the center and rotations, as well as in the number of rearings. The *post hoc* test showed no significant changes between *Negr1*$^{-/-}$ and WT mice for individual days (Figure 15A, B, C, D). For each mouse, AUC was calculated, and the results analyzed using the Mann-Whitney U test (Figure 15E, F, G, H) showed that *Negr1*$^{-/-}$ mice performed significantly less rearings compared to WT mice (p = 0.012) (Figure 14I). The AUC of distance travelled in the center of the box was significantly lower in *Negr1*$^{-/-}$ mice (p = 0.035) (Figure 15J).

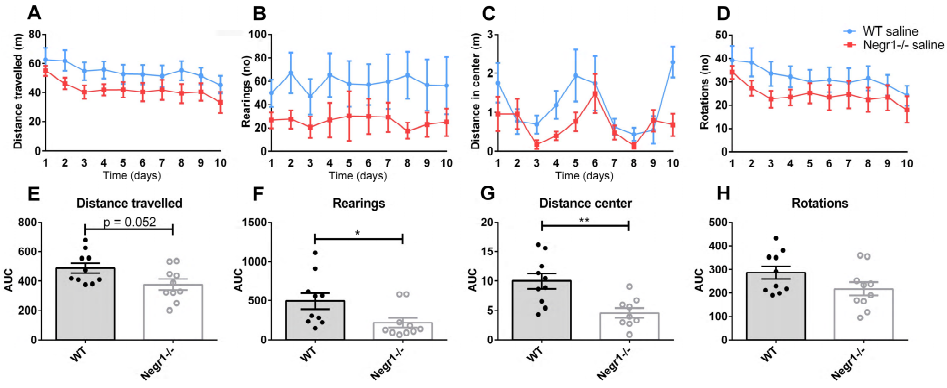

Figure 15. Effects of daily saline injections on activity of *Negr1*$^{-/-}$ and WT mice. The saline-injected groups showed significant effects in the open field test in (A) distance travelled there were time ($F_{9,162}$ = 2.14; < 0.05), genotype ($F_{1,18}$ = 4.91; < 0.05) effect (B) rearings had genotype effect ($F_{1,153}$ = 20.63; p < 0.0001), (C) distance travelled in center had time ($F_{9,162}$ = 3.701; p < 0.001) and genotype effect ($F_{1,18}$ = 5.414; p < 0.05) (D) rotations had time effect ($F_{9,162}$ = 2.072; p < 0.05) (only saline-injected groups from Figure 2A–D are displayed to visualize behavioral differences between genotypes without pharmacological intervention). (E–H) The same parameters quantified as area under the curve (AUC). Data represents mean ± SEM, ++p < 0.01 – genotype effect, *p < 0.05, **p < 0.01 – *post hoc* test, two-way ANOVA (Bonferroni *post hoc* test).

According to these results we saw that baseline open field test (7 days before injection started) and consequent housing in single cages induced the decrease in the body weight of WT mice, whereas the body weight of *Negr1*$^{-/-}$ mice stayed stable or even increased slightly during the same time period indicating reduced anxiety of *Negr1*$^{-/-}$ mice. During the course of daily chronic injections, housing in single cages and testing, however, saline-receiving *Negr1*$^{-/-}$ mice became less active in most of the behavioral parameters that were measured, including total distance traveled and distance in the center. We saw that 10-day administration of amphetamine induced significantly higher motor and stereotypic activity in *Negr1*$^{-/-}$ mice compared to WT mice, indicating a higher behavioral sensitivity to amphetamine.

5.3.4. Chronic administration of amphetamine increases the level of tyrosine hydroxylase (*Th*) in VTA

To assess the level of dopamine system related genes in VTA, qPCR was performed using both cohort VI (Figure 16A–D) and cohort IV mice (Figure 16E–I). *Post hoc* tests showed that chronic amphetamine treatment significantly increased the level of TH only in WT mice (p = 0.027). The level of TH was significantly higher in the WT amphetamine group compared to the *Negr1*$^{-/-}$ amphetamine group (p = 0.045) (Figure 16B). There were no other significant changes in the level of dopamine system related genes (*Dat*, *Drd2* and *Comt*) between the groups of cohort IV mice (Figure 16A, C, D).

Mann-Whitney U Test was used to compare WT and *Negr1*$^{-/-}$ groups. In the VTA, the level of *Dat* was significantly higher in *Negr1*$^{-/-}$ mice (p = 0.010) (Figure 16E). The levels of *Th* (p = 0.019) (Figure 16F), *MaoA* (p = 0.009) (Figure 16H) and *MaoB* (p = 0.005) (Figure 16I) were also statistically significantly higher in the VTA of *Negr1*$^{-/-}$ mice compared to WT mice. There were no significant changes in the level of *Drd2* in the VTA of cohort VI mice (Figure 16G).

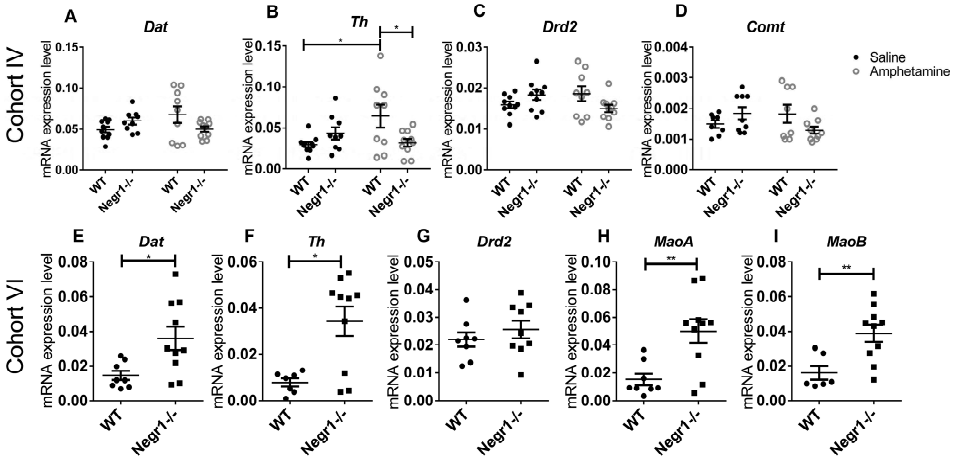

Figure 16. The level of dopamine system-related genes in the VTA of the mice. Relative mRNA expression levels of (A) dopamine transporter (*Dat*), (B) tyrosine hydroxylase (*Th*), (C) dopamine receptor D2 (*Drd2*), (D) catechol-*O*-methyltransferase (*Comt*) in *Negr1*$^{-/-}$ mice and their WT littermates after 10 days of chronic saline or amphetamine i.p. injection (cohort IV). The levels of (E) dopamine transporter (*Dat*), (F) tyrosine hydroxylase (*Th*), (G) dopamine receptor D2 (*Drd2*), (H) monoamine oxidase A (*MaoA*) and (I) monoamine oxidase B (*MaoB*) in uninjected *Negr1*$^{-/-}$ mice and their WT littermates kept in their home cages (cohort VI). Data represents mean ± SEM, *p < 0.05, **p < 0.01, two-way ANOVA (Bonferroni *post hoc* test).

5.3.5. Amphetamine increases the level of dopamine in DSTR

To identify the differences caused by chronic amphetamine administration between WT and *Negr1*$^{-/-}$ two-way ANOVA [treatment (amphetamine or saline) × genotype (WT or *Negr1*$^{-/-}$)] and Bonferroni *post hoc* test was used. The level of dopamine and its metabolites were measured in VSTR and DSTR. In the DSTR the level of DA was dependent on the treatment ($F_{1,36}$ = 9.19; p = 0.005) and Bonferroni's *post hoc* test showed that chronic treatment with amphetamine statistically significantly increased the level of DA in *Negr1*$^{-/-}$ mice (p = 0.026) (Figure 17A). Dopamine turnover (3-MT/DA) in the DSTR was affected by the genotype ($F_{1,36}$ = 5.30; p = 0.027) (Figure 17B), *post hoc* test showed no statistically significant changes between the groups. Immunohistochemical *Dat* staining of DSTR and VSTR did also not show any significant differences between WT and *Negr1*$^{-/-}$ mice (Figure 17C).

In the VSTR, the level of DA had no significant changes between the groups (Figure 17D). Dopamine turnover to 3-MT (3-MT/DA) was again affected by the genotype ($F_{1,34}$ = 12.51; p < 0.001) (Figure 17E). The level of DA metabolite 3-MT itself was affected by the treatment ($F_{1,34}$ = 9.77; p = 0.004) (Figure 17F) and *post hoc* test revealed that the level of 3-MT was significantly increased in the *Negr1*$^{-/-}$ group receiving amphetamine (p = 0.047) in comparison to the saline-injected *Negr1*$^{-/-}$. The level of 5-HT metabolite 5-HIAA was dependent on both treatment ($F_{1,34}$ = 10.61; p = 0.003) and genotype ($F_{1,34}$ = 10.06; p = 0.003) (Figure 17G). In the VSTR, the levels of dopamine system related genes *Dat* (p = 0.011) (Figure 17H) and *Comt* (p = 0.014) (Figure 17I) were significantly higher in *Negr1*$^{-/-}$ mice compared to WT mice.

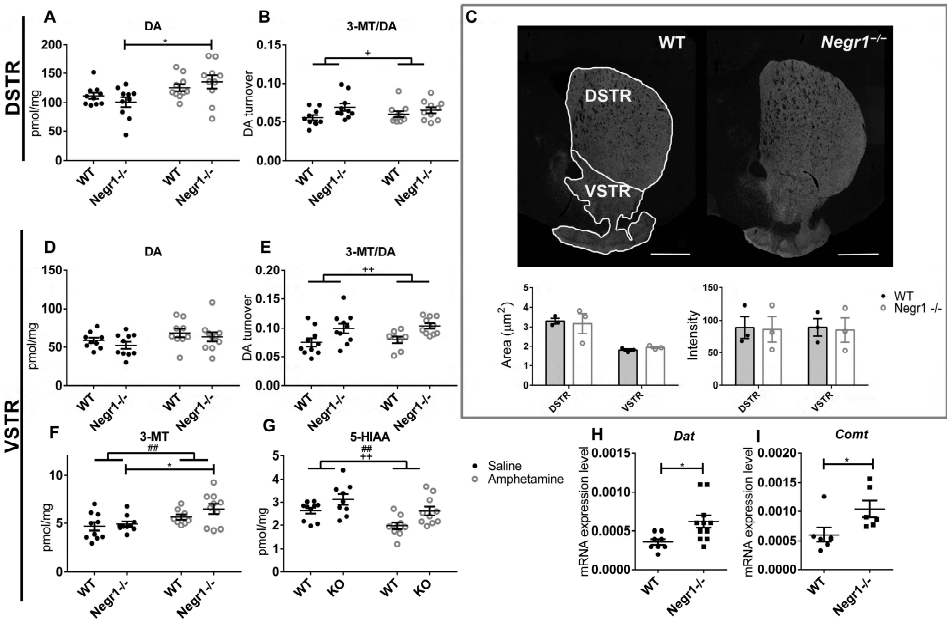

Figure 17. Effect of chronic amphetamine in the VSTR and DSTR. The level of (A) dopamine (DA) and (B) dopamine turnover (3-MT/DA) in the DSTR. (C) Immunohistochemical *Dat* stainings of DSTR and VSTR. The level of (D) dopamine (DA), (E) dopamine turnover (3-MT/DA), (F) 3MeOTyramine (3-MT), (G) 5-Hydroxyindoleacetic acid (5-HIAA), (H) dopamine transporter (*Dat*) and (I) catechol-*O*-methyltransferase (*Comt*) in the VSTR. Monoamines and their metabolites shown as pmol/mg. Data represents mean ± SEM, ##p < 0.01 – treatment effect, +p < 0.05, ++p < 0.01 – genotype effect, *p < 0.05 – *post hoc* test, two-way ANOVA (Bonferroni *post hoc* test).

5.3.6. Chronic amphetamine administration alters the level of monoamines in Hip and chronic escitalopram treatment causes weight difference of the Hip

Hip of the *Negr1*$^{-/-}$ mice weigh less compared to WT Hip (Figure 18C–D). Amphetamine had no effect on the hippocampal weights of either *Negr1*$^{-/-}$ or WT mice (Figure 18A–B). In the escitalopram treatment experiment, the weight of Hip was dependent on genotype ($F_{1,51} = 7.38$; $p = 0.009$) and there was a genotype × treatment interaction ($F_{1,51} = 5.06$; $p = 0.030$). The *post hoc* test showed that Hip of the *Negr1*$^{-/-}$ mice that received saline weigh less compared to WT saline group mice Hip ($p = 0.006$) and *Negr1*$^{-/-}$ escitalopram group Hip weigh significantly more compared to *Negr1*$^{-/-}$ saline group Hip ($p = 0.030$) (Figure 18C). If the weight of Hip was divided by the body weight of mice it was seen that the Hip/body weight relationship was dependent on genotype × treatment interaction ($F_{1,51} = 8.01$; $p = 0.007$). The *post hoc* test showed that this relationship was significantly higher in the *Negr1*$^{-/-}$ escitalopram group compared to *Negr1*$^{-/-}$ saline group ($p = 0.030$) (Figure 18D).

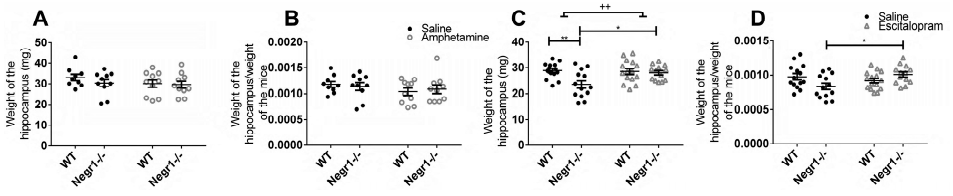

Figure 18. Hip of *Negr1*$^{-/-}$ mice weigh less compared to WT mice and escitalopram restores the weight of Hip of *Negr1*$^{-/-}$ mice. (A) The weight of the Hip of the mice after receiving 10 days of saline or amphetamine. (B) Weight of Hip divided by the weight of mice (after receiving 10 days of saline or amphetamine). (C) Weight of Hip of the mice receiving 23 days of saline or escitalopram. (D) Weight of Hip divided by the weight of mice (after receiving 23 days of saline or escitalopram). Data represents mean ± SEM, ++$p < 0.01$ – genotype effect, *$p < 0.05$, **$p < 0.01$ – *post hoc* test, two-way ANOVA (Bonferroni *post hoc* test).

The level of monoamines and their metabolites were measured in the Hip of mice receiving either chronic treatment of amphetamine (Figure 19A–H) or escitalopram (Figure 19I–P). In case of chronic amphetamine administration, the level of tyrosine was dependent on treatment ($F_{1,34} = 7.78$; $p = 0.09$). Bonferroni's *post hoc* test revealed that the level of tyrosine was significantly decreased by amphetamine in the *Negr1*$^{-/-}$ group ($p = 0.039$) (Figure 19A). The level of 3MT was dependent of genotype ($F_{1,35} = 6.00$; $p = 0.019$) (Figure 19C) and the level of tyramine was dependent on genotype × treatment interaction ($F_{1,35} = 5.82$; $p = 0.021$) (Figure 19D), but *post hoc* test showed no significant changes in case of neither of them. The level of 5-HT was affected by the treatment ($F_{1,35} = 17.51$; $p < 0.001$), the *post hoc* test showed that amphetamine increased the level of 5-HT in the WT mice group ($p = 0.005$) (Figure 19E). The level of 5-HIAA was dependent on the treatment ($F_{1,35} = 4.18$; $p = 0.049$) (Figure 19F), post hoc

comparison did not indicate significant differences in *Negr1*$^{-/-}$ or WT mice separately. The level of NA was affected by the genotype ($F_{1,35} = 4.36$; $p = 0.049$) (Figure 19G) and its metabolite NMN was affected by the treatment ($F_{1,33} = 19.44$, $p < 0.001$), *post hoc* test showed that amphetamine increased the level of NMN of the WT mice ($p = 0.002$) (Figure 19H).

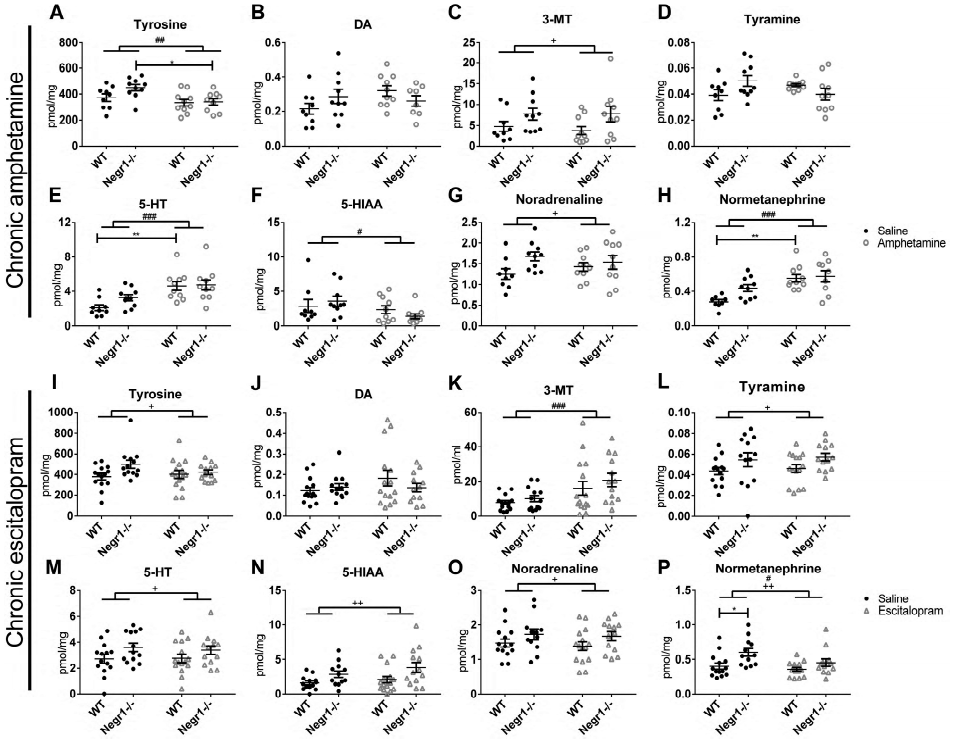

Figure 19. Effect of chronic administration of amphetamine (A–H) and escitalopram (I–P) on the level of monoamines and their metabolites in the Hip. The levels of (A) tyrosine, (B) dopamine (DA), (C) 3MeOTyramine (3-MT), (D) tyramine, (E) serotonin (5-HT), (F) 5-hydroxyindoleacetic acid (5-HIAA), (G) noradrenaline and (H) normetanephrine in the Hip of *Negr1*$^{-/-}$ mice and their WT littermates after 10 days of chronic amphetamine IP injections. The levels of (I) tyrosine, (J) dopamine (DA), (K) 3MeOTyramine (3-MT), (L) tyramine, (M) serotonin (5-HT), (N) 5-Hydroxyindoleacetic acid (5-HIAA), (O) noradrenaline and (P) normetanephrine in the Hip of *Negr1*$^{-/-}$ mice and their WT littermates after 23 days of chronic escitalopram IP injections. Monoamines and their metabolites shown as pmol/mg. Data represents mean ± SEM, #$p < 0.05$, ###$p < 0.001$– treatment effect, +$p < 0.05$, ++$p < 0.01$ – genotype effect, *$p < 0.05$, **$p < 0.01$ – *post hoc* test, two-way ANOVA (Bonferroni *post hoc* test).

In the chronic escitalopram experiment, the level of tyrosine was dependent on genotype ($F_{1,51} = 4.25$; $p = 0.045$) (Figure 19I), Bonferroni's *post hoc* test showed no significant changes. The level of 3-MT was affected by the treatment ($F_{1,51} = 10.36$; $p = 0.002$) (Figure 19K). The levels of tyramine ($F_{1,51} = 5.93$; $p = 0.018$) (Figure 19L), 5- HT ($F_{1,51} = 5.40$; $p = 0.024$) (Figure 19M), 5-HIAA ($F_{1,49} = 8.64$; $p = 0.005$) (Figure 19N) and NA ($F_{1,50} = 4.14$; $p = 0.047$) (Figure 19O) were dependent on the genotype. The level of NMN depended on both the treatment ($F_{1,50} = 4.57$; $p = 0.038$) and genotype ($F_{1,50} = 10.55$; $p = 0.002$), the *post hoc* test showed that the level of NMN was higher in the *Negr1*$^{-/-}$ saline group compared to WT saline group ($p = 0.023$) (Figure 19P).

5.4. High-fat diet induces pre-diabetes and distinct sex-specific metabolic alterations in *Negr1*-deficient mice (Paper IV)

5.4.1. *Negr1* deficiency induces lower intake of HF food but higher body weight gain in male mice

In the cohort VII of mice, the mice were weighed weekly from age 10±1 weeks during 9 weeks before the beginning of a HF diet; altogether the body weight was tracked for 16 weeks. The variation in body weight was relatively high, therefore no statistical genotype differences in body weight dynamics were detectable in the current study. In general, both male and female *Negr1*$^{-/-}$ mice tended to have slightly lower body weight when on a standard diet (Figure 20B). When consuming a HF diet, however, male *Negr1*$^{-/-}$ mice tended to gain more body weight compared to their WT littermates (Figure 20A). When mice consumed regular chow there were no significant weight differences between genotypes (Figure 20B). Male *Negr1*$^{-/-}$ mice consumed less HF food in the short-term food preference test, in which the food was individually measured for 24 hours (Figure 20D). Correspondingly, a tendency for a lower HF food intake in male *Negr1*$^{-/-}$ mice was also observed in group-housing settings 2 weeks before the glucose tolerance test (Figure 20E). Additionally, male *Negr1*$^{-/-}$ mice also consumed smaller amounts of standard food, when the consumption of food was individually measured during 96 hours (Figure 20C).

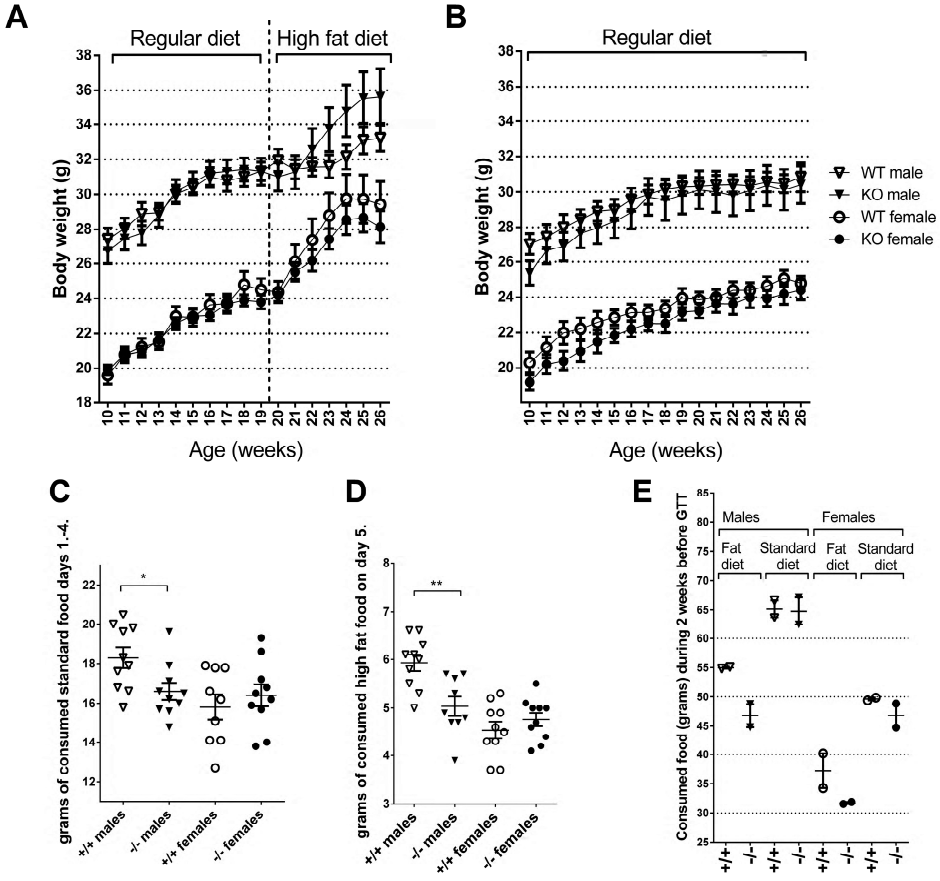

Figure 20. Body weight dynamics and food intake measurements. The body weight of the cohort VII mice was measured 10 weeks before the beginning of the HF diet. Mice received the HF diet for 7 weeks. Body weight dynamics of (A) HF diet groups and (B) standard chow group. Daily food intake measurements in single-housed mice prior to the food preference test showed that (C) WT males consumed significantly more standard food (days 1.–4.). (D) WT males also consumed significantly more HF food during the food preference test (day 5) compared to the *Negr1*$^{-/-}$ mice. (E) Food consumed (grams) during 2 weeks (14 days) before the glucose tolerance test in the cohort VIII of mice. The data points were calculated as food consumed per group of mice (n = 5 per group). Data represents mean ± SEM. *$p \leq 0.05$, **$p \leq 0.01$ (Mann-Whitney U test).

5.4.2. HF diet leads to higher levels of blood glucose in *Negr1*$^{-/-}$ mice, whereas phenotype difference in glucose tolerance test was apparent only in males

The HF diet elevated the level of basal blood glucose in both sexes, for male there was a diet effect ($p = 0.002$, $F = 10.23$) whereas females showed a genotype effect ($p < 0.001$, $F = 19.11$). However, the basal level of glucose was statistically higher in the HF diet fed *Negr1*$^{-/-}$ mice compared to the HF diet fed WT group ($p = 0.036$) in both sexes (Figure 21A). The HF diet increased the basal level of blood glucose in *Negr1*$^{-/-}$ male mice ($p = 0.0117$) (Figure 21B). In the female group there was no diet-effect ($F = 0.012$), on the other hand, the genotype effect was observed ($F= 19.11$). The basal level of glucose was significantly higher in the HF fed female *Negr1*$^{-/-}$ group compared to the HF diet fed WT group ($p = 0.001$) (Figure 21C).

For male mice, GTT was performed on the 6th week of the HF diet, and for females on the 6th and 13th week of the diet. In GTT, AUC was calculated for every mouse and two-way ANOVA and Tukey *post hoc* tests were used.

In male mice, the AUC of HF fed *Negr1*$^{-/-}$ mice was statistically significantly higher compared to *Negr1*$^{-/-}$ mice fed regular chow ($p < 0.001$) (Figure 21D). In female mice, the AUC of the HF diet fed mice on the 6th week of diet was statistically significantly higher compared to the regular chow group in both WT ($p = 0.002$) and *Negr1*$^{-/-}$ ($p = 0.018$) mice (Figure 21E). In the 13th week the results were similar to the 6th week; the AUC of female HF diet fed mice was statistically significantly higher than regular chow fed mice in both genotypes: WT ($p = 0.001$), *Negr1*$^{-/-}$ ($p = 0.0003$) (Figure 21F). When the different time points were analyzed separately, the blood sugar levels of HF diet fed male mice were significantly higher compared to HF diet fed WT mice at 30 min ($p = 0.001$) and 60 min ($p = 0.003$) time points (Figure 21G). The blood sugar levels of the HF diet fed *Negr1*$^{-/-}$ were significantly higher at 30 min ($p < 0.0001$), 60 min ($p < 0.0001$), 90 min ($p < 0.001$) and 120 min ($p = 0.013$) time points compared to regular chow fed *Negr1*$^{-/-}$ mice (Figure 21G). In female mice, on the 6th week of diet the blood sugar levels of the HF diet fed *Negr1*$^{-/-}$ mice were significantly higher at 30 min ($p < 0.001$) and 60 min ($p = 0.017$) time point compared to regular chow fed *Negr1*$^{-/-}$ mice, and for the HF diet fed WT mice the blood sugar levels were significantly higher at 30 min ($p < 0.0001$) and 60 min ($p < 0.001$) time points (Figure 21H). On the 13th week of the diet, the blood sugar levels of the HF diet fed *Negr1*$^{-/-}$ female mice were significantly higher at 30 min ($p = 0.011$), 60 min ($p = 0.003$), 90 min ($p < 0.001$) and 120 min ($p = 0.004$) time points compared to regular chow fed *Negr1*$^{-/-}$ mice (Figure 21I). In the WT group the blood sugar levels of the HF diet fed mice were significantly higher at 30 min ($p < 0.0001$), 60 min ($p = 0.002$), and 120 min ($p = 0.041$) timepoints (Figure 21I).

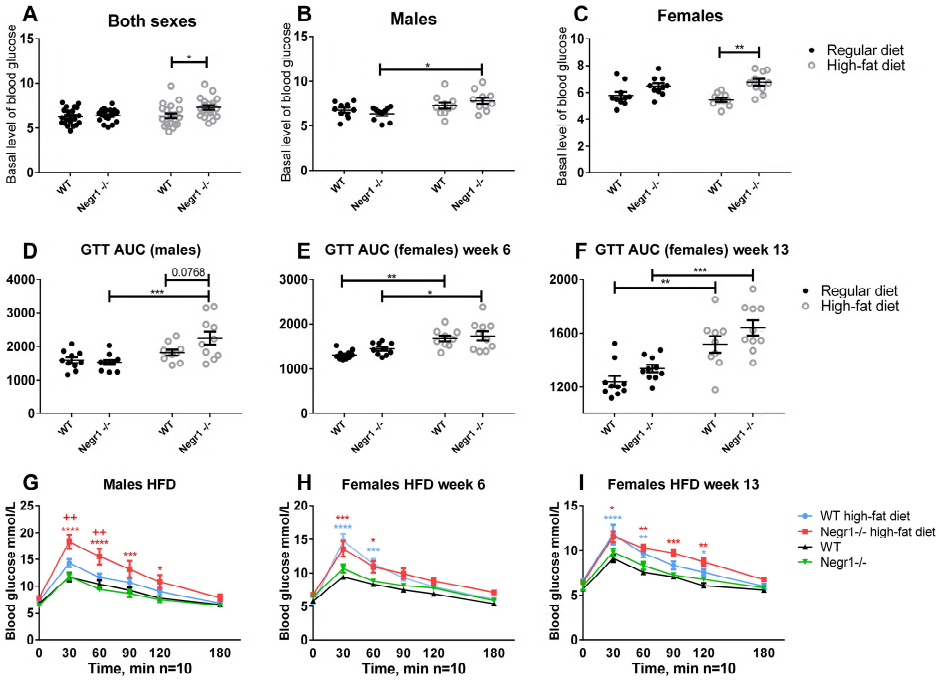

Figure 21. The basal level of glucose and glucose tolerance test. Basal level of glucose after 6 weeks of HF/standard diet when (A) both sexes were pooled together, (B) in the male group, and (C) in the female group. (D, G) Glucose tolerance test was performed for males after 6 weeks on the HF diet, and for females (E, H) after 6 and (F, I) 13 weeks of HF diet. (D–F) The bioavailability of glucose was estimated by calculating the area under the curve of plasma concentration (AUC) over the measured timepoints. (G–I) Mean values of blood sugar at different timepoints. Data represent mean ± SEM, *p ≤ 0.05, **p ≤ 0.01, ***p ≤ 0.001, ****p ≤ 0.0001 (diet effect), ++p ≥ 0.01 (genotype effect), two-way ANOVA (Bonferroni *post hoc* test (basal level of glucose), Tukey *post hoc* test (GTT).

5.4.3. HF diet induces an altered profile of circulating lipids sex-specifically *in Negr1*$^{-/-}$ mice

The level of saturated fatty acids (SFA) was markedly increased in the HF diet fed *Negr1*$^{-/-}$ male mice group ($p < 0.0001$) (Figure 22A). The level of SFAs were statistically significantly higher in the HF diet fed *Negr1*$^{-/-}$ group compared to regular chow fed *Negr1*$^{-/-}$ mice ($p = 0.017$) and HF diet fed WT mice ($p = 0.008$) (Figure 22A). In the female mice group the HF diet increased the level of SFAs similarly for both genotypes (Figure 22B).

Serum levels of phosphatidylcholines (PC), acylcarnitines and sphingomyelins (SM) were measured. Out of 100 quantifiable PC and SM species 87 were significantly altered due to HF diet. Among acylcarnitines C18 and C18:1 were significantly increased by HF diet, but C0, C2, C3, C4, C14 and C18:2 decreased significantly. If C2 level was looked at both sexes separately, there

were genotype effects only for females (p = 0.001) (Figure 22F). The level of C2 was statistically significantly lower in the regular chow fed *Negr1*$^{-/-}$ female mice group compared to the regular chow fed WT female mice group (p = 0.001) (Figure 22F).

There were not any statistically significant changes in the ratio of C2/C0 in male mice groups (Figure 22G). In female mice groups the HF diet decreased the ratio of C2/C0 in WT mice group (p < 0.0001) and in regular chow fed mice group the ratio of C2/C0 was statistically lower in *Negr1*$^{-/-}$ group (p = 0.047) (Figure 22H). The HF diet increased the ratio of unsaturated PC/SFA in the WT group for both males (p < 0.001) (Figure 22C) and females (p = 0.046) (Figure 22D). Although acylcarnitines with hydroxyacyl or dicarboxylic residues were frequently below the limit of quantification or even below the limit of detection their relative cumulative abundance among all acylcarnitines was higher in HF diet (p < 0.0001).

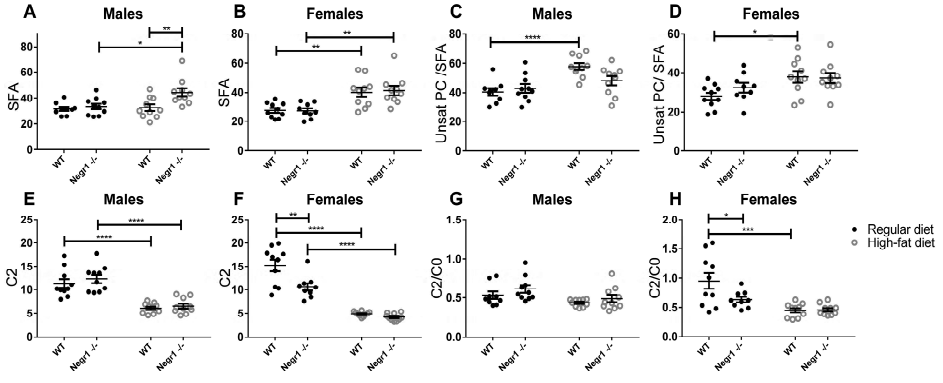

Figure 22. Effect of HF diet on the level of selected lipids and related ratios. Data represents mean ± SEM, *p ≤ 0.05, **p ≤ 0.01, ***p ≤ 0.001, ****p ≤ 0.0001, two-way ANOVA (Bonferroni *post hoc* test).

5.4.4. HF diet induced an increase in circulating amino acids in *Negr1*$^{-/-}$ mice, more prominently in males

To identify the differences caused by HF diet between WT and *Negr1*$^{-/-}$ two-way ANOVA [diet (regular or HF) × genotype (WT or *Negr1*$^{-/-}$)] and Bonferroni *post hoc* test was used. In WT animals, the HF diet had limited effect on serum amino acid levels.

When analyzed both sexes separately the total level of amino acids was statistically significantly increased only in the HF diet fed *Negr1*$^{-/-}$ male mice group (p = 0.023) (Figure 23A), in females there were no statistically significant changes (Figure 23B). The level of branched-chain amino acids (BCAA) was also statistically significantly increased only in the HF diet fed *Negr1*$^{-/-}$ male mice group (p = 0.05) (Figure 23G). If different BCAAs were looked at separately, the levels of Leu (p = 0.036) (Figure 23M) and Val (p = 0.031) were statistically significantly increased in the HF diet *Negr1*$^{-/-}$ group. When we analyzed both

sexes separately, the levels of Leu were significantly increased only in the HF diet fed *Negr1*$^{-/-}$ male mice group (p = 0.007) (Figure 23M). The HF diet increased the level of Val in both WT (p = 0.023) and *Negr1*$^{-/-}$ (p = 0.009) male mice.

In males the HF diet increased the level Lys (p = 0.005) (Figure 23K), in the *Negr1*$^{-/-}$ group. The level of Ala was not statistically significantly increased by HF diet but in the *Negr1*$^{-/-}$ group it showed a tendency towards increase (p = 0.061) (Figure 23I). In male group there were genotype effects for Gly (p = 0.011) (Figure 23Q), all three were statistically significantly higher in the HF diet fed *Negr1*$^{-/-}$ mice group compared to the HF diet fed WT mice group. In male WT groups the HF diet decreased the level of Gly (p = 0.001) (Figure 23Q).

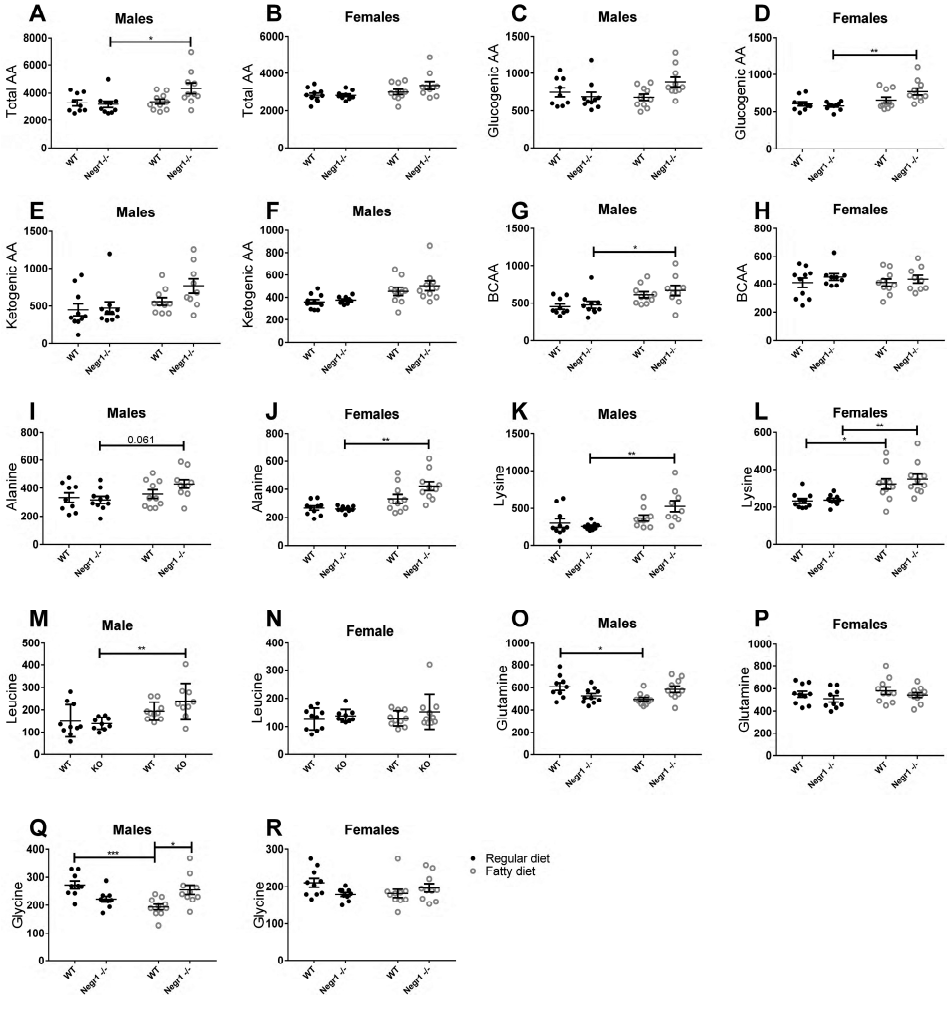

Figure 23. Effect of HF diet on the level of amino acids. In WT animals the HF diet had limited effect on serum amino acid levels. In *Negr1*$^{-/-}$ animals the HF diet increased the total pool of amino acids in blood. Data represents mean ± SEM, *p ≤ 0.05, **p ≤ 0.01, ***p ≤ 0.001, ****p ≤ 0.0001, two-way ANOVA (Bonferroni *post hoc* test).

In females HF diet increased the level of Ala ($p < 0.001$) (Figure 23J), Lys ($p = 0.006$) (Figure 23L) in the *Negr1*$^{-/-}$ group. The level of Lys was also increased in the WT group ($p = 0.036$). In other amino acids there were no statistically significant changes caused by the HF diet.

5.4.5. Altered profile of circulating organic acids in *Negr1*$^{-/-}$ mice

A few organic acids, including the citric acid cycle intermediates, were quantified in the blood serum in order to better identify the flux of metabolites. Male *Negr1*$^{-/-}$ mice had significantly higher citrate ($F = 5.5$, $p = 0.026$) (Figure 24A), beta-hydroxybutyrate ($F = 13.1$, $p = 0.001$) (Figure 24D), lactate ($F = 14.7$, $p < 0.001$) (Figure 24G), pyruvate ($F = 4.9$, $p = 0.035$), oxaloacetate ($F = 5.0$, $p = 0.034$) than WT male animals. Female mice had a weak oxaloacetate decrease due to diet ($F = 4.7$, $p = 0.040$), but other than that all diet and genotypes were similar. When both genders were combined, citrate ($F = 8.7$, $p = 0.005$) (Figure 24C) and lactate ($F = 4.3$, $p = 0.050$) (Figure 24I) remained significantly elevated in *Negr1*$^{-/-}$ animals. Lactate ratio to glucose was lowered by HF diet in female animals of both genotypes ($F = 9.7$, $p = 0.005$). In male, on the other hand, genotype had a significant effect with *Negr1*$^{-/-}$ having more lactate per glucose ($F = 11.1$, $p = 0.003$).

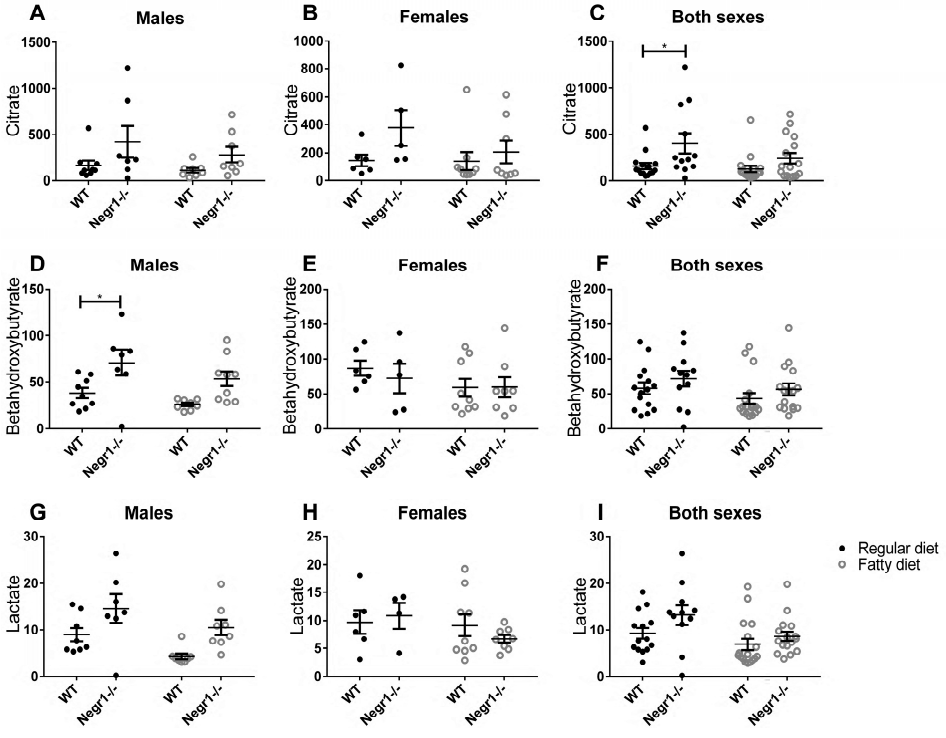

Figure 24. The levels of selected organic acids in males, females and in both sexes combined. Data represents mean ± SEM, *$p \leq 0.05$, two-way ANOVA (Bonferroni post hoc test).

5.5. *Negr1*$^{-/-}$ mice have increased levels of oxidative stress related proteins in Hip (Cohort X) (unpublished)

The levels of oxidative stress related proteins were measured using western blot analysis. Mann-Whitney U test showed that the levels of NOX2 ($p = 0.030$, WT – 0.43 ± 0.08, *Negr1*$^{-/-}$ – 0.71 ± 0.07) and GSH ($p = 0.003$, WT – 0.24 ± 0.03, *Negr1*$^{-/-}$ – 0.55 ± 0.08) (data not shown) are increased in the Hip of *Negr1*$^{-/-}$ mice.

6. DISCUSSION

6.1. Expression of *Lsamp* and *Negr1* in the monoaminergic nuclei and pathways

One of the aims of the current study is to explore the brain monoaminergic system in a mouse model deficient in either *Negr1* or *Lsamp* gene/protein for better understanding whether these neural circuits could be responsible for the links between *Negr1* and *Lsamp* polymorphisms and phenotypes of depression.

Several studies have shown associations between *Lsamp* and different neurotransmitter systems. Innos et al. have shown that deletion of *Lsamp* in mice induces alterations in GABAergic and dopaminergic neurotransmission (Innos et al., 2011; Innos et al., 2013a). It has been shown that *Lsamp* plays an important role as a leader molecule in dopaminergic axons (Schmidt et al., 2014). In addition, previous studies suggest that *Lsamp* is also involved in the serotonergic systems of the brain. We have previously reported that mice with *Lsamp*-deficiency have an increase in 5-HT turnover and changes in baseline 5-HT levels in several brain regions (Innos et al., 2013a).

In this study, we show that *Lsamp* transcripts are expressed both in the dorsal and median raphe nuclei, whereas the signal is slightly more intense in the dorsal raphe. The expression of *Lsamp* gene promoters varies in distinct nuclei; while both *Lsamp* 1a and 1b promoters are active in the dorsal raphe (Figure 4B), most of the expression in the median raphe comes from 1b promoter and most of the *Lsamp* expression in the caudal subgroup of raphe nuclei derives from 1a promoter (Figure 4). That indicates to us that *Lsamp* is expressed in the brain areas that receive input from raphe or send output towards raphe nuclei. Those stainings support the hypothesis that decreased anxiety-like phenotype in *Lsamp*-deficient mice could be regulated by changes in the serotonergic system. Both dorsal and median raphe nuclei project to the dorsal and ventral striatum, but more significantly to the ventral striatum. Additionally, dorsal raphe nuclei have a stronger projection to the ventral striatum (Hassanzadeh and Behzadi, 2007). Serotonin from the dorsal raphe nucleus activates a subpopulation of neurons in the bed nucleus of the stria terminalis (BST) in mice (Marcinkiewcz et al., 2017) and a prominent projection from the BST, which controls anxiety-related behaviors, directly targets DR serotonergic neurons (Dorocic et al., 2014). Strong LSAMP expression on the protein (Levitt, 1984) and transcript level (Reinoso et al., 1996) has been shown in the ventral striatum (both in the nucleus accumbens and BST) and we have meanwhile specified that most of the Lsamp expression in that area comes from 1a promoter (Philips et al., 2015). It has been shown that 5-HT from the dorsal raphe nucleus enhances fear and anxiety and activates a subpopulation of corticotropin-releasing factor neurons in the BST in mice (Marcinkiewcz et al., 2017). The serotonergic projection from DR also targets the basolateral nucleus of the amygdala (Gao et al., 2002), which shows a strong Lsamp 1a isoform specific staining (Philips et al., 2015). Intense Lsamp 1b isoform specific staining

has been shown in the central amygdala nucleus (Philips et al., 2015), which displays a major projection from the amygdala to the DR region (Dorocic et al., 2014). Basolateral nucleus of the amygdala and central amygdala nucleus, and the increase or decrease of connectivity between these nuclei has been shown to have an acute impact on anxiety-related behavior (Tye et al., 2011). Hippocampus receives serotonergic projections both from the DR (Kocsis et al., 2006) and median raphe nucleus (Cui et al., 2013). We have previously shown that the density of cells exhibiting 1b promoter activity is remarkably higher in the subgranular zone of the dentate gyrus in the hippocampal formation; 1a promoter, on the contrary, is selectively active in the pyramidal and granule cell layers (Heinla et al., 2015).

In human GWAS studies, the neural adhesion molecule encoding *NEGR1* gene has been linked with both depression and obesity (Thorleifsson et al., 2009; Speliotes et al., 2010; Hyde et al., 2016; Howard et al., 2018). Altered monoaminergic neurotransmission has also been linked with both obesity (Geiger et al., 2009; Sjödin et al., 2010) and depression (Belujon & Grace, 2017) and these conditions could be connected to the neural pathways that are guided and maintained in the presence of NEGR1 protein. The expression of *Negr1* has been shown in both dopaminergic nuclei and projection areas such as substantia nigra pars compacta, VTA, islands of Calleja in the VSTR (Singh et al., 2019) and in the fasciculus retroflexus, which serves as a molecular scaffold for dopaminergic axons that grow from the midbrain towards the habenula (Schmidt et al., 2014). Additionally, *Negr1* has been identified as a differentially expressed gene across 5-HT neuron subtypes, whereas the expression of *Negr1* was highest in the median raphe (Okaty et al., 2015).

In our earlier studies with *Negr1*, we have shown that compared to other brain areas, the expression of NEGR1 is sparse in the striatal areas, especially in the DSTR of adult mice (Jagomäe et al., 2021). To estimate NEGR1 protein expression and impact in the dopaminergic signaling in the striatal area, we performed *Negr1* and tyrosine hydroxylase co-stainings in the striatal area (results not shown in the dissertation, see paper II). We found that *Negr1* in the striatum is highly expressed in the fibers and moderately on cell bodies where *Negr1* also shows co-localization with tyrosine hydroxylase, indicating that *Negr1* is expressed in the same cells where dopamine is synthesized. This staining indicated that at least some amount of the NEGR1 protein in the striatum is not synthesized in the cell bodies in the striatum but is expressed on the axon bundles projecting through it. The more specific identification of these bundles remains to be clarified in future studies.

Next, we also studied potential expression of NEGR1 in the region from midbrain to pons, by using triple immuno-stainings for tryptophan hydroxylase, tyrosine hydroxylase and NEGR1 (results not shown in the dissertation, see paper II). Additionally, to striatum, we found co-expression of tyrosine hydroxylase and NEGR1 also in the VTA/substantia nigra region. Our findings of more prevalent NEGR1 expression in the median raphe compared to dorsal raphe are in line with the findings from Okaty et al. (2015) and stainings available in the

Allen Brain Atlas. In the median raphe, NEGR1 is present in both the tyrosine hydroxylase and tryptophan hydroxylase-positive cells, whereas in the dorsal raphe, the expression of NEGR1 is minor (results not shown in the dissertation, see paper II).

In conclusion, we show that *Lsamp* is expressed both in the dorsal and median raphe nuclei and the expression of *Lsamp* gene promoters varies in distinct nuclei. NEGR1 protein is present in both dopaminergic and serotonergic pathways; in the tyrosine hydroxylase-positive cells in both striatum and midbrain and in the raphe where NEGR1 is mostly present in the median raphe.

6.2. Effects of escitalopram on the *Lsamp*- and *Negr1*- deficient mice

We challenged the monoaminergic neurotransmission of mice lacking *Negr1* or *Lsamp* and their WT littermates with chronic injection of escitalopram. The behavior of these mice was tested, and brain monoamines and gene expression were measured from the brain consequently.

In previous studies we have shown that the average body weight of *Lsamp* deficient mice tends to be 5–10% lower compared to their WT littermates (Innos et al., 2011). In this study, we also saw that *Lsamp* deficient tended to have lower baseline bodyweight compared to WT littermates but after escitalopram treatment the weight difference is lost. But we did not detect any statistically significant *post hoc* differences due to high variance of the data (Figure 5). Nevertheless, the observation that 5-HT turnover was increased in most of the brain areas tested in *Lsamp* deficient mice fits well with the current view that increased 5-HT activity is linked to reduced body weight (Voigt and Fink, 2015).

Lsamp-deficient mice showed signs of reduced anxiety, increased exploratory activity and behavioral disinhibition, entering more frequently to both open and closed arms, as well as making more head dips, both protected and unprotected (genotype effects, Figure 6A, B, C). During the first five minutes in the open field test, chronic escitalopram treatment significantly increased exploratory activity in both genotypes (Figure 6F). In the elevated plus-maze, escitalopram significantly increased entries to the closed arms in *Lsamp*-deficient mice (Figure 6A). *Lsamp*-deficient mice displayed a specific behavioral pattern in the tail suspension test that was not dependent on the injected substance: a significantly higher number of short (1–2 s) episodes of immobility compared with their WT littermates (Figure 6J). The meaning or physiological basis of short immobility episodes remains to be clarified in the future studies.

In this study we found that *Lsamp*-deficient mice had higher levels of 5-HIAA, the main 5-HT metabolite, in the raphe region and in the dorsal striatum. (Figure 7B). Therefore, as demonstrated in the two independent studies (Innos et al 2013a; Bregin et al, 2020), elevated 5-HT turnover in the brain is typical for the pharmacologically unaffected *Lsamp*-deficient animals (saline group) both after acute and chronic injections. In the current experiment, this effect was

significantly detected only in the Hip of WT mice (Figure 7B). Escitalopram decreased 5-HIAA levels in the raphe region, DSTR, and Hip of *Lsamp*-deficient animals. Escitalopram also decreased 5-HT turnover in the raphe, VSTR, DSTR and Hip of *Lsamp*-deficient animals. These findings confirm our earlier findings that the 5-HT turnover in the brains of *Lsamp*-deficient animals is increased (Innos et al., 2013a, Innos et al., 2013b). Increased activity in the elevated plus-maze following SSRI treatment in the current study was associated by a decrease in 5-HT turnover levels, demonstrating less anxiety in *Lsamp*-deficient animals. Human studies have shown that people with panic disorder (Esler et al., 2007) and MDD (Barton et al., 2008) who are not taking medication had higher levels of brain 5-HT turnover. High brain 5-HT turnover may also be a significant biological substrate for both MDD and panic disorder, as evidenced by the fact that 5-HT turnover in these patients significantly decreased after receiving SSRI medication, and by the symptomatic improvement that followed (Esler et al., 2007; Barton et al., 2008).

In this study, we also investigated the effect of chronic escitalopram treatment on *Negr1*-deficient mice, another member of IgLON superfamily. Differently from *Lsamp*-deficient mice, *Negr1* deletion did not induce alterations in the behavior of mice after chronic administration of escitalopram. (Table 2). However, we found that escitalopram could rescue the significantly smaller volumes of hippocampi that *Negr1*$^{-/-}$ mice have compared to WT (Figure 18), the phenotype that we have shown earlier (Singh et al, 2019). This result is intriguing, especially as it has been demonstrated earlier that depression-related changes in the hippocampal volume could be prevented by antidepressant treatment (Czéh et al., 2001). Still, several other studies indicate that hippocampal atrophy is persisting despite treatment of depression and long-term remission (Sapolsky, 2001). It is questionable if *Negr1*$^{-/-}$ mice could be model for depression despite the strong links of the human *NEGR1* gene with depression phenotypes in accumulating studies, because higher levels of NEGR1 have been described in the tissues and body fluids of depressed patients. However, it is likely that *Negr1* is regulating pathways that are linked with depression and therefore its role in the reactivity to escitalopram deserves further studies.

Similarly, to *Lsamp*-deficient mice, escitalopram induced a decrease in 5-HT turnover in both genotypes of mice, but this effect was highly significant only in the raphe of *Negr1*$^{-/-}$ mice (Figure 11). This indicates an overlapping function of these homologous proteins. In *Negr1*$^{-/-}$ mice, however, we could not see an increased 5-HT, which was evident in *Lsamp*$^{-/-}$ mice. Furthermore, escitalopram induced a robust decrease in dopamine turnover only in *Negr1*$^{-/-}$ mice; this effect was amplified by the increased baseline turnover of dopamine (DOPAC/DA) in the *Negr1*$^{-/-}$ raphe compared to WT. In fact, the significant treatment effect suggests that escitalopram induced the elevation of 5-HT in the raphe of both *Negr1*$^{-/-}$ and WT mice, but the significant elevation of dopamine was induced only in the raphe of WT mice, suggesting that alterations in the dopamine system could affect the serotonergic neurotransmission in *Negr1*$^{-/-}$ raphe. We detected dopamine-related changes in the raphe of *Negr1*$^{-/-}$ mice that were not seen in

Lsamp$^{-/-}$ mice suggesting distinct functions of these proteins in specific mono-aminergic pathways. Accumulating evidence suggests that serotonergic system has an impact on the activity of dopaminergic neurons in the striatum (Navailles & De Deurwaerdère, 2011), thus, the altered interplay of dopamine and 5-HT might also be responsible for the altered sensitivity to amphetamine in *Negr1*$^{-/-}$ mice, possibly indicated by the increased 5-HT metabolite 5-HIAA in the VSTR of *Negr1*$^{-/-}$ mice (Table 3).

Differently from *Lsamp*-deficient mice, in *Negr1*-deficient mice we saw an upregulation of the serotonin transporter (*Slc6a4*) (Figure 11) which is the main target of escitalopram in the raphe of *Negr1*$^{-/-}$ mice. In *Lsamp*-deficient mice we detected a significant elevation in *MaoA* transcript expression specifically in the raphe area, which is in line with the most prominent elevation of 5-HIAA in this area in *Lsamp*-deficient mice. Moreover, the levels of DOPAC, another product of *MaoA*, were also elevated only in the raphe of *Lsamp*-deficient mice. Both 5-HIAA and DOPAC were restored to the levels of WT mice by escitalopram treatment. These findings together with the elevation of *MaoA* transcript in the raphe suggest elevated activity of serotonin transporter (SERT) in *Lsamp*-deficient mice. Although elevated brain 5-HT turnover is influenced by the SERT genotype in human patients (Barton et al., 2008), we did not detect any alterations in serotonin transporter gene (*Slc6a4*) mRNA expression in the raphe area of *Lsamp*-deficient mice. Nevertheless, the activity of SERT is most probably increased in *Lsamp*-deficient mice since the SERT blocker escitalopram reverses their 5-HT turnover (Table 4).

Table 2. Comparison of the behavioral effect of escitalopram on *Lsamp*- and *Negr1*-deficient mice.

	Lsamp	***Negr1***
Elevated plus maze		
Closed arm entries	In *Lsamp*$^{-/-}$ mice, escitalopram administration significantly increased the number of closed arm entries.	No significant post hoc effects
Open field test		
Distance travelled in first 5 minutes	In WT mice, escitalopram administration significantly increased the distance travelled.	No significant post hoc effects
Corner visits in first 5 minutes	In *Lsamp*$^{-/-}$ mice, escitalopram administration significantly increased the number of corner visits.	No significant post hoc effects

Table 3. Comparison of the effect of escitalopram on the monoamine levels of *Lsamp*- and *Negr1*-deficient mice. Some results shown in this table are not shown in the dissertation result section, for more information see paper I (Bregin et al., 2020).

	Lsamp	***Negr1***
Monoamines in Hip		
5-HIAA	Escitalopram reduced 5-HIAA levels in both groups but notably, to a greater extent in in *Lsamp*$^{-/-}$ mice.	No significant post hoc effects
5-HT turnover	Escitalopram administration reduced 5-HT turnover significantly in *Lsamp*$^{-/-}$ mice.	No significant post hoc effects
Monoamines in raphe		
Serotonin (5-HT)	Chronic escitalopram reduced the level of 5-HT significantly in *Lsamp*$^{-/-}$ mice.	No significant post hoc effects
5-HIAA	In *Lsamp*$^{-/-}$ mice receiving saline, 5-HIAA level was significantly higher than in WT groups. Escitalopram reduced the level of 5-HIAA significantly in *Lsamp*$^{-/-}$ mice.	No significant post hoc effects
5-HT turnover (5-HIAA/5-HT)	Escitalopram treatment decreased 5-HT turnover significantly only in *Lsamp*$^{-/-}$ mice. However, the baseline 5-HT turnover was significantly higher in *Lsamp*-deficient mice receiving saline compared to the WT mice receiving saline.	Escitalopram significantly decreased the 5-HT turnover in the *Negr1*$^{-/-}$ group.
Dopamine (DA)	No significant post hoc effect	Escitalopram significantly increased the level of DA in the WT group.
DOPAC	*Lsamp*$^{-/-}$ mice had a significantly higher level of DOPAC. Escitalopram decreased the level of DOPAC significantly in *Lsamp*$^{-/-}$ mice.	In *Negr1*$^{-/-}$ mice, escitalopram significantly decreased the level of DOPAC.
DA turnover (DOPAC/DA)	No significant post hoc effect	DA turnover was significantly higher in the *Negr1*$^{-/-}$ saline group compared to the WT saline group and escitalopram significantly decreased the DA turnover in the *Negr1*$^{-/-}$ group.

Table 4. Comparison of the gene expression levels of *Lsamp*- and *Negr1*-deficient mice.

	Lsamp	***Negr1***
MaoA	Significantly increased in the *Lsamp*$^{-/-}$ mice raphe area.	No significant change
Slc6a4	No significant change	Significantly increased in the *Negr1*$^{-/-}$ mice raphe area.
Dat	Significantly decreased in the VTA (Innos et al, 2013).	Significantly increased in the VTA.

In conclusion, deficiency of either *Negr1* or *Lsamp* causes several changes in the level of monoamines. While the *Lsamp* affects more the level of 5-HT and its metabolites, *Negr1* is more associated with dopamine system and affects more the level of dopamine and its metabolites. In *Lsamp*$^{-/-}$ we saw increased 5-HT turnover, which was reduced by the escitalopram, higher 5-HT turnover has also been described in the individuals with depression and also is decreased by the SSRI treatment. Any imbalance in the level of monoamines can lead to a wider range of changes in the brain that can eventually lead to development of psychiatric disorders.

6.3. Effects of amphetamine in the *Negr1*-deficient mice

Since we saw changes in the turnover of dopamine particularly in *Negr1*-deficient mice compared to controls, we tested the effect of amphetamine on these mice. Amphetamine increases dopaminergic and noradrenergic neurotransmission, and its effect could highlight potential impairments in dopaminergic signalling in *Negr1*-deficient mice.

6.3.1. Increased behavioral sensitization to amphetamine and upregulation of *Dat* transcript in *Negr1*$^{-/-}$ mice

We studied whether *Negr1*-deficient mice show altered sensitivity to chronic amphetamine treatment. Ten-day administration of amphetamine induced significantly higher motor and stereotypic activity in *Negr1*$^{-/-}$ compared to WT mice, indicating a higher behavioral sensitivity to amphetamine (Figure13) (Table 5). It has been shown earlier that time-dependent changes in behavioral sensitization to amphetamine are associated with time-dependent changes in amphetamine-stimulated DA release in the striatum (Paulson & Robinson, 1995).

Table 5. Comparison of the behavioural effects of amphetamine in *Lsamp*- and *Negr1*-deficient mice.

	Acute amphetamine	**Chronic amphetamine**
Negr1 –/– vs WT	Tendency towards decreased sensitivity to the acute amphetamine in Negr1$^{-/-}$ mice in dose response experiment (6 mg/kg) and on the first day of chronic amphetamine administration (3 mg/kg) (current study, Kaare et al., 2022)	Increased time-dependent sensitivity to chronic amphetamine (10 days) in Negr1$^{-/-}$ mice (current study, Kaare et al., 2022)
Lsamp –/– vs WT	Decreased sensitivity to the acute amphetamine in Lsamp$^{-/-}$ mice both in case of 5 mg/kg and 7.5 mg/kg but not 2.5 mg/kg (Innos et al., 2013)	not available

Transcripts encoding proteins regulating dopaminergic neurotransmission were mostly significantly increased in the striatum and VTA of *Negr1*$^{-/-}$ mice. Namely, *Dat* transcripts were significantly upregulated both in the VTA and VSTR in *Negr1*$^{-/-}$ mice at baseline (Figures 16 and 17). The *Dat* plays a central role in the regulation of dopaminergic signaling; *Dat* overexpressing transgenic mice demonstrate markedly increased locomotor responses to amphetamine compared with WT animals (Salahpour et al., 2008). Likewise, reduced *Dat* expression has been shown to diminish amphetamine's locomotor stimulatory effects (Cagniard et al., 2014). Furthermore, similarly to our current finding in the VSTR in *Negr1*$^{-/-}$ mice, an increase in the amount of DA released by amphetamine has been shown in the *Dat* overexpressing mice (Salahpour et al., 2008). Transcripts encoding tyrosine hydroxylase, *MaoA* and *MaoB* were also upregulated in the VTA, whereas *Comt* was upregulated in the VSTR at baseline (Figures 16 and 17).

From our previous studies we have shown that deletion of other IgLONs, both *Lsamp* (Table 5) and *Ntm,* induces reduced sensitivity for the acute amphetamine in mice (Innos et al, 2013, Singh et al, 2018a). Moreover, this phenotype is the only overlapping phenotype in mice deficient for either *Lsamp* or *Ntm* and the insensitivity phenotype is magnified in *Lsamp*$^{-/-}$*Ntm*$^{-/-}$ double mutant mice. Indeed, in the current study we could not see clear genotype difference in behavior of amphetamine groups, however our data indicates tendency toward reduced sensitivity in case of acute administration of amphetamine, therefore IgLON family of neural adhesion molecules could be collectively responsible for the fine tuning of neural circuits involved in both acute and chronic responses of amphetamine.

6.3.2. Altered molecular reactivity to the amphetamine in the brains of *Negr1*$^{-/-}$ mice

The expected effect of amphetamine on the turnover of DA was similar in the striatum in both *Negr1*$^{-/-}$ mice and their WT controls. In our current study, significantly increased DA levels after 10-day administration of amphetamine were

evident in the DSTR in *Negr1*$^{-/-}$ mice. However, the DA metabolite 3-MT was elevated in the VSTR in *Negr1*$^{-/-}$ mice, indicating that DA release was increased there as well. Increased levels of the *Comt* transcript in the VSTR are further fitting with the higher dopamine release along with higher DA turnover in the VSTR in *Negr1*$^{-/-}$ mice (Figure17). The difference that we see between DSTR and VSTR, could indicate a differential effect of amphetamine on the DA release and uptake in DSTR and VSTR (Avelar et al., 2013; Siciliano et al., 2014) (Figure 17).

The baseline levels of DA itself were not found to be altered in the brain areas of *Negr1*$^{-/-}$ mice, however, several significant alterations in several brain areas of the *Negr1*$^{-/-}$ mice suggest increased turnover of DA but also increased turnover of serotonin. Increased turnover of DA to 3-MT was evident in both dorsal and VSTR. Interestingly, serotonin metabolite 5-HIAA was increased only in the VSTR of *Negr1*$^{-/-}$ mice. Although amphetamine suppressed 5-HIAA in both genotypes, the 5-HIAA still remained higher in *Negr1*$^{-/-}$ mice. The upregulation or the tendency for upregulation of monoamines and their metabolites in saline-injected *Negr1*$^{-/-}$ mice was most evident in the Hip area. The results from mice receiving saline chronically from amphetamine study and escitalopram study could be regarded as replicates (Figure 19) and they indicate genotype differences between knockout and control groups in two distinct age groups; the age of mice at the end of escitalopram study was 3 months and the age of mice in the end of amphetamine study was 5 months. Significantly higher levels of 3-MT, tyramine, 5-HT, 5-HIAA, noradrenaline and normetanephrine in *Negr1*$^{-/-}$ mice compared to WT could be detected tyrosine.

Increased *Dat* and tyrosine hydroxylase in the midbrain after amphetamine have been described earlier in wild type animals (Shilling et al., 1997; Dietz et al., 2005), likewise, in the current study, amphetamine induced an increase in tyrosine hydroxylase and a tendency for increased levels of *Dat*, *Comt* and *Drd2* in WT mice in the VTA. In *Negr1*$^{-/-}$ mice, on the contrary, these transcripts showed a tendency for reduction after amphetamine, indicating altered molecular reactivity to amphetamine in the brains of *Negr1*$^{-/-}$ mice (Figures 16). Similarly, in the Hip of WT mice, amphetamine significantly increased the levels of 5-HTand normetanephrine and induced a tendency for increase of several monoamines including dopamine. In the Hip, however, the changes that amphetamine induced in monoamine profile were quite different in *Negr1*$^{-/-}$ mice; the only significant effect of amphetamine was the reduced level of tyrosine (Figure 19).

The stronger behavioral effect of amphetamine in *Negr1*$^{-/-}$ mice could have also been modulated by the trace amine associated receptor 1 (TAAR1) that has been shown to serve as a direct intracellular target for amphetamines in dopaminergic neurons (Underhill et al., 2019). TAAR1 is stimulated by amphetamine, but also by a variety of trace amines and monoamines, which are upregulated in the brains of *Negr1*$^{-/-}$ mice, such as tyramine and 3-MT. The increased levels of endogenous agonists could have an impact on the sensitivity of TAAR1, which could in turn, influence the effects of amphetamine.

6.3.3. *Negr1*$^{-/-}$ mice display reduced sensitivity to stress and show less activity during chronic injections/testing

In the chronic amphetamine study, the genotype differences appeared already prior to injections, as the open field test for baseline activity (7 days before injections started) and a consequent housing in single cages induced the expected decrease in the body weight of WT mice, whereas the body weight of *Negr1*$^{-/-}$ mice stayed stable or even increased slightly during the same time period (Figure 14) resulting in the disappearance of previously significant body weight difference between genotypes. This indicates that *Negr1*$^{-/-}$ mice were less sensitive to the single-housing stress similarly to the phenotype we have previously described in *Lsamp*$^{-/-}$ mice (Innos et al., 2012). In the baseline open field test, *Negr1*$^{-/-}$ mice spent significantly more time in the center of the open field, indicating higher exploratory activity and reduced anxiety (the results of this experiment have been published in Singh et al., 2019). During the course of daily chronic injections, housing in single cages and testing, however, saline-receiving *Negr1*$^{-/-}$ mice became less active in most of the behavioral parameters that were measured, including total distance traveled and distance in the center (Figure 14). Interestingly, *Negr1*$^{-/-}$ mice performed significantly less rearings both during baseline testing (Singh et al., 2019) and during the course of chronic testing/ injections in the current study. Previous studies have found that damage to the Hip impairs rearing due to failures in spatial memory, where novelty detection is impaired (Barth et al., 2018). The hypothesis that reduced rearing in *Negr1*$^{-/-}$ mice could be the expression of impaired hippocampal morphology is supported by accumulating data of reduced size of Hip in *Negr1*$^{-/-}$ mice and numerous molecular and cellular alterations in the hippocampi of *Negr1*$^{-/-}$ mice (Singh et al., 2018; Singh et al., 2019; Noh et al., 2019).

6.4. *Negr1* deficiency-induced alterations in the monoaminergic neurotransmission could explain links of *NEGR1* with both depression and obesity phenotypes

Depression and obesity are leading public health concerns worldwide. Shared genetic risk factors between depression and obesity have been reported, which could be mediated through shared etiological pathways, such as dysfunction of the hypothalamic–pituitary axis (Bornstein et al., 2006; Ouakinin et al., 2018; Leidmaa et al., 2020). Imbalance of monoaminergic neurotransmission in the brain areas, such as mesolimbic pathways (Belujon & Grace, 2017), raphe (Fazecas et al., 2021) and Hip have been shown to underlie depressive conditions. This study showed that *Negr1*$^{-/-}$ mice display a time-dependent increase in behavioral sensitization to amphetamine associated with changes in amphetamine-stimulated DA release in the ventral and DSTR, indicating altered reactivity of mesolimbic pathways in mice lacking NEGR1 protein. Mesolimbic pathways underlying reward processing were our special interest as dysfunctional reward

processing that has been described both in depressive patients (Admon & Pizzagalli, 2015; Ng et al., 2019) and obese subjects (Kenny, 2011; Volkow et al., 2011). Thus, there could be a shared mechanism underlying both obesity and depression. Anhedonia, one of the core symptoms of depression, has been linked to dysfunctions in the reward system, and in particular the DA system (Yadid et al., 2008). Therefore, we next studied hedonic eating and metabolism in *Negr1*$^{-/-}$ mice. More specifically, our purpose was to add evidence that would enable us to determine whether the impact of NEGR1 is established mainly through its function as a cell adhesion molecule in the hypothalamus, or whether it also has a distinct role in the systemic metabolism, which could, in turn, contribute to the etiology of psychiatric disorders.

6.5. Body weight and metabolic profile of *Negr1*-deficient mice on HF diet

6.5.1. Effects of HF diet on the body weight and food consumption of *Negr1*-deficient mice

In the final part of the current study, we found that both male and female *Negr1*$^{-/-}$ mice tended to have slightly lower body weight when on a standard diet, in accordance with an earlier study in *Negr1*$^{-/-}$ mice (Lee et la., 2012). Male *Negr1*$^{-/-}$ mice also consumed smaller amounts of standard food when measured individually for 96 h. A HF diet leads to body weight gain in both genotypes and both genders. Surprisingly, genotype difference occurred only in male mice (Figure 20). The WT males tended to gain less body weight when on HF diet compared to *Negr1*$^{-/-}$ male mice; however, this effect was not related to higher amounts of consumed food. On the contrary, the WT males consumed higher amounts of HF food in the food preference test, in which the consumed food was individually measured for 24 h. Furthermore, male *Negr1*$^{-/-}$ mice had a tendency to eat less HF food but nevertheless gain more weight also in group-housing settings. Our data indicate that *Negr1*-deficiency induces alterations in the efficiency of energy storage.

Interestingly, the initial approach to and consumption of the HF food during the first hours of the food preference test was not altered in *Negr1*$^{-/-}$ mice. Measuring the acute consumption of energy-dense and palatable HF food allows us to estimate the changes in the reward processing (hedonic liking/wanting), as well as the acute homeostatic mechanisms that regulate the control of food intake (Leidmaa et al., 2020). *Negr1*$^{-/-}$ mice seem to have a normal hedonic appetite and the corresponding satiety induction in the beginning of the food preference test. During a longer exposure to HF food (24 h), however, the *Negr1*$^{-/-}$ males reduce their energy intake more than the WT. This could be explained by the impaired glucose tolerance and corresponding metabolic alterations in these mice, discussed in the next paragraph. Reduced food intake could be an attempt to compensate for the metabolic challenge present in the *Negr1*$^{-/-}$ males, particularly

during the HF diet exposure. Previous studies have also shown that a restricted feeding schedule increases *Negr1* (22%) in the arcuate nucleus/ventromedial hypothalamus of rats (Boender et al. 2014), and that NEGR1 protein is increased in the lateral hypothalamus of fasted chicks (Liu et al., 2019). NEGR1 in certain hypothalamic nuclei might, therefore, lead to increased appetite, which would be in line with our findings of decreased food consumption in *Negr1*$^{-/-}$ mice. These effects may be site-specific, however, as administration of NEGR1 ectodomains into the paraventricular nucleus of the hypothalamus is shown to induce an opposite effect: a 20% decrease in food intake in rats (Venkannagari et al., 2020). Reduced intake of HF food during the first 24 hours could also be a sign of altered reward processing, which, however, needs further research.

6.5.2. HF diet alters the glucose tolerance of male *Negr1*-deficient mice

The role of *NEGR1* in glucose homeostasis has been previously demonstrated in many instances. Schlauch et al. (2020) have shown by GWAS studies that, besides obesity in the general population, *NEGR1* gene also associates with BMI in type 2 diabetes patients, with abnormal glucose levels and impaired fasting glucose. A direct impact on serum glucose levels has been demonstrated in *Negr1*$^{-/-}$ mice with a >1.3-fold increase in serum glucose and insulin levels (Joo et al., 2019). While the level of leptin was substantially higher, the level of insulin-sensitizing adipokine adiponectin was lower in the *Negr1*$^{-/-}$ mice (Joo et al., 2019).

Our experiments in this study indicate that, when on the standard diet, males and females from both genotypes have similar basal glucose levels (Figure 21). HF food, however, leads to higher levels of blood sugar in *Negr1*$^{-/-}$ mice, as reported by earlier studies. In male mice, HF diet resulted in altered glucose tolerance only in *Negr1*$^{-/-}$ mice. In females, HF diet altered glucose tolerance in both genotypes, and no genotype effect appeared after either 6 weeks or 13 weeks. Although males are more likely to develop insulin resistance and hyperglycemia in response to nutritional challenges (Tramunt et al., 2020), impaired glucose tolerance is more prevalent in women (Mauvais-Jarvis et al., 2018). The gender dependence of glucose metabolism is in fact a complex outcome of many factors, such as muscle mass, muscle-to-fat ratio, and the nature of dysfunction in insulin signaling (Mauvais-Jarvis et al., 2018). It should also be noted that the animals in our experiment did not develop diabetes, although the glucose tolerance test indicated a significant impairment in glucose homeostasis under some experimental conditions. With WT male mice having a slightly elevated basal glucose, and females performing worse in the glucose tolerance test, current results are in accordance with previous reports.

6.5.3. Gender-specific changes in the metabolism of lipids of *Negr1*-deficient mice caused by HF diet

The HF diet is expected to overload fatty acid metabolism in one way or another. If ketogenic, HF would upregulate beta-oxidation, ketogenesis, and gluconeogenesis. If the HF diet has enough carbohydrates, a large portion of dietary fats would be stored as fat and none of the previously mentioned metabolic pathways need to be activated.

We observed nearly unanimous increases in serum PC and SM lipids due to the HF diet. Acylcarnitines at the same time decreased, with the exception of stearyl- and oleyl-carnitine, which increased. According to the manufacturer, palmitoyl, stearyl, and oleyl residues are the most dominant lipids in the HF diet formula. A high load of long-chain acyl residues increased various species of lipids, while the amount of free carnitine and short-chain acylcarnitines decreased due to activity and low substrate specificity of carnitine-acyl transferases. Hence, the pattern of changes due to the HF diet was as expected (Figure 22).

Hydroxylated acylcarnitines and acyl residues with two carboxylic acids could not be properly quantified in most samples. Therefore, the observed relative increase in the total amount of all hydroxylated and dicarboxylic acyl residues may be erroneous. Even more, an overload of acyl residues is expected to activate omega oxidation, which generates dicarboxylic acids and, thereby, alleviates the overload of lipid catabolism pathways. Ketone bodies appeared not to be increased by HF diet, and the individual acylcarnitines, as well as their ratios, did not imply that beta-oxidation and ketogenesis intensified because of our dietary intervention.

The fact that serum lipoproteins have gender-dependent reference values is common knowledge in clinical chemistry. Variations in male and female serum PC species, besides cholesterol and triglycerides, have also been shown previously (Rauschert et al., 2017). Higher beta-hydroxybutyrate levels in females on a standard diet have been reported before as well (Cochran et al., 2018). Thus, the gender differences in lipids found here are in accordance with previously published data. Somewhat surprisingly, the genotype effect on lipid profile appeared to be marginal in our experiment.

6.5.4. Gender-specific changes in the metabolism of amino acids of *Negr1*-deficient mice caused by HF diet

In WT animals, the diet had a limited effect on serum amino acid levels (Figure 23). In *Negr1*$^{-/-}$ animals, particularly in males, the HF diet increased the total pool of amino acids in blood. It did not seem to be related to the essentiality of glucogenicity of the amino acids. The most significant was the increase for Lys, Thr, Ala, Ser, and His. With the reduced relative abundance of proteins in the HF diet, the increased level of essential amino acids (Lys, Thr, and His, in particular) implies increased protein breakdown in the body. Indeed, decreased muscle mass has been demonstrated in another strain of *Negr1*$^{-/-}$ mice (Joo et la., 2019) and

the same result was replicated in the current study, suggesting that *Negr1*$^{-/-}$ mice might also be prone to the protein breakdown in the case of standard feeding.

If the increased protein breakdown is accompanied by increased amino acid usage in peripheral tissues, Ala and Gln should increase in serum because of shuttling of the amino group to the urea production in the liver. Female mice had a relative increase in Ala, but males, on the contrary, showed a weakly significant decrease in Gln. Additionally, the urea cycle intermediates (Arg, Cit, Orn) and their ratios did not indicate an overload of the urea cycle. The ratio of short-chain acylcarnitines and BCAA decreased with HF diet for both sexes, which indicates that, although BCAA levels increase, they are not catabolized into short-chain acyl radicals, which would be a necessary step in their oxidation.

The decrease in Glu and Gln on HF while nearly all other amino acids are either unchanged or increased might be a meaningful anomaly. Most logically, Glu could be transaminated to alpha-ketoglutarate, enter the tricarboxylic acid cycle, and be used for energy, either directly or indirectly via gluconeogenesis. Indeed, there was a tendency of reduced levels of alpha-ketoglutarate and oxaloacetate in animals consuming the HF diet.

Interestingly, Ala and Ser have elevated concentrations in *Negr1*$^{-/-}$ on HF, although they are closely related to pyruvate and 3-phosphoglycerate, serving as potential substrates for gluconeogenesis. Ala generation in the periphery/muscles may simply exceed its use in the liver. This notion is supported by the fact that lactate, another gluconeogenesis substrate closely related to Ala and pyruvate, is not increased by the HF diet. However, comparing Ala and Gln levels and Ser- and alpha-ketoglutarate-related amino acids, there seems to be a preference to use carbons in alpha-ketoglutarate form rather than any gluconeogenic substrate. Alpha-ketoglutarate would be converted to oxaloacetate, which, besides being a starting point for gluconeogenesis, can be converted to aspartate by transamination. The latter is needed for the urea cycle and elimination of excessive nitrogen from increased amino acid catabolism. Gluconeogenesis from pyruvate also goes over oxaloacetate, but requires energy investment for pyruvate carboxylation, and may, therefore, be less economic.

In male *Negr1*$^{-/-}$ animals, Leu and Val are increased. BCAAs are generally upregulated in glucose intolerance (Wang et al., 2011) and, particularly, Leu is known to regulate glucose and protein metabolism (Liu et al., 2014). Whether the BCAA increase stems from protein breakdown and contributes to glucose intolerance or whether their higher level is maintained to counter peripheral glucose resistance cannot be answered from this study. Interestingly, high Leu should inhibit protein breakdown and enhance protein synthesis (Lynch et al., 2014).

Altogether, *Negr1*$^{-/-}$ mice, particularly males, break down proteins in the body in order to be able to use some amino acids, while others accumulate. This reprogramming of metabolism does not seem to overload amino acid catabolic pathways but causes reduced muscle fiber size phenotype. This reprograming also reduces metabolic flexibility and paves the way to glucose intolerance.

6.5.5. Gender-specific changes in the metabolism of citric of *Negr1*-deficient mice caused by HF diet

The citric acid cycle is a central mitochondrial pathway, which is closely related to catabolic and anabolic pathways of many biomolecules, including fatty acids, amino acids, and glucose. Above, we discussed how certain amino acids in *Negr1*$^{-/-}$ mice are more important gluconeogenic source than in WT mice. An important note and maybe the root of all metabolic alterations are the increased citrate levels in *Negr1*$^{-/-}$ mice. High citrate is a signal of energy excess which activates fatty acid synthesizing enzymes allosterically (Kornacker et al., 1965; Munday et al., 2002); on the other hand, citrate inhibits glycolytic enzymes. Thus, even on a normal diet, *Negr1*$^{-/-}$ mice are biased towards fatty acid synthesis and have reduced glycolytic efficiency. Alpha-ketoglutarate, succinate, malate, and oxaloacetate did follow citrate's pattern only in male mice, though. In *Negr1*$^{-/-}$, a part of citrate is diverted away from the citrate cycle into lipid synthesis. The latter is intense in hepatocytes and might cause the fatty liver phenotype if up-regulated (Figure 24).

A GWAS suggests that insulin suppresses NEGR1 in adipocytes and the synthetic glucocorticoid dexamethasone induces *NEGR1* expression (Walley et al., 2012). Insulin is known to enhance fatty acid synthesis from citrate; whether it does so via NEGR1 or independently, we cannot answer, but our results are in good accordance with these findings. Another study on monozygotic twins discordant for type 2 diabetes found *NEGR1* being upregulated in adipocytes of type 2 diabetic twins (Nilsson et al., 2014). Here, the insulin level is expected to be high, but adipocytes do not recognize it properly. Upregulation of *NEGR1* in relative insulin deficiency suggests that NEGR1 has a functional role in how insulin regulates the activities of enzymes of glycolysis, citric acid cycle, and/or lipogenesis. Even more, Joo et al. (2019) have shown that *Negr1* deficiency induces abnormal fat deposition in various peripheral cells, especially fat and liver tissue cells.

Still, *Negr1*$^{-/-}$ did not display increased levels of acyl residues that would be expected if high citrate diverges from glycolysis into lipid synthesis. As the synthesis also demands high amounts of ATP and reductive NADPH, it may be ineffective. Therefore, on a normal diet, the mice do not gain excessive fat or body weight and display a normal serum lipid profile. If glycolysis is inhibited, more amino acids are catabolized for energy production, leading to a risk of muscle wasting. HF diet impairs glucose utilization even further (Jana et al., 2019); thus, the *Negr1*$^{-/-}$, who already have trouble with glucose usage, are forced to utilize amino acids as a source of energy (Figure 25).

To expand our knowledge of how the metabolic shift present in *Negr1*$^{-/-}$ could be linked with the brain endophenotypes of *Negr1*$^{-/-}$, the western blot estimating proteins related to the cellular energetics in the brain tissue was performed. A statistically significant increase of glutathionylated proteins and NOX2 enzyme was found in the Hip of *Negr1*$^{-/-}$ but not in the frontal cortex of the same mice. NOX2 is NADPH oxidase, which is a superoxide generating enzyme that is

forming reactive oxygen species (ROS). In previous studies it has been shown that superoxide overproduction as a result of NOX2 activation leads to the loss of inhibitory capacity of parvalbumin interneurons (Schiavone et al., 2009). NOX2 is also one factor that has been implicated in causing inflammation associated with a HF diet. A study with NOX2 knockout mice on a HF diet showed that NOX2 knockout mice do not experience all the deleterious metabolic and inflammatory effects in the body and brain caused by HF diet to the same degree as WT mice (Costford et al., 2014). There is also another study where a mouse model was genetically engineered with the intent of inhibiting NOX2 solely within macrophages. Similar to the first study, these macrophage-deficient NOX2 knockout mice were placed on a HF diet, the results showed that macrophage-deficient NOX2 knockout mice were protected from the deleterious effects of a HF diet (Pepping et al., 2017). Those two studies showed that the deletion of NOX2 can have a protective benefit against the effects of obesity in the context of a HF diet. In our study we saw an increased level of NOX2 in *Negr1*$^{-/-}$ mice, at the same time we saw that in *Negr1*$^{-/-}$ mice, HF diet promotes prediabetes and fat accumulation. These results support the hypothesis that higher levels of NOX2 can promote worse outcomes of HF diet and lower levels of NOX2 in WT animals protect them from deleterious effects of HF diet. GSH is an antioxidant and is capable of preventing damage to important cellular components caused by ROS. These results further suggest that systemic metabolism in *Negr1*$^{-/-}$ organisms is shifted towards ineffective metabolic alterations that may produce more oxidative stress and Hip may be especially sensitive compared to other brain regions.

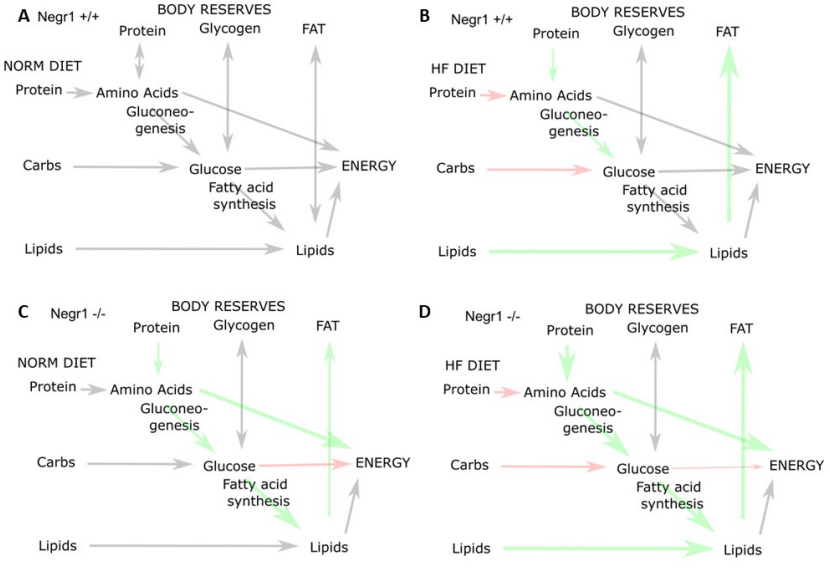

Figure 25. A hypothetical and simplified scheme of the metabolic differences in WT (*Negr1*$^{+/+}$) (**A, B**) and *Negr1*$^{-/-}$ (**C, D**) mice on a normal diet (**A, C**) and high-fat diet (**B, D**). Increased size and green color indicate increased metabolic flux, reduced arrow size and red color indicate inhibited process.

6.6. Concluding remarks and future prospects

In conclusion, in the current study we showed that *Negr1* and *Lsamp*, members of the IgLON gene family, are strongly associated with behavioral and biochemical changes in the mice that are analogous to changes described in psychiatric patients. *Negr1* also showed strong sex dependent associations with regulation of body metabolism and obesity. In several studies it has also been shown that depression and obesity can have shared etiology, and in our study, we saw that *Negr1* is a gene that has an impact on both.

In the future, the role of NEGR1 in systemic metabolism should be studied further. In this study we studied the level of glucose and performed GTT analysis on *Negr1*$^{-/-}$ and WT mice on a HF diet, but the levels of insulin and insulin tolerance should also be measured. Since we saw differences between male and female mice, the sex differences should also be studied further. For example, measurement of sex hormones in the context of HF diet and also the level of other enzymes related to metabolism (glucagon, leptin, adiponectin etc.).

CONCLUSIONS

Both NEGR1 and LSAMP have distinct impact on the monoaminergic neurotransmission. As the impact of NEGR1 is stronger for the dopaminergic system, this neural transmission system could affect both depressive and obesity-related phenotypes linked with *NEGR1* gene.

1. LSAMP is expressed in the raphe, whereas the distribution of *Lsamp* is isoform specific in the dorsal and median raphe nuclei. *Lsamp* 1a and 1b promoters are active in the DR (dorsal raphe); most of the expression in MnR (median raphe) comes from 1b promoter, whereas most of the *Lsamp* expression in the caudal subgroup of raphe, such as raphe magnus (RMg) derives from 1a promoter.

2. In *Lsamp*-deficient mice, chronic escitalopram induces alterations in behavior and changes in brain biochemistry that are highly analogous to the changes described in major depressive disorder patients. We also detected significant upregulation of *MaoA* gene in the raphe area of *Lsamp*-deficient mice, which can be a response to the higher activity of serotonin transporter (SERT) protein, as indicated by higher serotonin (5-HT) turnover, which transport more 5-HT from the synapse, leading to increased supply of 5-HT to *MaoA*.

   In *Negr1*$^{-/-}$ mice, reduction of 5-HT and DA turnover induced by chronic escitalopram is enhanced in raphe nuclei. Escitalopram could rescue reduced hippocampal weight in *Negr1*$^{-/-}$ mice.

3. *Negr1*$^{-/-}$ mice show a time-dependent increase in behavioral sensitization to amphetamine associated with increased dopamine turnover in both dorsal (DSTR) and ventral striatum (VSTR). Upregulation of transcripts encoding for dopamine and SERT and higher levels of several monoamines, and their metabolites was evident in distinct brain areas of Negr1$^{-/-}$ mice.

4. *Negr1*$^{-/-}$ mice have a higher protein catabolism than WT mice. With higher usage of amino acids, the energy from carbohydrates and lipids can be diverted into reserves, e.g., formation of fat stores. The high-fat (HF) diet does promote prediabetes and fat accumulation in Negr1$^{-/-}$ mice, which indicates that the metabolic pathways are already activated by the absence of *Negr1*. Our data show that *Negr1* is one of the genetic factors that, together with other signaling molecules (e.g., sex hormones) and consumed diet, contributes to the balance of systemic metabolism, including glucose homeostasis.

   Figures 26 and 27 summarize the findings of this theses concerning the transcripts in monoaminergic synapses.

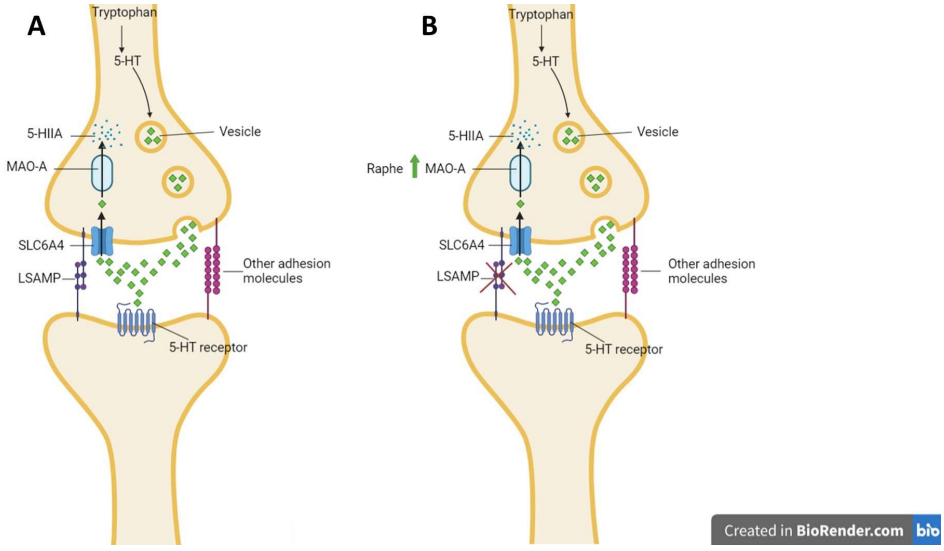

Figure 26. Serotonergic synapse. Schematic overview of LSAMP in a serotonergic synapse (A) and changes in the serotonergic synapse caused by LSAMP-deficiency (B). Green arrow indicates an increase.

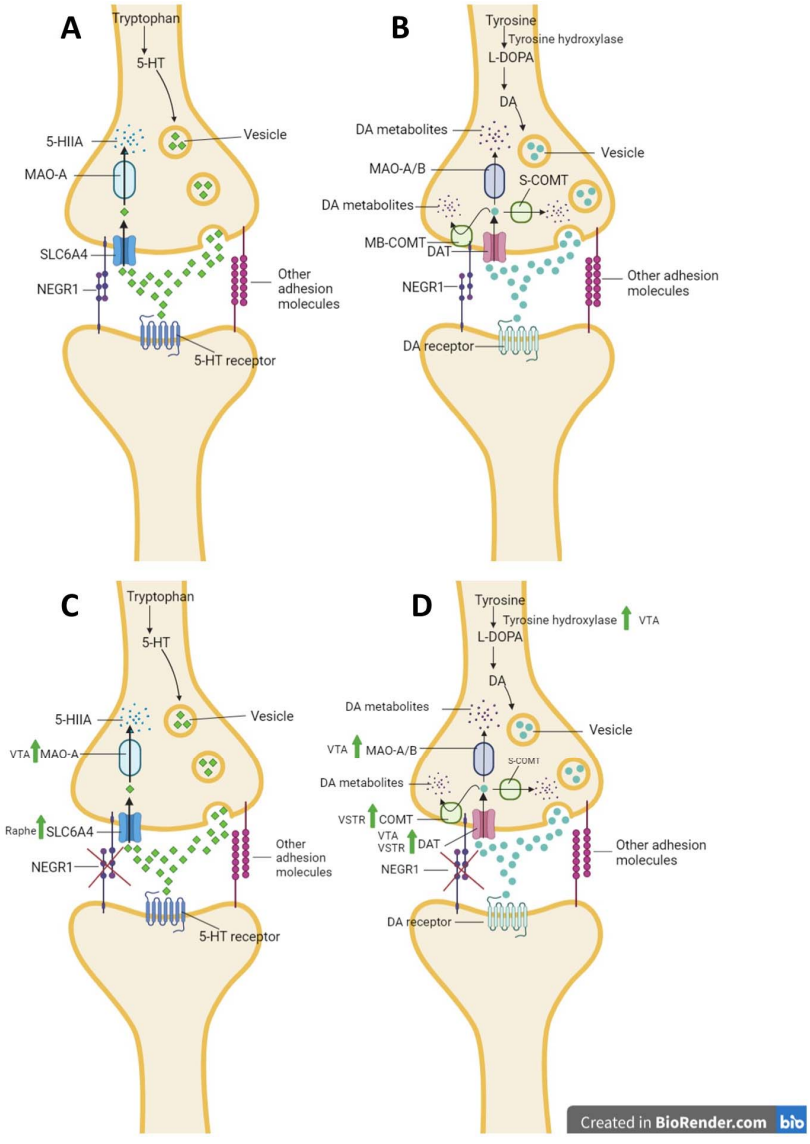

Figure 27. Serotonergic and dopaminergic synapse. Schematic overview of NEGR1 in serotonergic (A) and dopaminergic (B) synapse. Changes in the serotonergic (C) and dopaminergic (D) synapse in the case of NEGR1-deficiency. Green arrow indicates an increase.

REFERENCES

Admon, R. and Pizzagalli, D.A. (2015). Dysfunctional Reward Processing in Depression. *Current opinion in psychology* 4: 114–118. 10.1016/j.copsyc.2014.12.011.

Alttoa, A., Kõiv, K., Hinsley, T.A., Brass, A., Harro, J. (2010). Differential gene expression in a rat model of depression based on persistent differences in exploratory activity. *Eur. Neuropsychopharmacol.* 20: 288–300. https://doi.org/10.1016/j.euroneuro.2009.09.005.

An D., Joo Y., Kim H. (2019). The role of NEGR1 in the formation of lipid droplets. *FASEB J.* 34: 1. doi: 10.1096/fasebj.2020.34.s1.09960.

Avelar, A.J., Juliano, S.A and Garris, P.A. (2013). Amphetamine augments vesicular dopamine release in the dorsal and ventral striatum through different mechanisms. *J Neurochem.* 125: 373–385. 10.1111/jnc.12197.

Bakker, R., Tiesinga, P. and Kötter, R. (2015). The Scalable Brain Atlas: Instant Web-Based Access to Public Brain Atlases and Related Content. *Neuroinform* 13: 353–366. 10.1007/s12021-014-9258-x.

Barøy, T., Kresse, S.H., Skårn, M., Stabell, M., Castro, R., Lauvrak, S., Llombart-Bosch, A., Myklebost, O. and Meza-Zepeda, L.A. (2014). Reexpression of LSAMP inhibits tumor growth in preclinical osteosarcoma model. *Mol Cancer* 13:93. 10.1186/1476-4598-13-93.

Barth, A.M., Domonkos, A., Fernandez-Ruiz, A., Freund, T.F. and Varga, V. (2018). Hippocampal Network Dynamics during Rearing Episodes. *Cell Rep*. 23: 1706–1715. 10.1016/j.celrep.2018.04.021.

Barton, D.A., Esler, M.D., Dawood, T., Lambert, E.A., Haikerwal, D., Brenchley, C., Socratous, F., Hastings, J., Guo, L., Wiesner, G., Kaye, D.M., Bayles, R., Schlaich, M.P., Lambert, G.W. (2008). Elevated brain serotonin turnover in patients with depressioon: effect of genotype and therapy. *Arch. Gen. Psychiatry* 65: 38–46. https://doi.org/10.1001/arch gen psychiatry.2007.11.

Behan, A.T., Byrne, C., Dunn, M.J., Cagney, G., Cotter, D.R. (2009). Proteomic analysis of membrane microdomain-associated proteins in the dorsolateral prefrontal cortex in schizophrenia and bipolar disorder reveals alterations in LAMP, STXBP1 and BASP1 protein expression. *Mol. Psychiatry* 14: 601–613. https://doi.org/10.1038/mp. 2008.7.

Belujon, P. and Grace, A. A. (2017). Dopamine System Dysregulation in Major Depressive Disorders. *The international journal of neuropsychopharmacology* 20: 1036–1046. 10.1093/ijnp/pyx056.

Bernhard F., Landgraf K., Klöting N., Berthold A., Büttner P., Friebe D., Kiess W., Kovacs P., Blüher M., Körner A. (2020). Functional relevance of genes implicated by obesity genome-wide association study signals for human adipocyte biology. *Diabetol.* 56: 311–322. doi: 10.1007/s00125-012-2773-0.

Bethea, C.L., Reddy, A.P. (2012). Effect of ovarian steroids on gene expression related to synapse assembly in serotonin neurons of macaques. *J. Neurosci. Res.* 90: 1324–1334. https://doi.org/10.1002/jnr.23004.

Boender A.J., van Gestel M.A., Garner K.M., Luijendijk M.C.M., Adan R.A.H. (2012). The obesity-associated gene Negr1 regulates aspects of energy balance in rat hypothalamic areas. *Physiol. Rep.* 2:e12083. doi: 10.14814/phy2.12083.

Bornstein, S. R., Schuppeines, A., Wong, M.-L. and Licinio, J. (2006). Approaching the shared biology of obesity and depression: the stress axis as the locus of gene-environment interactions. *Molecualr Psychiatry* 11: 892–902. https://doi.org/10.1038/sj.mp.4001873.

Bregin, A., Mazitov, T., Aug, I., Philips, M.A., Innos, J., Vasar, E. (2019). Increased sensitivity to psychostimulants and GABAergic drugs in Lsamp-deficient mice. *Pharmacol. Biochem. Behav.* 183: 87–97. https://doi.org/10.1016/j.pbb.2019.05. 010.

Cagniard, B., Sotnikova, T.D., Gainetdinov, R.R. and Zhuang, X. (2014). The Dopamine Transporter Expression Level Differentially Affects Responses to Cocaine and Amphetamine. *Journal of Neurogenetics* 28: 112–121. 10.3109/01677063.2014. 908191.

Carboni, L., Pischedda, F., Piccoli, G., Lauria, M., Musazzi, L., Popoli, M., Mathé, A.A. and Domenici, E. (2020). Depression-Associated Gene *Negr1-Fgfr2* Pathway Is Altered by Antidepressant Treatment. *Cell* 9: 1818. 10.3390/cells9081818.

Catania, E.H., Pimenta, A., Levitt, P. (2008). Genetic deletion of Lsamp causes exaggerated behavioral activation in novel environments. *Behav. Brain Res.* 188: 380–390. https://doi.org/10.1016/j.bbr.2007.11.022.

Chang L. C., Jamain S., Lin C. W., Rujescu D., Tseng G. C., Sibille E. A. (2014). Conserved BDNF, glutamate- and GABA-enriched gene module related to human depression identified by coexpression meta-analysis and DNA variant genome-wide association studies. *PLOS ONE* 9:e90980. 10.1371/journal.pone.0090980

Chen, X., Long, F., Cai, B., Chen, X., Chen, G. (2017). A novel relationship for schizophrenia, bipolar and major depressive disorder. Part 3: evidence from chromosome 3 high density association screen. *J. Comp. Neurol.* 526: 59–79. 10. 1002/cne.24311.

Cochran J., Taufalele P.V., Lin K.D., Zhang Y., Abel E.D. (2011). Sex Differences in the Response of C57BL/6 Mice to Ketogenic Diets. *Diabetes*. 67: 1884. 10.2337/db18-1884-P.

Costain G., Bassett A. S. (2012). Clinical applications of schizophrenia genetics: genetic diagnosis, risk, and counseling in the molecular era. *Appl. Clin. Genet.* 5: 1–18. 10.2147/TACG.S21953.

Cox, D.A., Gottschalk, M.G., Wesseling, H., Ernst, A., Cooper, J.D., Bahn, S. (2016). Proteomic systems evaluation of the molecular validity of preclinical psychosis models compared to schizophrenia brain pathology. *Schizophr. Res.* 177: 98–107. 0.1016/j.schres.2016.06.012.

Cross-Disorder Group of the Psychiatric Genomics Consortium. (2019). Genomic Relationships, Novel Loci, and Pleiotropic Mechanisms across Eight Psychiatric Disorders. *Cell* 179: 1469–1482.e11. 10.1016/j.cell.2019.11.020.

Czéh, B., Michaelis, T., Watanabe, T., Frahm, J., de Biurrun, G., van Kampen, M., Bartolomucci, A., & Fuchs, E. (2001). Stress-induced changes in cerebral metabolites, hippocampal volume, and cell proliferation are prevented by antidepressant treatment with tianeptine. Proceedings of the *National Academy of Sciences of the United States of America* 98: 12796–12801. 10.1073/pnas.211427898.

Cui, Z., Gerfen, C.R., Young 3rd., W.S. (2013). Hypothalamic and other connections with the dorsal CA2 area of the mouse hippocampus. J. Comp. Neurol. 521, 1844–1866.

Dall'Aglio, L., Lewis, C.M., Pain, O. (2021). Delineating the Genetic Component of Gene Expression in Major Depression. *Biol Psychiatry* 89: 627–636. 10.1016/ j.biopsych.2020.09.010.

Deng, Y.-T., Ou, Y.-N., Wu, B.-S., Yang, Y.-X., Jiang, Y., Huang, Y.-Y., Liu, Y. and Tan, L. (2022). Identifying casual genes for depression via integration of the proteome and transcriptome from brain and blood. Molecular psychiatry 27: 2849–2857. 10.1038/s41380-022-01507-9.

Dietz, D.M., Tapocik, J., Gaval-Cruz, M. and Kabbaj, M. (2005). Dopamine transporter, but not tyrosine hydroxylase, may be implicated in determining individual differences in behavioral sensitization to amphetamine. *Physiol Behav*. 86: 347–355. 10.1016/ j.physbeh.2005.08.005.

Dorocic, I.P., Fürth, D., Xuan, Y., Johansson, Y., Pozzi, L., Silberberg, G., Carlén, M., Meletis, K. (2014). A whole-brain atlas of inputs to serotonergic neurons of the dorsal and median raphe nuclei. *Neuron* 83: 663–678. 10.1016/j.neuron. 2014.07.002.

Esler, M., Lambert, E., Alvarenga, M., Socratous, F., Richards, J., Barton, D., Pier, C., Brenchley, C., Dawood, T., Hastings, J., Guo, L., Haikerwal, D., Kaye, D., Jennings, G., Kalff, V., Kelly, M., Wiesner, G., Lambert, G. (2007). Increased brain serotonin turnover in panic disorder patients in the absence of a panic attack: reduction by a selective serotonin reuptake inhibitor. *Stress* 10: 295–304. 10.1080/10253890701300904.

Fox, M. E. and Lobo, M. K. (2019). The molecular and cellular mechanisms of depression: a focus on reward circuitry. *Mol Psychiatry* 24(12): 1798–1815. 10.1038/ s41380-019-0415-3.

Franklin, K.B.J., Paxinos, G. (1997). The Mouse Brain in Stereotaxic Coordinates. Academic Press, San Diego, CA. Gao, J., Zhang, J.-X., Xu, T.-L., 2002. Modulation of serotonergic projections from dorsal raphe nucleus to basolateral amygdala on sleep-waking cycle of rats. *Brain Res.* 945: 60–70. 10.1016/S0006-8993(02)02625-2.

Gao, J., Zhang, J.-X., Xu, T.-L. (2002). Modulation of serotonergic projections from dorsal raphe nucleus to basolateral amygdala on sleep-waking cycle of rats. *Brain Res*. 945: 60–70.

Geiger, B.M., Haburcak, M., Avena, N.M., Moyer, M.C., Hoebel, B.G. and Pothos, E.N. (2009). Deficits of mesolimbic dopamine neurotransmission in rat dietary obesity. *Neuroscience* 159: 1193–1199. 10.1016/j.neuroscience.2009.02.007.

Genovese, A., Cox, D. M. and Butler, M. G. (2015). Partial Deletion of Chromosome 1p31.1 Including only the Neuronal Growth Regulator 1 Gene in Two Siblings. *J Pediatr Genet.* 23–8. 10.1055/s-0035-1554977.

Gil, O.D., Zhang, L., Chen, S., Ren, Y.Q., Pimenta, A., Zanazzi, G., Hillman, D., Levitt, P., Salzer, J.L. (2002). Complementary expression and heterophilic interactions between IgLON family members neurotrimin and LAMP. *J. Neurobiol.* 51: 190–204. 10.1002/neu.10050.

Hansson, C., Alvarez-Crespo, M., Taube, M., Skibicka, K.P., Schmidt, L., Karlsson-Lindahl, L., Egecioglu, E., Nissbrandt, H., Dickson, S.L. (2014). Influence of ghrelin on the central serotonergic signaling system in mice. *Neuropharmacology* 79: 498–505. 10.1016/j.neuropharm.2013.12.012.

Hashimoto, T., Yamada, M., Maekawa, S., Nakashima, T. and Miyata, S. (2008) IgLON cell adhesion molecule Kilon is a crucial modulator for synapse number in hippocampal neurons. *Brain Research* 1224: 1–11. 10.1016/j.brainres.2008.05.069.

Hashimoto, T., Maekawa, S., Miyata, S. (2009). IgLON cell adhesion molecules regulate synaptogenesis in hippocampal neurons. *Cell Biochem. Funct.* 27: 496–498. 10.1002/ cbf.1600.

Hassanzadeh, G.R., Behzadi, G. (2007). Projections of dorsal and median raphe nuclei to dorsal and ventral striatum. *Acta Med. Iranica* 45: 339–344.

Heinla, I., Leidmaa, E., Kongi, K., Pennert, A., Innos, J., Nurk, K., Tekko, T., Singh, K., Vanaveski, T., Reimets, R., Mandel, M., Lang, A., Lilleväli, K., Kaasik, A., Vasar, E., Philips, M.-A. (2015). Gene expression patterns and environmental enrichment-induced effects in the hippocampi of mice suggest importance of Lsamp in plasticity. Front. *Neurosci*. 9, 205

Hosak L., Silhan P., Hosakova J. (2012). Genome-wide association studies in schizophrenia, and potential etiological and functional implications of their results. *Acta Medica* 55: 3–11. 10.14712/18059694.2015.67.

Howard D.M., Adams M.J., Shirali M., Clarke T.-K., Marioni R.E., Davies G., Coleman J.R.I., Alloza C., Shen X., Barbu M.C., et al. (2018). Genome-wide association study of depression phenotypes in UK Biobank identifies variants in excitatory synaptic pathways. *Nat. Commun.* 9: 1470. 10.1038/s41467-018-03819-3.

Huang, K.W., Ochandarena, N.E., Philson, A.C., Hyun, M., Birnbaum, J.E., Ciccotnet, M., Sabatini, B.L. (2019). Molecular and anatomical organization of the dorsal raphe nucleus. *Elife* 8: e46464. 10.7554/eLife.46464.

Hyde C. L., Nagle M. W., Tian C., Chen X., Paciga S. A., Wendland J. R., et al. (2016). Identification of 15 genetic loci associated with risk of major depression in individuals of European descent. *Nat. Genet.* 48: 1031–1036. 10.1038/ng.3623.

Innos, J., Philips, M.-A., Leidmaa, E., Heinla, I., Raud, S., Reemann, P., Plaas, M., Nurk, K., Kurrikoff, K., Matto, V., Visnapuu, T., Mardi, P., Kõks, S., Vasar, E. (2011). Lower anxiety and a decrease in agonistic behaviour in Lsamp-deficient mice. *Behav. Brain Res.* 217: 21–31. 10.3389/fnins.2015.00205.

Innos, J., Philips, M.-A., Raud, S., Lilleväli, K., Kõks, S., Vasar, E. (2012). Deletion of the Lsamp gene lowers sensitivity to stressful environmental manipulations in mice. *Behav. Brain Res.* 228: 74–81. 10.1016/j.bbr.2011.11.033.

Innos, J., Leidmaa, E., Philips, M.-A., Sütt, S., Alttoa, A., Harro, J., Kõks, S., Vasar, E. (2013a). Lsamp$^{-/-}$ mice display lower sensitivity to amphetamine and have elevated 5-HT turnover. Biochem. *Biophys. Res. Commun*. 430: 413–418. 10.1016/j.bbrc.2012.11.077.

Innos, J., Koido, K., Philips, M.-A., Vasar, E. (2013b). Limbic system associated membrane protein as a potential target for neuropsychiatric disorders. *Front. Pharmacol.* 4: 32. 10.3389/fphar.2013.00032.

Jana B.A., Chintamaneni P.K., Krishnamurthy P.T., Wadhwani A., Mohankumar S.K. (2019). Cytosolic lipid excess-induced mitochondrial dysfunction is the cause or effect of high fat diet-induced skeletal muscle insulin resistance: A molecular insight. *Mol. Biol. Rep.* 46: 957–963. 10.1007/s11033-018-4551-7.

Joo Y., Kim H., Lee S., Lee S. (2020). Neuronal growth regulator 1-deficient mice show increased adiposity and decreased muscle mass. *Int. J. Obes.* 43: 1769–1782. 10.1038/s41366-019-0376-2.

Karis, K., Eskla, K.L., Kaare, M., Täht, K., Tuusov, J., Visnapuu, T., Innos, J., Jayaram, M., Timmusk, T., Weickert, C.S., Väli, M., Vasar, E., Philips, M.A. (2018). Altered expression profile of IgLON family of neural cell adhesion molecules in the dorsolateral prefrontal cortex of schizophrenic patients. *Front. Mol. Neurosci*. 10.3389/fnmol.2018.00008.

Keller, F., Rimvall, K., Barbe, M.F., Levitt, P. (1989). A membrane glycoprotein associated with the limbic system mediates the formation of the septo-hippocampal pathway in vitro. *Neuron* 3: 551–561. 10.1016/0896-6273(89)90265-1.

Kenny P. J. (2011). Reward mechanisms in obesity: new insights and future directions. *Neuron* 69: 664–679. 10.1016/j.neuron.2011.02.016.

Kim H., Chun Y., Che L., Kim J., Lee S., Lee S. (2017). The new obesity-associated protein, neuronal growth regulator 1 (NEGR1), is implicated in Niemann-Pick disease Type C (NPC2)-mediated cholesterol trafficking. *Biochem. Biophys. Res. Commun*. 482: 1367–1374. 10.1016/j.bbrc.2016.12.043.

Kocsis, B., Varga, V., Dahan, L., Sik, A. (2006). Serotonergic neuron diversity: identification of raphe neurons with discharges time-locked to the hippocampal theta rhythm. *PNAS* 103, 1059–1064.

Koido, K., Traks, T., Balõtšev, R., Eller, T., Must, A., Koks, S., Maron, E., Tõru, I., Shlik, J., Vasar, V., Vasar, E. (2012). Associations between LSAMP gene polymorphisms and major depressive disorder and panic disorder. *Transl. Psychiatry* 2: e152.

Koido, K., Janno, S., Traks, T., Parksepp, M., Ljubajev, Ü., Veiksaar, P., Must, A., Shlik, J., Vasar, V., Vasar, E. (2014). Associations between polymorphisms of LSAMP gene and schizophrenia. *Psychiatry Res.* 215: 797–798. 10.1016/j.psychres.2014.01.016.

Kõks, S., Luuk, H., Nelovkov, A., Areda, T., Vasar, E. (2004). A screen for genes induced in the amygdaloid area during cat odor exposure. *Genes Brain Behav*. 3: 80–89. 10.1046/j.1601-183x.2003.00047.x.

Lamprecht, R., Dracheva, S., Assoun, S., LeDoux, J.E. (2009). Fear conditioning induces distinct patterns of gene expression in lateral amygdala. *Genes Brain Behav*. 8: 735–743. 10.1111/j.1601-183X.2009.00515.x.

Lee A.W.S., Hengstler H., Schwald K., Diaz M.B., Loreth D., Kirsch M., Kretz O., Haas C.A., de Angelis M.H., Herzig S., et al. (2012). Functional Inactivation of the Genome-Wide Association Study Obesity Gene Neuronal Growth Regulator 1 in Mice Causes a Body Mass Phenotype. *PLoS ONE.* 7:e41537. 10.1371/journal.pone.0041537.

Leidmaa E., Gazea M., Patchev A.V., Pissioti A., Gassen N.C., Kimura M., Liposits Z., Kallo I., Almeida O.F.X. (2020). Blunted leptin sensitivity during hedonic overeating can be reinstated by activating galanin 2 receptors (Gal2R) in the lateral hypothalamus. *Acta Physiol.* 228:e13345. 10.1111/apha.13345.

Levey D.F., Stein M.B., Wendt F.R., Pathak G.A., Zhou H., Aslan M., Quaden R., Harrington K.M., Nuñez Y.Z., Overstreet C., et al. (2021). Bi-ancestral depression GWAS in the Million Veteran Program and meta-analysis in >1.2 million individuals highlight new therapeutic directions. *Nat. Neurosci*. 954–963. 10.1038/s41593-021-00860-2.

Levitt, P. (1984). A monoclonal antibody to limbic system neurons. *Science* 223: 299–301. 10.1126/science.6199842.

Livak K. J., Schmittgen T. D. (2001). Analysis of relative gene expression data using real-time quantitative PCR and the $2^{-\Delta\Delta C}{}_{T}$ method. *Methods* 25: 402–408. 10.1006/meth.2001.1262.

Liu H., Liu R., Xiong Y., Li X., Wang X., Ma Y., Guo H., Hao L., Yao P., Liu L., et al. (2014). Leucine facilitates the insulin-stimulated glucose uptake and insulin signaling in skeletal muscle cells: Involving mTORC1 and mTORC2. *Amino Acids* 46: 1971–1979. 10.1007/s00726-014-1752-9.

Locke A.E., Kahali B., Berndt S.I., Justice A.E., Pers T.H., Day F.R., Powell C., Vedantam S., Buchkovich M.L., Yang J., et al. (2015). Genetic studies of body mass index yield new insights for obesity biology. *Nature* 518: 197–206. 10.1038/nature14177.

Lynch C.J., Adams S. (1965). Branched-chain amino acids in metabolic signalling and insulin resistance. *Nat. Rev. Endocrinol*. 10: 723–736. 10.1038/nrendo.2014.171.

Maccarrone, G., Ditzen, C., Yassouridis, A., Rewerts, C., Uhr, M., Uhlen, M., Holsboer, F. and Turck, C.W. (2013). Psychiatric patient stratification using biosignatures based on cerebrospinal fluid protein expression clusters. *Journal of Psychiatric Research* 47: 1572–1580. 10.1016/j.jpsychires.2013.07.021.

Mann, F., Zhukareva, V., Pimenta, A., Levitt, P., Bolz, J. (1998). Membrane-associated molecules guide limbic and non limbic thalamocortical projections. *J. Neurosci*. 18: 9409–9419. 10.1523/JNEUROSCI.18-22-09409.

Marcinkiewcz, C.A., Mazzone, C.M., D'Agostino, G., Halladay, L.R., Hardaway, J.A., DiBerto, J.F., Navarro, M., Burnham, N., Cristiano, C., Dorrier, C.E., Tipton, G.J., Ramakrishnan, C., Kozicz, T., Deisseroth, K., Thiele, T.E., McElligott, Z.A., Holmes, A., Heisler, L.K., Kash, T.L., 2017. Serotonin engages an anxiety and fear-promoting circuit in the extended amygdala. Nature 537, 97–101. https://doi.org/ 10.1038/ nature19318.

Marshall, C.R., Noor, A., Vincent, J.B., Lionel, A.C., Feuk, L., Skaug, J., Shago, M., Moessner, R., Pinto, D., Ren, Y. et al. (2008). Structural variation of chromosomes in autism spectrum disorder. *Am J Hum Genet.* 82: 477–88. 10.1016/j.ajhg.2007.12.009.

Mauvais-Jarvis F. (2017). Gender differences in glucose homeostasis and diabetes. *Physiol. Behav.* 187: 20–23. 10.1016/j.physbeh.2017.08.016.

Michaelson, J. J., Shi, Y., Gujral, M., Zheng, H., Malhotra, D., Jin, X., Jian, M., Liu, G., Greer, D., Bhandari, A. et al. (2012) Whole-genome sequencing in autism identifies hot spots for de novo germline mutation. *Cell* 151: 1431–42. 10.1016/j.cell.2012. 11.019.

Munday M.R. (2014). Regulation of mammalian acetyl-CoA carboxylase. *Biochem. Soc. Trans.* 30: 1059–1064. 10.1042/bst0301059.

Mustard, C., Whitfield, P., Megson, I. and Wei, J. (2012). P-1104 – The Effect of Clozapine on the Expression of Obesity Genes. *European Psychiatry* 27(S1): 1–1. 10.1016/S0924-9338(12)75271-9

Must, A., Tasa, G., Lang, A., Vasar, E., Kõks, S., Maron, E., Väli, M. (2008). Association of limbic system-associated membrane protein (LSAMP) to male completed suicide. *BMC Med. Genet*. 9: 34. 10.1186/1471-2350-9-34.

Mäki P., Veijola J., Jones P. B., Murray G. K., Koponen H., Tienari P., et al. (2005). Predictors of schizophrenia – a review. *Br. Med. Bull.* 73–75: 1–15. 10.1093/bmb/ ldh046.

Nascimento J. M., Martins-de-Souza D. (2015). The proteome of schizophrenia. *NPJ Schizophr.* 1: 14003. 10.1038/npjschz.2014.3.

Navailles, S. and De Deurwaerdère, P. (2011). Presynaptic control of serotonin on striatal dopamine function. *Psychopharmacology (Berl).* 213: 213–242. 10.1007/s00213-010-2029-y.

Ng, T.H., Alloy, L.B. and Smith, D.V. (2019). Meta-analysis of reward processing in major depressive disorder reveals distinct abnormalities within the reward circuit. *Transl Psychiatry* 9**:** 293. 10.1038/s41398-019-0644-x.

Nelovkov, A., Philips, M.-A., Kõks, S., Vasar, E. (2003). Rats with low exploratory activity in the elevated plus-maze have the increased expression of limbic system-associated membrane protein gene in the periaqueductal grey. *Neurosci. Lett.* 352: 179–182. 10.1016/j.neulet.2003.08.061.

Nilsson E., Jansson P.A., Perfilyev A., Volkov P., Pedersen M., Svensson M.K., Poulsen P., Ribel-Madsen R., Pedersen N.L., Almgren P., et al. (2019). Altered DNA Methylation and Differential Expression of Genes Influencing Metabolism and Inflammation in Adipose Tissue from Subjects with Type 2 Diabetes. *Diabetes* 63: 2962–2976. 10.2337/db13-1459.

Noh K., Lee H., Choi T.-Y., Joo Y., Kim S.-J., Kim H., Kim J.Y., Jahng J.W., Lee S., Choi S.-Y., et al. (2019). Negr1 controls adult hippocampal neurogenesis and affective behaviors. *Mol. Psychiatry* 24: 1189–1205. 10.1038/s41380-018-0347-3.

Ntougkos, E., Rush, R., Scott, D., Frankenberg, T., Gabra, H., Smyth, J.F. and Sellar, G.C. (2005). The IgLON family in epithelial ovarian cancer: expression profiles and clinicopathologic correlates. *Clin Cancer Res.* 11: 5764–8. 10.1158/1078-0432.CCR-04-2388.

Okaty, B. W., Freret, M.E., Rood, B.D., Brust, R.D., Hennessy, M.L., Bairos, D., Kim, J.K., Cook, M.N., Dymecki, S.M. et al. (2015). Multi-Scale Molecular Deconstruction of the Serotonin Neuron System. *Neuron* 88: 774–91. 10.1016/j.neuron.2015.10.007.

Ouakinin, S. R. S., Barreira, D. P. and Gois, C. J. (2018). Depression and besity: Integrating the Role of Stress, Neuroendocrine Dysfunction and Innflamatory Pathways. *Front Endocrinol (Lausanne)* 9:431. 10.3389/fendo.2018.00431.

Pepping, J. K., Vandanmagsar, B., Fernandez-Kim, S.-O., Zhang, J., Mynatt, R., L. and Bruce-Keller, A. J. (2017). Myeloid-specific deletion of NOX2 prevents the metabolic and neurologic consequences of high fat diet. *PLoS One* 12: e0181500. 10.1371/journal.pone.0181500.

Paulson, P. E., and Robinson, T. E. (1995). Amphetamine-induced time-dependent sensitization of dopamine neurotransmission in the dorsal and ventral striatum: a microdialysis study in behaving rats. *Synapse (New York, N.Y.)* 19: 56–65. 10.1002/syn.890190108.

Philips M. A., Kingo K., Karelson M., Rätsep R., Aunin E., Reimann E., et al. (2010). Promoter polymorphism –119C/G in MYG1 (C12orf10) gene is related to vitiligo susceptibility and Arg4Gln affects mitochondrial entrance of Myg1. *BMC Med. Genet*. 11:56. 10.1186/1471-2350-11-56.

Philips, M.-A., Lilleväli, K., Heinla, I., Luuk, H., Hundahl, C.A., Kongi, K., Vanaveski, T., Tekko, T., Innos, J., Vasar, E. (2015). Lsamp is implicated in the regulation of emotional and social behavior by use of alternative promoters in the brain. *Brain Struct. Funct*. 220: 1381–1393. 10.1007/s00429-014-0732-x.

Pischedda F., Szczurkowska J., Cirnaru M. D., Giesert F., Vezzoli E., Ueffing M., et al. (2014). A cell surface biotinylation assay to reveal membrane-associated neuronal cues: negr1 regulates dendritic arborization. *Mol. Cell. Proteomics* 13: 733–748. 10.1074/mcp.M113.031716.

Pischedda, F. and Piccoli, G. (2015). The IgLON Family Member Negr1 Promotes Neuronal Arborization Acting as Soluble Factor via FGFR2. (2015). *Front Mol Neurosci.* 8:89. 10.3389/fnmol.2015.00089.

Pimenta, A.F., Zhukareva, V., Barbe, M.F., Reinoso, B.S., Grimley, C., Henzel, W., Fischer, I., Levitt, P. (1995). The limbic system-associated membrane protein is an Ig superfamily member that mediates selective neuronal growth and axon targeting. *Neuron* 15: 287–297. 10.1016/0896-6273(95)90034-9.

Pompili M., Amador X. F., Girardi P., Harkavy-Friedman J., Harrow M., Kaplan K., et al. (2007). Suicide risk in schizophrenia: learning from the past to change the future. *Ann. Gen. Psychiatry* 6:10. 10.1186/1744-859X-6-10.

Rauschert S., Uhl O., Koletzko B., Mori T.A., Beilin L.J., Oddy W.H., Hellmuth C. (2018). Sex differences in the association of phospholipids with components of the metabolic syndrome in young adults. *Biol. Sex Differ.* 8:10. 10.1186/s13293-017-0131-0.

Reed J., McNamee C., Rackstraw S., Jenkins J., Moss D. (2004). Diglons are heterodimeric proteins composed of IgLON subunits, and diglon-CO inhibits neurite outgrowth from cerebellar granule cells. *J. Cell Sci*. 117: 3961–3973. 10.1242/jcs.01261.

Salahpour, A., Ramsey, A.J., Medvedev, I.O., Kile, B., Sotnikova, T.D., Holmstrand, E., Ghisi, V., Nicholls, P.J., Wong, L., Murphy, K. et al. (2008). Increased amphetamine-induced hyperactivity and reward in mice overexpressing the dopamine transporter. *Proc Natl Acad Sci U S A* 105: 4405–4410. 10.1073/pnas.0707646105.

Sandholt C.H., Vestmar M.A., Bille D.S., Borglykke A., Almind K., Hansen L., Sandbæk A., Lauritzen T., Witte D., Jørgensen T., et al. (2011). Studies of Metabolic Phenotypic Correlates of 15 Obesity Associated Gene Variants. *PLoS ONE* 6:e23531. 10.1371/journal.pone.0023531.

Sapolsky R. M. (2001). Depression, antidepressants, and the shrinking hippocampus. *Proceedings of the National Academy of Sciences of the United States of America* 98: 12320–12322. 10.1073/pnas.231475998.

Schiavone, S., Sorce, S., Dubois-Dauphin, M., Jaquet, V., Colaianna, M., Zotti, M., et al. (2009). Involvement of NOX2 in the development of behavioral and pathologic alterations in isolated rats. *Biol. Psychiatry* 66: 384–392. 10.1016/j.biopsych.2009. 04.033

Schlauch K.A., Read R.W., Lombardi V.C., Elhanan G., Metcalf W.J., Slonim A.D., Twenty Three & Me Research Team. Grzymski J.J. (2020). A Comprehensive Genome-Wide and Phenome-Wide Examination of BMI and Obesity in a Northern Nevadan Cohort. G3 Genes Genomes *Genet.* 10: 645–664. 10.1534/g3.119.400910.

Schmidt, E.R.E., Brignani, S., Adolfs, Y., Lemstra, S., Demmers, J., Vidaki, M., Donahoo, A.-L., Lilleväli, K., Vasar, E., Richards, L.J., Karagogeos, D., Kolk, S.M., Pasterkamp, R.J. (2014). Subdomain-mediated axon-axon signaling and chemoattraction cooperate to regulate afferent innervation of the lateral habenula. *Neuron* 83: 372–387. 10.1016/j.neuron.2014.05.036.

Scholl, J.L., Feng, N., Watt, M.J., Renner, K.J., Forster, G.L. (2009). Individual differences in amphetamine sensitization, behavior and central monoamines. *Physiol Behav*. *96(3)*, 493–504. 10.1016/j.physbeh.2008.12.001.

Sellar, G.C., Watt, K.P., Rabiasz, G.J, Stronach, E.A., Li, L., Miller, E.P., Massie, C.E., Miller, J., Contreras-Moreira, B., Scott, D., Brown, I., Williams, A.R., Bates, P.A., Smyth, J.F. and Gabra, H. (2003). OPCML at 11Q25 is epigenetically inactivated and has tumor-supressor function in epithelial ovarian cancer. *Nature Genetics* 34: 337–343.10.1038/ng1183.

Sharma, K., Schmitt, S., Bergner, C.G., Tyanova, S., Kannaiyan, N., Manrique-Hoyos, N., A. Bregin, et al. (2020). *Pharmacology, Biochemistry and Behavior* 198: 173017 11.

Costford, S. R., Castro-Alves, J., Chan, K. L., Bailey, L. J., Woo, M., Belsham, D. D., Brumell, J. H. and Klip, A. (2014). Mice lacking NOX2 are hyperphagic and store fat preferentially in the liver. *American journal of physiology* 306: 1341–1353. 10.1152/ajpendo.00089.2014.

Shilling, P.D., Kelsoe, J.R. and Segal, D.S. (1997). Dopamine transporter mRNA is upregulated in the substantia nigra and the ventral tegmental area of amphetamine-sensitized rats. *Neuroscience Letters* 236: 131–134. 10.1016/S0304-3940(97)00768-4.

Siciliano, C.A., Calipari, E.S. and Jones, S.R. (2014). Amphetamine potency varies with dopamine uptake rate across striatal subregions. *J Neurochem.* 131: 348–355. 10.1111/jnc.12808.

Singh, K., Lilleväli, K., Gilbert, S.F., Bregin, A., Narvik, J., Jayaram, M., Rahi, M., Innos, J., Kaasik, A., Vasar, E., Philips, M.-A. (2018). The combined impact of IgLON family proteins Lsamp and Neurotrimin on developing neurons and behavioral profiles in mouse. *Brain Res. Bull.* 140: 5–18. 10.1016/j.brainresbull.2018.03. 013.

Singh K., Loreth D., Pöttker B., Hefti K., Innos J., Schwald K., Hengstler H., Menzel L., Sommer C.J., Radyushkin K., et al. (2018). Neuronal Growth and Behavioral Alterations in Mice Deficient for the Psychiatric Disease-Associated Negr1 Gene. *Front. Mol. Neurosci*. 11: 1662–5099. 10.3389/fnmol.2018.00030.

Singh K., Jayaram M., Kaare M., Leidmaa E., Jagomäe T., Heinla I., Hickey M., Kaasik A., Schäfer M.K., Innos J., et al. (2019). Neural cell adhesion molecule Negr1 deficiency in mouse results in structural brain endophenotypes and behavioral deviations related to psychiatric disorders. *Sci. Rep.* 9: 5457. 10.1038/s41598-019-41991-8.

Sjödin, A., Gasteyger, C., Nielsen, A.L., Raben, A., Mikkelsen, J.D., Jensen, J. K.S., Meier, D. and Astrup, A. (2010) . The effect of the triple monoamine reuptake inhibitor tesofensine on energy metabolism and appetite in overweight and moderately obese men. *Int J Obes.* 34**:** 1634–1643. 10.1038/ijo.2010.87.

Sniekers, S., Stringer, S., Watanabe, K., Jansen, P.R., Coleman, J.R.I., Krapohl, E., Taskesen, E., Hammerschlag, A.R., Okbay, A., Zabaneh, D. et al. (2017). Genome-wide association meta-analysis of 78,308 individuals identifies new loci and genes influencing human intelligence. *Nat Genet.* 49: 1107–1112. 10.1038/ng.3869.

Sokolowski, M., Wasserman, J., Wasserman, D. (2016). Polygenic associations of neurodevelopmental genes in suicide attempt. *Mol. Psychiatry* 21: 1381–1390. 10.1038/mp.2015.187.

Speliotes E.K., Willer C.J., Berndt S.I., Monda K.L., Thorleifsson G., Jackson A.U., Allen H.L., Lindgren C.M., Mägi R., Randall J.C., et al. (2010). Association analyses of 249,796 individuals reveal 18 new loci associated with body mass index. *Nat. Genet.* 42: 937–948. 10.1038/ng.686.

Szczurkowska, J., Pischedda, F., Pinto, B., Managò, F., Haas, C.A., Summa, M., Bertorelli, R., Papaleo, F., Schäfer, M.K., Piccoli, G. et al. (2018). NEGR1 and FGFR2 cooperatively regulate cortical development and core behaviours related to autism disorders in mice. *Brain* 141: 2772–2794. 10.1093/brain/awy190.

Stefansson H., Ophoff R. A., Steinberg S., Andreassen O. A., Cichon S., Rujescu D., et al. (2009). Common variants conferring risk of schizophrenia. *Nature* 460: 744–747. 10.1038/nature08186.

Tamási, V., Petschner, P., Adori, C., Kirilly, E., Ando, R. D., Tothfalusi, L., Juhasz, G. and Bagdy, G. (2014). Transcriptional Evidence for the Role of Chronic Venlafaxine Treatment in Neurotrophic Signaling and Neuroplasticity Including also Glutatmatergic- and Insulin-Mediated Neuronal Processes. *PLoS ONE* 9: e113662. 10.1371/journal.pone.0113662.

Taylor, K.M. and Snyder, S. H. (1970). Amphetamine: differentiation by d and l isomer of behavior involving brain norepinephrine or dopamine. *Science* 168: 1487–1489. 10.1126/science.168.3938.1487.

Tramunt B., Smati S., Grandgeorge N., Lenfant F., Arnal J.-F., Montagner A., Gourdy P. (2018). Sex differences in metabolic regulation and diabetes susceptibility. *Diabetologia* 63: 453–461. 10.1007/s00125-019-05040-3.

Thorleifsson G., Walters G.B., Gudbjartsson D.F., Steinthorsdottir V., Sulem P., Helgadottir A., Styrkarsdottir U., Gretarsdottir S., Thorlacius S., Jonsdottir I., et al. (2009). Genome-wide association yields new sequence variants at seven loci that associate with measures of obesity. Nat. *Genet.* 41: 18–24. 10.1038/ng.274.

Tsou, J. A., Galler, J.S., Siegmund, K.D., Laird, P.W., Turla, S., Cozen, W., Hagen, J. A., Koss, M. N. and Laird-Offringa, I.A. (2007). Identification of a panel of sensitive and specific DNA methylation markers for lung adenocarcinoma. *Mol Cancer* 6: 70. 10.1186/1476-4598-6-70.

Tye, K.M., Prakash, R., Kim, S.-Y., Fenno, L.E., Grosenick, L., Zarabi, H., Thompson, K.R., Gradinaru, V., Ramakrishnan, C., Deisseroth, K. (2011). Amygdala circuitry mediating reversible and bidirectional control of anxiety. *Nature* 471: 358–362.

Underhill, S.M., Hullihen, P.D., Chen, J., Fenollar-Ferre, C., Rizzo, M. A., Ingram, S.L. and Amara, S.G. (2021). Amphetamines signal through intracellular TAAR1 receptors coupled to $G\alpha_{13}$ and $G\alpha_S$ in discrete subcellular domains. *Mol Psychiatry* 26: 1208–1223. 10.1038/s41380-019-0469-2.

Vanaveski T., Singh K., Narvik J., Eskla K.-L., Visnapuu T., Heinla I., et al. (2017). Promoter-specific expression and genomic structure of IgLON family genes in mouse. *Front. Neurosci.* 11:38. 10.3389/fnins.2017.00038.

Varul, J., Eskla, K.-L., Piirsalu, M., Innos, J., Philips, M.-A., Visnapuu, T., Plaas, M. and Vasar, E. (2021). Dopamine System, NMDA Receptor and EGF Family Expressions in Brain Structures of Bl6 and 129Sv Strains Displaying Different Behavioral Adaptation. *Brain Sci.* 11: 725. 10.3390/brainsci11060725.

Veerappa, A. M., Saldanha, M., Padakannaya, P. and Ramachandra, N. B. (2013). Family-based genome-wide copy number scan identifies five new genes of dyslexia involved in dendritic spinal plasticity. *J Hum Genet.* 58: 539–47. 10.1038/jhg. 2013.47.

Velásquez, E., Nogueira, F.C.S., Velásquez, I., Schmitt, A., Falkai, P., Domont, G.B., Martins-de-Souza, D. (2017). Synaptosomal proteome of the orbitofrontal cortex from schizophrenia patients using quantitative label-free and iTRAQ-based shotgun proteomics. *J. Proteome Res.* 16: 4481–4494. 10.1021/acs.jproteome. 7b00422.

Venkannagari H., Kasper J., Misra A., Rush S., Fan S., Lee H., Sun H., Seshadrinathan S., Machius M., Hommel J.D., et al. (2020). Highly Conserved Molecular Features in IgLONs Contrast Their Distinct Structural and Biological Outcomes. *J. Mol. Biol.* 432: 5287–5303. 10.1016/j.jmb.2020.07.014.

Voigt, J.P., Fink, H. (2015). Serotonin controlling feeding and satiety. *Behav. Brain Res.* 277: 14–31. 10.1016/j.bbr.2014.08.065.

Walley A.J., Jacobson P., Falchi M., Bottolo L., Andersson-Assarsson J., Petretto E., Bonnefond A., Vaillant E., Lecoeur C., Vatin V., et al. (2017). Differential co-expression analysis of obesity-associated networks in human subcutaneous adipose tissue. *Int. J. Obes.* 36: 137–147. 10.1038/ijo.2011.22.

Wang, L., Zhu, J. S., Song, M. Q., Chen, G. Q. and Chen, J. L. (2006). Comparison of gene expression profiles between primary tumor and metastatic lesions in gastric cancer patients using laser microdissection and cDNA microarray. *World J Gastroenterol* 12: 6949–54. 10.3748/wjg.v12.i43.6949.

Wang K. S., Liu X. F., Aragam N. (2010). A genome-wide meta-analysis identifies novel loci associated with schizophrenia and bipolar disorder. *Schizophr. Res.* 124: 192–199. 10.1016/j.schres.2010.09.002.

Wheeler E., Huang N., Bochukova E., Keogh J.M., Lindsay S., Garg S., Henning E., Blackburn H., Loos R., Wareham N.J., et al. (2013). Genome-wide SNP and CNV analysis identifies common and low-frequency variants associated with severe early-onset obesity. *Nat. Genet.* 45: 513–517. 10.1038/ng.2607.

Winkler T.W., Justice A.E., Graff M., Barata L., Feitosa M.F., Chu S., Czajkowski J., Esko T., Fall T., Kilpeläinen T.O., et al. (2016). The Influence of Age and Sex on Genetic Associations with Adult Body Size and Shape: A Large-Scale Genome-Wide Interaction Study. *PLoS Genet.* 11:e1005378. 10.1371/journal.pgen.1006166.

Wray, N.R., Ripke, S., Mattheisen, M., Trzaskowski, M., Byrne, E.M., Abdel, A., Adams, M.J., Agerbo, E., Air, T.M., Andlauer, T.M.F. et al. (2018). Genome-wide association analyses identify 44 risk variants and refine the genetic architecture of major depression. *Nat Genet.* 50: 668–681. 10.1038/s41588-018-0090-3.

Yadid, G. and Friedman, A. (2008). Dynamics of the dopaminergic system as a key component to the understanding of depression. *Prog Brain Res.* 172: 265–286. 10.1016/S0079-6123(08)00913-8.

Yue W., Yu X., Zhang D. (2017). Progress in genome-wide association studies of schizophrenia in Han Chinese populations. *NPJ Schizophr.* 3:24. 10.1038/s41537-017-0029-1.

SUMMARY IN ESTONIAN

NEGR1 ja LSAMP toime psühhiaatrilistele häiretele on vahendatud monoamiinergilise närviülekande ning süsteemse metabolismi mõjutamise kaudu

NEGR1 ja LSAMP kuuluvad mõlemad IgLON perekonna adhesioonimolekulide hulka. IgLONid mängivad olulist rolli rakkude vahelisel adhesioonil, neuriitide väljakasvul ning sünapside moodustumisel. Inimestel on seostatud muutuseid IgLON geenides mitmete erinevate psühhiaatriliste häiretega. Ülegenoomsetes GWAS uuringutes on *NEGR1* geeni tugevalt seostatud depressiooniga. Samuti on leitud seoseid teiste psühhiaatriliste häiretega. Depressiooni monoamiini hüpoteesi alusel on depressiooni sümptomite põhjuseks häired monoamiinergilistes närviülekande süsteemides. Kuigi mitmed tõendid viitavad sellele, et depressiooni tekkega on seotud ka mitmed teised rajad, mängivad monoamiinid siiski olulist rolli meeleolu häirete tekkes ning on põhilisteks hetkel kasutuses olevate antidepressantide sihtmärkideks (Belujon et al., 2017). On näidatud muutuseid *Negr1* ekspressioonis peale mitmete antidepressantide manustamist, mille sihtmärgiks on monoamiinergilised neurotransmitterid. Lisaks psühhiaatrilistele häiretele on NEGR1 geeni seostatud ka ülekaalulisusega. Ülegenoosetes GWAS uuringutes on NEGR1 geeni korduvalt seostatud kehamassi indeksiga, mis viitab sellele, et NEGR1 omab rolli keha kaalu reguleerimisel ja ülekaalulisuse tekkel. Samuti on näidatud seoseid LSAMP-i ning psühhiaatriliste häirete vahel. LSAMP valgu taseme tõusu otsmikukoores on näidatud nii skisofreenia kui ka depressiooni patsientidel võrreldes tervete kontrollidega. Hiirtel on näidatud, et suurenenud Lsamp tase on seotud vähenenud aktiivsuse, suurenenud ärevuse ning akuutse hirmu reaktsiooniga.

Hoolimata tugevast seosest *Negr1* ja depressiooni vahel, pole veel uuritud *Negr1* puudulikkusega hiire serotonergilist ja dopamiinergilist süsteemi. Arvestades seda, et NEGR1 geen inimesel seostub nii depressiooni kui ülekaalulisusega, on töö eesmärgiks uurida *Negr1*-puudulikkusega hiire mudelis nii kehakaalu fenotüüpi, depressiooni ja kehakaalu regulatsiooniga seotud biokeemilisi radasid ning täpsemalt hinnata *Negr1* puudulikkusega hiire monoamiinergilisi radu, kasutades selleks amfetamiini ja estsitalopraami. Veel on antud töö eesmärgiks uurida *Lsamp* puudulikkusega hiire serotonergilist süsteemi, kasutades selleks estsitalopraami.

Hiiremudelit kasutades leidsime, et nii LSAMP kui NEGR1 on ekspresseerunud serotonergilistes rakkudes ning kroonilise SSRI estsitalopraami manustamine tingib nii *Lsamp*- kui *Negr1*-puudulikkusega hiirtel ajus erineva monoamiinide profiili muutuse võrreldes nende metsiktüüpi pesakonnakaaslastega. Kui *Lsamp* välja lülitamise järgselt domineerib kõrgem serotoniini käive, siis NEGR1 puudulikus hiires nägime muutusi esmajoones dopamiinisüsteemis. Samuti näitasime me *MaoA* taseme tõusu *Lsamp* puudulikkusega hiirte raphe piirkonnas.

Veel näitasid tulemused, et *Negr1*-puudulikkusega hiirel esineb ajast-sõltuv suurenenud käitumuslik sensitiseerumine amfetamiini suhtes, mis on seotud suurenenud dopamiini vabanemisega nii dorsaalses kui ka ventraalses striaatumis. Mitmetes aju piirkondades oli märgata nii dopamiini kui serotoniini transporterite ekspressiooni taseme tõusu *Negr1*-puudulikkusega hiirel, samuti oli *Negr1*-puudulikkusega hiirel suurenenud mitmes ajupiirkonnas mitmete monoamiinide ning nende metaboliitide tasemed. Kroonilise estsitalopraami katse näitas, et *Negr1*-puudulikkusega hiirtel oli võimendunud estsitalopraami poolt põhjustatud serotoniini ning dopamiini ringkäigu vähenemine. Samuti oli näha, et estsitalopraam võib leevendada *Negr1*-puudulikkuse poolt põhjustatud hipokampuste kaalu vähenemist.

Metaboloomika uuringud *Negr1*-puudulikkusega hiirtega näitasid, et 6 nädalat kõrge rasvasisaldusega toitu põhjustas *Negr1*-puudulikkusega hiirtel suurenenud glükoosi taseme tõusu veres. Glükoosi tolerantsuse testis (GTT) põhjustas kõrge rasvasisaldusega toit genotüübi erinevusi ainult isastel hiirtel. *Negr1*-puudulikkusega isastel hiirtel esines vähenenud tolerantsus glükoosile ning samuti esines neil hargnenud ahelaga aminohapete (BCAA) taseme tõus veres. Üldine metaboolne profiil viitab sellele, et *Negr1*-puudulikkusega hiirte metabolism kaldub glükoneogeneesi, rasvhapete *de novo* sünteesi ja kõrgema valkude katabolismi suunas, seda kõike võimendab veel omakorda kõrge rasvasisaldusega toit.

Kokkuvõttes näitab käesolev uurimistöö, et nii *Negr1* kui ka *Lsamp* puudulikkusega hiirtel esinevad käitumuslikud ning biokeemilised muutused, mis on sarnased muutustele, mis esinevad psühhiaatriliste häiretega patsientidel ning IgLON adhesioonivalkude mõju psühhiaatrilistele häiretele toimib vähemalt osaliselt läbi monoamiinergiliste ühenduste mõjutamise. Meie leid, et NEGR1 mõjutab lisaks aju biokeemiale ka süsteemset metabolismi, kinnitab, et psühhiaatrilisi sündroome peaks käsitlema kui kogu keha homöostaasi häireid.

ACKNOWLEDGEMENT

I would like to thank my supervisors Mari-Anne Philips, Eero Vasar and Este Leidmaa for accepting me to their lab and helping and guiding me throughout all these years. Without them I would not have the opportunity to work with this very interesting project. Thanks to them I have gotten a lot of new knowledge and skills. They have always given me good advice and helped me whenever I needed it. Their comprehensive help of planning the experiments have been very important to me. Thanks to them I had the opportunity to visit the Italy and do part of my experimental work in there.

I would also thank all my coworkers from the lab, especially Mohan Jayaram and Kaie Mikheim who helped me a lot with animal experiments. I would not have been able to do them without their help. I would also like to thank Tanel Visnapuu, who help me with the dissection of the brains. I would also like to thank all the other colleagues and co-authors who have helped me throughout these years.

Huge thank goes also to the workers of the animal house who have helped a lot when it comes to animal experiments. And I would also like to thank people from biochemistry department, especially Kalle Kilk who helped a lot with metabolic studies and also with monoamine measurements.

And finally, I would like thank my parents and the rest of my family and friends. They have offered me support in difficult times and encouraged me to carry on. Without them I would not have reached where I am now.

ORIGINAL PUBLICATIONS

CURRICULUM VITAE

Name: Maria Kaare
Date of birth: 06.03.1994, Tartu
Citizenship: Estonia
Address: University of Tartu, Institute of Physiology, Ravila 19, Tartu 50411, Estonia
Phone: +372 53 488 352
E-mail: maria.kaare@ut.ee

Education:

2001–2011	Tartu Mart Reiniku Gymnasium
2011–2013	Tartu Jaan Poska Gymnasium
2013–2016	University of Tartu, Faculty of Science and Technology, B.Sc.
2016–2018	University of Tartu, Faculty of Science and Technology, M.Sc.
2018–2022	University of Tartu, Faculty of Medicine, doctoral studies in neuroscience

Career:

2020–	Solis Biodyne, laboratory assistant

Courses and conferences:

2019	Competence course on Laboratory Animal Science (Tartu)
2019	Baltic Summer School on Behavioural Characterization of Rodent Models of Major Brain Disorders (Pühajärve)
2019	32nd ECNP Congress (Copenhagen)
2022	35th ECNP Congress (Vienna)

List of publications:

Kaare, M., Jayaram, M., Jagomäe, T., Singh, K., Kilk, K., Leevik, M., Varul, J., Leidmaa, E., Visnapuu, T., Nõmm, H., Rähn, K., Plaas, M., Lilleväli, K., Schäfer, M. K.E., Philips, M.-A., Vasar, E. (2022). Depression-associated *Negr1* gene-deficiency induce alterations in the monoaminergic neurotransmission enhancing time-dependent sensitization to amphetamine in male mice. Brain Sciences 12(12), 1696.

Kaare, M., Mikheim, K., Lilleväli, K., Kilk, K., Jagomäe, T., Leidmaa, E., Piirsalu, M., Porosk, R., Singh, K., Reimets, R., Taalberg, E., Schäfer M. K. E., Plaas, M., Vasar, E., Philips, M.-A. (2021). High-Fat Diet Induces Pre-Diabetes and Distinct Sex-Specific Metabolic Alterations in Negr1-Deficient Mice. Biomedicine 9(9), 1148. 10.3390/biomedicines9091148.

Bregin, A.*, Kaare, M.*, Jagomäe, T., Karis, K., Singh, K., Laugus, K., Innos, J., Leidmaa, E., Heinla, I., Visnapuu, Oja, E.-M., Kõiv, K., Lilleväli, K., Harro, J., Philips, M.-A., Vasar, E. (2020). Expression and impact of Lsamp neural adhesion molecule in the serotonergic neurotransmission system. Pharmacol. Biochem. Behav. 198, 173017. 10.1016/j.pbb.2020.173017.

Singh, K., Jayaram, M., Kaare, M., Leidmaa, E., Jagomäe, T., Heinla, I., Hickey, M. A., Kaasik, A., Schäfer, M. K., Innos, J., Lilleväli, K., Philips, M.-A. and Vasar, E. (2019). Neural cell adhesion molecule Negr1 deficiency in mouse results in structural brain endophenotypes and behavioral deviation related to psychiatric disorders. Sci. Rep. 9, 5457. 10.1038/s41598-019-41991-8.

Karis, K., Eskla, K.-L., Kaare, M., Täht, K., Tuusov, J., Visnapuu, T., Innos, J., Jayaram, M., Timmusk, T., Weickert, C. S., Väli, M., Vasar, E., Philips, M.-A. (2018). Altered Expression Profile of IgLON Family of Neural Cell Adhesion Molecules in the Dorsolateral Prefrontal Cortex of Schizophrenic Patients. Front Mol Neurosci. 10.3389/fnmol.2018.00008.

ELULOOKIRJELDUS

Nimi: Maria Kaare
Sünniaeg: 06.03.1994, Tartu
Kodakondsus: Eesti
Aadress: TÜ füsioloogia instituut, Ravila 19, Tartu 50411, Eesti
Telefon: +372 53 488 352
E-post maria.kaare@ut.ee

Haridus:

2001–2011	Tartu Mart Reiniku Gümnaasium
2011–2013	Tartu Jaan Poska Gümnaasium
2013–2016	Tartu Ülikool, Loodus- ja täppisteaduste valdkond, geenitehnoloogia, BSc
2016–2018	Tartu Ülikool, Loodus- ja tõppisteaduste valdkond, biomeditsiin, MSc
2018–2022	Tartu Ülikool, meditsiiniteaduste valdkond, neuroteadused, PhD

Töökogemus:

2020–	Solis Biodyne

Erialane enesetäiendus:

2019	Katseloomateaduse kursus (Tartu)
2019	Balti suvekool: Behavioural Characterization of Rodent Models of Major Brain Disorders (Pühajärve)
2019	32. ECNP konverents (Kopenhaagen)
2022	35. ECNP konverents (Viin)

Artiklid eelretsentseeritavates ajakirjades:

Kaare, M., Jayaram, M., Jagomäe, T., Singh, K., Kilk, K., Leevik, M., Varul, J., Leidmaa, E., Visnapuu, T., Nõmm, H., Rähn, K., Plaas, M., Lilleväli, K., Schäfer, M. K.E., Philips, M.-A., Vasar, E. (2022). Depression-associated *Negr1* gene-deficiency induce alterations in the monoaminergic neurotransmission enhancing time-dependent sensitization to amphetamine in male mice. Brain Sciences 12(12), 1696.

Kaare, M., Mikheim, K., Lilleväli, K., Kilk, K., Jagomäe, T., Leidmaa, E., Piirsalu, M., Porosk, R., Singh, K., Reimets, R., Taalberg, E., Schäfer M. K. E., Plaas, M., Vasar, E., Philips, M.-A. (2021). High-Fat Diet Induces Pre-Diabetes and Distinct Sex-Specific Metabolic Alterations in Negr1-Deficient Mice. Biomedicine 9(9), 1148. 10.3390/biomedicines9091148.

Bregin, A.*, Kaare, M.*, Jagomäe, T., Karis, K., Singh, K., Laugus, K., Innos, J., Leidmaa, E., Heinla, I., Visnapuu, Oja, E.-M., Kõiv, K., Lilleväli, K., Harro, J., Philips, M.-A., Vasar, E. (2020). Expression and impact of Lsamp neural adhesion molecule in the serotonergic neurotransmission system. Pharmacol. Biochem. Behav. 198, 173017. 10.1016/j.pbb.2020.173017.

Singh, K., Jayaram, M., Kaare, M., Leidmaa, E., Jagomäe, T., Heinla, I., Hickey, M. A., Kaasik, A., Schäfer, M. K., Innos, J., Lilleväli, K., Philips, M.-A. and Vasar, E. (2019). Neural cell adhesion molecule Negr1 deficiency in mouse results in structural brain endophenotypes and behavioral deviation related to psychiatric disorders. Sci. Rep. 9, 5457. 10.1038/s41598-019-41991-8.

Karis, K., Eskla, K.-L., Kaare, M., Täht, K., Tuusov, J., Visnapuu, T., Innos, J., Jayaram, M., Timmusk, T., Weickert, C. S., Väli, M., Vasar, E., Philips, M.-A. (2018). Altered Expression Profile of IgLON Family of Neural Cell Adhesion Molecules in the Dorsolateral Prefrontal Cortex of Schizophrenic Patients. Front Mol Neurosci. 10.3389/fnmol.2018.00008.

DISSERTATIONES NEUROSCIENTIAE UNIVERSITATIS TARTUENSIS

1. **Sirli Raud.** Cholecystokinin$_2$ receptor deficient mice: changes in function of GABA-ergic system. Tartu, 2005.
2. **Kati Koido.** Single-nucleotide polymorphism profiling of 22 candidate genes in mood and anxiety disorders. Tartu, 2005.
3. **Dzhamilja Safiulina.** The studies of mitochondria in cultured cerebellar granule neurons: characterization of mitochondrial function, volume homeostasis and interaction with neurosteroids. Tartu, 2006.
4. **Tarmo Areda.** Behavioural and neurogenetic study of mechanisms related to cat odour induced anxiety in rodents. Tartu, 2006.
5. **Aleksei Nelovkov.** Behavioural and neurogenetic study of molecular mechanisms involved in regulation of exploratory behaviour in rodents. Tartu, 2006.
6. **Annika Vaarmann**. The studies on cystatin B deficient mice: neurochemical and behavioural alterations in animal model of progressive myoclonus epilepsy of Unverricht-Lundborg type. Tartu, 2007.
7. **Urho Abramov.** Sex and environmental factors determine the behavioural phenotype of mice lacking CCK_2 receptors: implications for the behavioural studies in transgenic lines. Tartu, 2008.
8. **Hendrik Luuk.** Distribution and behavioral effects of WFS1 protein in the central nervous system. Tartu, 2009.
9. **Anne Must.** Studies on molecular genetics of male completed suicide in Estonian population. Tartu, 2009.
10. **Kaido Kurrikoff**. Involvement of cholecystokinin in chronic pain mechanisms and endogenous antinociception. Tartu, 2009.
11. **Anu Aonurm-Helm.** Depression-like phenotype and altered intracellular signalling in neural cell adhesion molecule (NCAM)-deficient mice. Tartu, 2010.
12. **Silva Sütt.** Role of endocannabinoid system and *Wfs1* in regulation of emotional behaviour: behavioural, pharmacological and genetic studies. Tartu, 2010.
13. **Mari-Anne Philips.** Characterization of *Myg1* gene and protein: expression patterns, subcellular localization, gene deficient mouse and functional polymorphisms in human. Tartu, 2010.
14. **Ranno Rätsep.** Genetics of psoriasis and vitiligo, focus on IL10 family cytokines. Tartu, 2010.
15. **Kairit Joost.** Selective screening of metabolic diseases in Estonia: the application of new diagnostic methods. Tartu, 2012, 143 p.
16. **Monika Jürgenson.** A complex phenotype in mice with partial or complete deficiency of the NCAM protein. Tartu, 2012, 117 p.

17. **Ene Reimann.** Description of the cytokines and cutaneous neuroendocrine system in the development of vitiligo. Tartu, 2012, 117 p.
18. **Jürgen Innos.** Behavioural, pharmacological and neurochemical characterisation of limbic system-associated membrane protein (LSAMP) deficient mice. Tartu, 2013, 113 p.
19. **Kaili Anier.** The role of DNA methylation in the development of cocaine-induced behavioural sensitisation. Tartu, 2013, 147 p.
20. **Maarika Liik.** Cognitive functioning, perceived cognition, subjective complaints and symptoms of depression in patients with epilepsy: neuropsychological assessment and spet brain imaging study. Tartu, 2014, 124 p.
21. **Sten Ilmjärv.** Estimating differential expression from multiple indicators. Tartu, 2015, 125 p.
22. **Paula Reemann.** The effects of microenvironment on skin cells. Tartu, 2015, 146 p.
23. **Tanel Visnapuu.** Pharmacological and behavioral characterization of the monoaminergic and GABA-ergic systems of Wfs1-deficient mice. Tartu, 2015, 107 p.
24. **Indrek Heinla.** Behavioural and genetic comparison of B6 and 129Sv mouse lines focusing on the anxiety profile and the expression of *Lsamp* gene. Tartu, 2016, 115 p.
25. **Liina Haring.** Cognitive functioning after first psychotic episode. Tartu, 2017, 146 p.
26. **Triin Tekko.** Neurodevelopmental Approach in the Study of the Function of *Wfs1* and *Lsamp*, Potential Targets in the Regulation of Emotional Behaviour. Tartu, 2018, 194 p.
27. **Alina Altpere.** Targeting of mechanisms of elevated anxiety in female Wfs1-deficient mice. Tartu, 2018, 98 p.
28. **Maarja Toots.** Pharmacological challenge in rodent models of Wolfram syndrome with emphasis on diabetic phenotype. Tartu, 2018, 114 p.
29. **Katyayani Singh.** Neuropsychiatric endophenotypes – focusing on IgLON adhesion molecules in the mouse brain. Tartu, 2019, 148 p.
30. **Kattri-Liis Eskla.** Therapeutic strategies for ischemia reperfusion injury. Tartu, 2019, 138 p.
31. **Hardo Lilleväli**. Hyperphenylalaninaemias and neurophysiological disorders associated with the condition. Tartu, 2020, 134 p.
32. **Roman Balõtšev**. Interaction between the immune and metabolic systems in different stages of schizophrenia spectrum disorders. Tartu, 2020, 164 p.
33. **Mari Urb**. DNA methylation in the predisposition, expression and abstinence of cocaine addiction. Tartu, 2020, 147 p.
34. **Liisa Leppik.** Alterations in metabolomic profile of lipids, amino acids and biogenic amines in the early course of schizophrenia spectrum disorders. Tartu, 2021, 173 p.
35. **Kadri Seppa.** The neuroprotective effect of GLP-1 receptor agonist liraglutide in a rat model of Wolfram syndrome. Tartu, 2021, 154 p.

36. **Akbar Zeb.** The novel mechanisms of Parkin-dependent mitophagy. Tartu, 2022, 146 p.
37. **Aleksandr Bregin.** Alterations of emotional behaviour induced by the genetic invalidation of the limbic system associated membrane protein (Lsamp) – potential implications for neuropsychiatric disorders. Tartu, 2022, 176 p.
38. **Jane Varul.** Different stress coping strategies of 129Sv and C57/Bl6 mouse strains – evidence from behavioural, pharmacological, metabolomics and gene expression studies. Tartu, 2022, 177 p.